Rep. Prog. Phys. 53 (1990) 1559-1619. Printed in the UK

Planetary nebulae

Manuel Peimbert

Instituto de Astronomía, Universidad Nacional Autónoma de México, Apartado Postal 70-264, México D F, 04510 Mexico

Abstract

Planetary nebulae (PN) are shells of low-density ionized gas that have been expelled by their central stars. Intermediate-mass stars, while leaving the red giant stage to become white dwarfs, undergo mass loss, producing PN.

The main emphasis of the review is on the properties of the shell and their relation to other branches of astrophysics. Recent studies on the distance scale to galactic PN, the extragalactic distance scale, and the PN birth rate are described. The relevance of the PN chemical composition to the study of stellar evolution and the chemical evolution of galaxies is discussed.

This review was received in its present form in August 1990.

0034-4885/90/121559+61$14.00

Contents

1. Introduction

Planetary nebulae (PN) are shells of low-density ionized gas that have been ejected by their central stars. The shells are expelled at low velocity and are expanding away from the central stars with typical velocities of about 25 km s^{-1}; they are expected to dissipate in about 25 000 years. In this time interval the central star also modifies appreciably its luminosity and effective temperature. Typical densities in the shell range from 10^5 cm^{-3}, for young and compact PN, to about 1 cm^{-3}, for very extended objects or faint outer halos of objects with higher-density inner shells. The electron temperatures, T_e, for the ionized region of the shell, range from 5000 to 20 000 K. The central star surface temperatures range from 25 000 to 300 000 K. The ionized shell is easily observable in the visible spectrum since it produces bright recombination lines of H and He and also bright forbidden lines of O, N, Ne, S and Ar. An excellent review with emphasis on the physical processes taking place in the low-density ionized gas was presented by Seaton (1960).

The study of PN includes research into the properties of the ejected envelope, or nebular shell, and research into the central star, or nucleus. Very often the term PN is used to denote only the shell, but sometimes it is also used to denote the shell and the nucleus. The name planetary nebula dates from the end of the eighteenth century and is based on the disk-like greenish appearance of some bright PN seen through small telescopes, similar to the appearance of Uranus and Neptune. The name is kept for historical reasons but there is no connection between PN and planets. Figures 1 and 2 show two classic galactic PN.

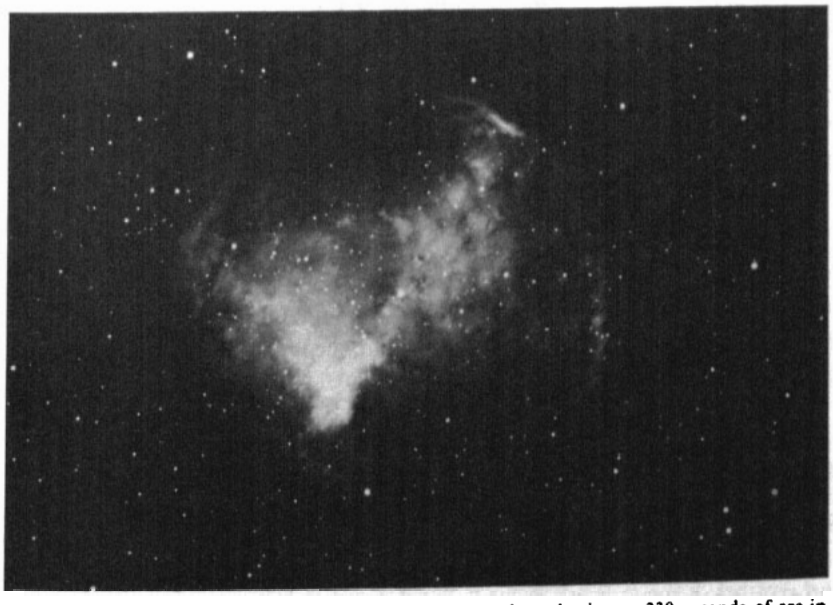

Figure 1. NGC 6853, the Dumbbell nebula, a nearby galactic PN, 330 seconds of arc in diameter. Original photograph was taken with the 3 m Shane reflector and a plate-filter combination emphasizing [N II] λλ6548, 6583 and Hα. (Lick Observatory photograph.)

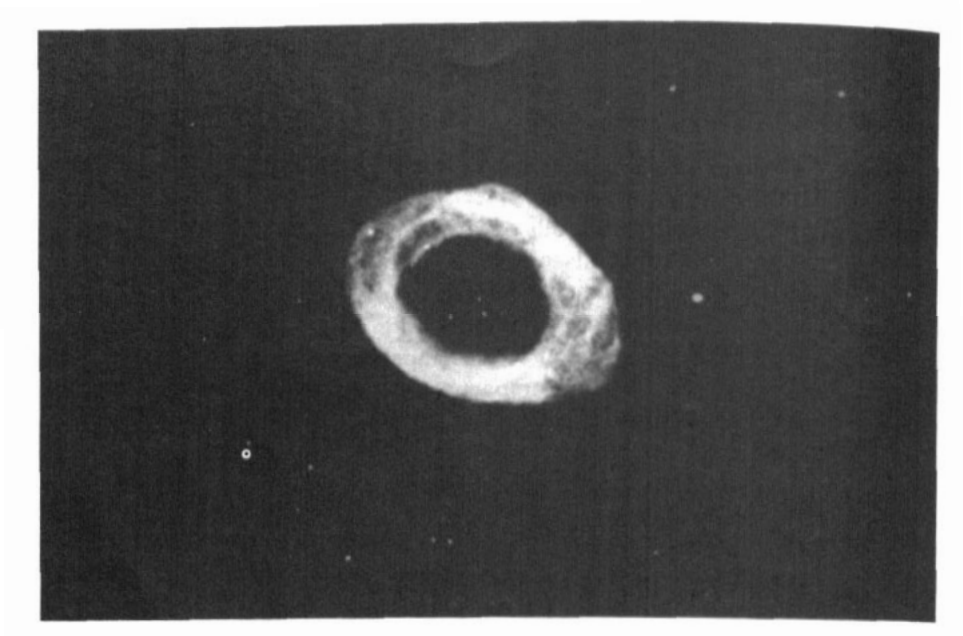

Figure 2. NGC 6720, the Ring nebula, a nearby galactic PN, 75 seconds of arc in diameter. Original photograph taken with the same equipment as figure 1. (Lick Observatory photograph.)

Intermediate mass stars (IMS), those with masses in the range $0.8 \leqslant M_i/M_\odot \leqslant 8$, where M_i is their initial mass and $M_\odot$ is the solar mass, are considered to be the progenitors of PN. IMS spend most of their life in the main sequence transforming hydrogen into helium in their nuclei; after leaving the main sequence they become red giants and develop a degenerate carbon-oxygen core. It is thought that a considerable fraction of the IMS while leaving the red giant phase and before becoming white dwarfs eject their outer envelope, forming a PN. The central star evolves toward higher surface temperatures during the shell ejection and the emergent flux of wavelength less than 912 Å becomes intense enough to ionize most or all of the ejected gas. Figure 3 is a graph of stellar luminosity as a function of stellar temperature (an HR diagram) where the direction of the evolution is represented by arrows.

Stars with $M_i \geqslant 8\ M_\odot$ ignite carbon in a non-degenerate core; their final evolutionary stages are greatly different from those of the IMS, probably producing supernovae. Stars with $M_i \leqslant 0.8\ M_\odot$ have not had time to evolve off the main sequence during the lifetime of the Galaxy (e.g. Iben and Rood 1970), moreover they may lose their hydrogen-rich envelope before the central star becomes hot enough to ionize the ejected envelope (Renzini and Voli 1981).

From the study of the gaseous envelope of a PN it is possible to determine its chemical composition. There are two types of elements: those affected by the stellar evolution of IMS, such as H, He, C and N and those not affected by it, such as Ne, S and Ar. Data on the abundances of the elements of the first group provide constraints for stellar evolution models, while data on the abundances of the elements of the second group indicate the relative abundances of those elements at the time the progenitors of the PN were formed. The determination of the chemical composition of PN is paramount for the study of the chemical evolution of the Galaxy.

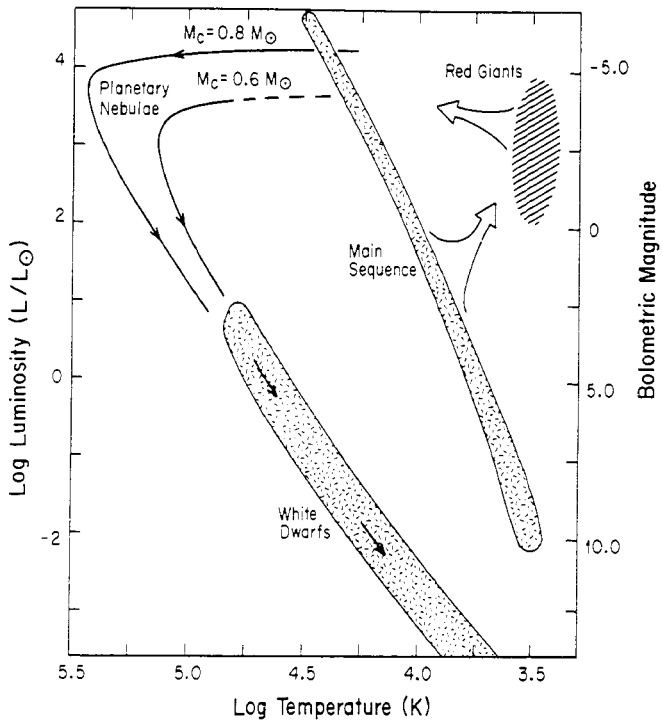

Figure 3. HR diagram showing the location of: central stars of PN, main sequence stars, white dwarf stars and red giants. The evolutionary tracks for central stars of PN for $M_c = 0.6\ M_\odot$ and $M_c = 0.8\ M_\odot$ by Paczynski (1971) are also shown schematically.

There are several recent books dedicated to the study of the physical conditions within ionized gaseous nebulae (Osterbrock 1989, Pottasch 1984, Aller 1984). The topic has been of considerable interest and every five years since 1967 there has been a major symposium dedicated to all aspects of PN; the last three, those of 1977, 1982 and 1987, contain very useful review articles that are still relevant to current research (Terzian 1978, Flower 1983, Torres-Peimbert 1989). A recent review on PN has been presented by Khromov (1989).

As of 1967 there were 1067 galactic objects in the PN catalogue compiled by Perek and Kohoutek (1967). This catalogue contains most of the PN observations available up to 1966. At present the sample of galactic PN has grown to about 1600. The number of known extragalactic PN reaches many hundreds and includes objects as far away as 15 Mpc from us. With present techniques it is possible to discover many thousands of them.

This review concentrates on the properties of the PN shell and their relevance to other astrophysical problems. In sections 2 and 3 we describe the ionization structure of the shell and the methods used to derive the electron temperature and the electron density. In section 4 we describe the determination of the chemical abundances. In section 5 we present a classification of PN based on their chemical composition and compare the abundances of PN with those predicted by stellar evolution theory. In section 6 we review the galactic distance determinations to PN and how they are used to determine masses, birth rates and the total number of galactic PN. In section 7 we

discuss the information on abundances and on the extragalactic distance scale (the determination of the Hubble constant) that can be derived from extragalactic PN. Also in section 7 we discuss the PN birth rate in extragalactic systems and their relation with the galactic distance scale. In section 8 we discuss the relevance of PN research to the problem of galactic chemical evolution, in particular to the primordial or pregalactic He/H abundance ratio. The concluding remarks are presented in section 9.

Very important advances have been achieved during the last ten years in other areas of PN research, that will not be reviewed here, including: (a) properties and evolution of the central stars (e.g. Kaler 1985, Méndez *et al* 1988, Schönberner 1989), (b) stellar mass loss and its effects on the late stages of stellar evolution (e.g. Kwok 1987, Renzini 1989, Perinotto 1989), (c) protoplanetary nebulae (e.g. Preite-Martinez 1987 and other articles in the same book), (d) dust content of the shell (e.g. Roche 1989), (e) molecules in the shell (e.g. Zuckerman and Gatley 1988, Rodríguez 1989), and (f) multiple shells (e.g. Chu 1989).

2. Ionization structure

The ionization structure of a PN depends on the physical processes occurring within the nebula. We will discuss equilibrium structures that do not include gas motions; this approach simplifies our task considerably. The processes that determine the ionization structure and the kinetic temperature have been widely studied and are in general well understood.

2.1. Photoionization and recombination of a hydrogen nebula: Strömgren spheres

Typical PN envelopes are composed of H, He and trace elements such as C, N, O and Ne. The envelope is ionized by a hot central star that produces a significant photon flux above the Lyman limit, $h\nu_0 = 13.6$ eV. The envelope radiates through recombination and collisional excitation processes. We will simplify our discussion by assuming a pure hydrogen nebula of uniform density with spherical symmetry.

It is necessary to consider the transfer of UV radiation through the nebula. This radiation is the ultimate source of energy for all the physical processes at each point in the nebula. The stellar radiation flux at frequency ν impinging upon a unit area at a distance r from the exciting star is:

$$4\pi J_\nu(r) = \pi F_\nu(r_*)\left(\frac{r_*}{r}\right)^2 \exp(-\tau_\nu(r)) \tag{2.1}$$

where $\pi F_\nu(r_*)$, in erg cm^{-2} s^{-1} Hz^{-1}, is the stellar flux at the surface of the star of radius r_*, $\pi F_\nu(r_*) = L_\nu/4\pi r_*^2$, L_ν is the luminosity of the star at frequency ν, in erg s^{-1} Hz^{-1}, and τ_ν is the optical depth due to absorption by hydrogen atoms and is given by

$$\mathrm{d}\tau_\nu = N(\mathrm{H}^0)a_\nu(\mathrm{H}^0)\mathrm{d}r \tag{2.2}$$

where $N(\mathrm{H}^0)$ is the number of neutral H atoms per unit volume at the distance r and $a_\nu(\mathrm{H}^0)$, in cm^2, is the absorption cross section for the H^0 ground state. The dependence of a_ν on frequency may be represented as

$$a_\nu(\mathrm{H}^0) = \begin{cases} 0 & \nu < \nu_0 \\ 6.3\times10^{-18}(\nu_0/\nu)^3 & \nu \geq \nu_0 \end{cases}. \tag{2.3}$$

2.1.1. Ionization equilibrium. Equilibrium of ionization prevails if, in each volume element, the photoionization rate is equal to the recombination rate; that is if the capture rate of H^0 ionizing photons is balanced by the recombination rate of protons with free electrons. This can be expressed as

$$N(H^0)\int_{\nu_0}^{\infty}\frac{4\pi J_\nu}{h\nu}\,a_\nu\,d\nu = N(H^+)N_e\alpha_A(T_e) \tag{2.4}$$

where $\alpha_A(T_e)$, the recombination coefficient to all levels defined as $\alpha_A=\Sigma_{i=1}^{\infty}\alpha_i$, is related to a_ν through the Milne relation and is equal to $4\times10^{-13}\,cm^3\,s^{-1}$ for $T_e=10\,000$ K. The radiation intensity, J_ν, consists of the stellar component, J_ν^*, and the 'diffuse' component, J_ν^d, i.e.

$$J_\nu = J_\nu^* + J_\nu^d \tag{2.5}$$

where J_ν^d is produced by the nebula itself upon recombination of electrons to the H ground state and in general is assumed to be isotropic. The diffuse radiation consists predominantly of photons with frequencies just above ν_0 and, to a good approximation, it can be assumed to be absorbed locally on the spot. Under this approximation, the photoionization rate by diffuse radiation is equal to the rate of recombination to the ground state at every point, consequently the ionization equilibrium condition (equation (2.4)) can be written as

$$N(H^0)\int_{\nu_0}^{\infty}\frac{4\pi J_\nu^d}{h\nu}\,a_\nu\,d\nu = N(H^+)N_e\alpha_1 \tag{2.6}$$

and

$$N(H^0)\int_{\nu_0}^{\infty}\frac{4\pi J_\nu^*}{h\nu}\,a_\nu\,d\nu = N(H^+)N_e\alpha_B \tag{2.7}$$

where $\alpha_B=\Sigma_{i=2}^{\infty}\alpha_i$ (equal to $2.6\times10^{-13}\,cm^3\,s^{-1}$ for $T_e=10\,000$ K) is the recombination coefficient to all levels but the first.

The ionization structure of the nebula is obtained by solving the transfer equation (equation (2.1)) coupled with the optical depth and the ionization equilibrium equations (equations (2.2) and (2.7)). In a pure-H nebula the following relations apply:

$$N(H) = N(H^0) + N(H^+) \qquad N_e = N(H^+). \tag{2.8}$$

This problem was originally solved by Strömgren (1939), who found that H is almost completely ionized within a sphere of radius R_s and that the degree of ionization decreases rapidly at the outer edge of the ionization zone ($r=R_s$), achieving neutrality in a distance $\Delta s\sim[a_\nu N(H^0)]^{-1}$. These configurations have been named Strömgren spheres.

The Strömgren or critical radius, R_s, can be derived by assuming that within it, the rate of recombinations to all levels but the first is equal to the number of ionizing photons produced by the central star, $Q(H^0)$, i.e.

$$Q(H^0) = \int_{\nu_0}^{\infty}\frac{L_\nu}{h\nu}\,d\nu = \frac{4\pi}{3}R_s^3N_e^2\alpha_B. \tag{2.9}$$

If the number of ionizing photons is larger than the number of recombinations, then a fraction of the ionizing photons escape the PN and the object is considered to be optically thin; if this is not the case all the ionizing photons are trapped inside the

nebula and the PN is optically thick. Under conditions of inhomogeneous density a PN could be optically thick in some directions and not in others. Optically thin and optically thick nebulae are also called density bounded and ionization bounded, respectively.

2.2. Helium

After H the next most abundant element in PN is He, its relative abundance is ~10% by number and a better approximation to the ionization structure of an actual nebula is provided by taking it into account. The ionization potential of He^0 is 24.6 eV, or 1.8 $h\nu_0$, and that of He^+ is 54.4 eV, or 4 $h\nu_0$. The photons of energy $13.6 < h\nu < 24.6$ eV can only ionize H^0, while those of energy $24.6 < h\nu < 54.4$ eV can ionize both H^0 and He^0. Different types of ionizing structures are present depending on the spectrum of the ionizing radiation and on the He abundance.

In the presence of He, the on-the-spot approximation can also be adopted, and ionization equilibrium equations can be written for H^0, He^0 and He^+. The additional complication is that some photons produced by He recombination processes are energetic enough to ionize H and have to be taken into account. The ionization cross sections reach their maximum value at the threshold energies, and also show a very rapid decrease with increasing energy. Table 1 shows the interrelation between the H and He recombination fields for typical conditions within a PN. Moreover, He^0 and He^+ have to be taken into account for the calculation of τ_1 and N_e.

Table 1. Relative absorption* of the diffuse radiation field by H^0, He^0 and He^+.

Process	Absorber		
	H^0	He^0	He^+
H I Lyman continuum	1	—	—
He I Lyman continuum	0.13	0.87	—
He II Lyman continuum	0.03	0.56	0.41
He II Balmer continuum	1	—	—
He I Lyman lines	1	—	—
He II Lyman lines	0.08	0.92	—
He I Two-photon emission	1	—	—
He II Two-photon emission $(1\text{-}1.8)h\nu_0$	1	—	—
He II Two-photon emission $(1.8\text{-}3)h\nu_0$	0.11	0.89	—

* Given in $\dfrac{\int J_\nu^d N(X^+) a_\nu(X^+) d\nu}{\int J_\nu^d [N(H^0) a_\nu(H^0) + N(He^0) a_\nu(He^0) + N(He^+) a_\nu(He^+)] d\nu}$.

2.3. Heavy elements

In PN the abundance of heavy elements is very small, and thus they do not affect significantly the ionization structure of the radiation field. However, through collisional excitation, the heavy elements emit forbidden and semiforbidden lines that radiate energy away very efficiently.

The ionization equilibrium for consecutive stages of ionization, i and $i+1$, of any element X may be written as:

$$N(X^{+i})\int_{\nu_i}^{\infty}\frac{4\pi J_\nu}{h\nu}a_\nu(X^{+i})\,d\nu = N(X^{+i+1})N_e\alpha_G(X^{+i},T_e) \tag{2.10}$$

where $N(X^{+i})$ and $N(X^{+i+1})$ are the number densities of the two successive stages of ionization, $a_\nu(X^{+i})$ is the photoionization cross section for the ground level of X, with threshold ν_i, and α_G is the recombination coefficient of the ground level of X^{+i+1} to all levels of X^{+i}. Additional terms should be added to equations of this type to take into account charge exchange reactions and dielectronic recombinations.

The ionization equilibrium equations, together with the condition that the ionic abundances add up to the total element abundance.

$$N(X^0)+N(X^+)+N(X^{+2})+\ldots = N(X) \tag{2.11}$$

completely determine the ionization equilibrium at each point.

2.4. Heating and cooling mechanisms

In the static case the temperature is fixed by the equilibrium between heating by photoionization and cooling by recombination, collisional excitation of low lying energy levels which upon de-excitation produce photons that leave the nebula, and free-free radiation or bremsstrahlung. When hydrogen absorbs an ultraviolet photon of energy $h\nu > h\nu_0$ it becomes ionized, the electron released has an initial kinetic energy given by $\frac{1}{2}mv^2 = h(\nu-\nu_0)$. The electron interacts with other electrons and ions, rapidly redistributing its kinetic energy and becoming 'thermalized'. Upon recombination the inverse process occurs and an electron with an energy equal to $\frac{1}{2}mv^2$ is captured by an ion. The balance of energy gains and losses defines the kinetic energy of the gas. Therefore to construct a model that solves for the temperature distribution of a nebula it is necessary to assess these processes at each point.

The energy input by photoionization of hydrogen (in erg $cm^{-3}\,s^{-1}$) is

$$G(H) = N(H^0)\int\frac{4\pi J_\nu}{h\nu}h(\nu-\nu_0)a_\nu(H^0)\,d\nu. \tag{2.12}$$

While the kinetic energy lost by the electron gas in recombinations (in erg $cm^{-3}\,s^{-1}$) is

$$L_R(H) = N_eN_pkT_e\beta_A(H^0,T_e) \tag{2.13}$$

where

$$\beta_A(H^0,T_e) = \sum_{n=1}^{\infty}\beta_n(H^0,T_e) \tag{2.14}$$

and

$$\beta_n = \frac{1}{kT_e}\int v\sigma_n(H^0,T_e)\tfrac{1}{2}mv^2f(v)\,dv. \tag{2.15}$$

In addition, free-free emission is more effective in cooling the nebula than recombination. The rate of cooling is in this case

$$L_{FF}(Z) = (1.42\times10^{-27})Z^2T_e^{\frac{1}{2}}g_{ff}N_eN_{ion} \tag{2.16}$$

where Z is the charge of the cooling ions and g_{ff} is the mean Gaunt factor for free-free emission, for nebular conditions g_{ff} is close to 1.3 (Osterbrock 1989). The collisional excitation of low lying levels of common ions, with subsequent radiation, is the most important of all cooling processes. These ions make a significant contribution, in spite of their low abundances, because they have energy levels with excitation potential $\sim kT_e$. These processes are more laborious to calculate since for each element the excitation to several levels has to be computed for different stages of ionization. We can represent the energy lost by radiation following collisional excitation as

$$L_C = \sum_{i,k,a} N_a(X^{+k})_i \sum_{j<i} A_{ij} h\nu_{ij} \tag{2.17}$$

where i is the excited level, k is the stage of ionization, a is the atomic mass and A_{ij} is the Einstein transition probability coefficient.

At each point in the nebula the kinetic temperature is determined by the equilibrium between the heating and cooling mechanisms discussed above, i.e.

$$G = L_R + L_{FF} + L_C. \tag{2.18}$$

Given the ultraviolet spectrum of the ionizing star, as well as the density distribution and the chemical composition of the surrounding gas, it is possible to compute model ionization structures for gaseous nebulae.

3. Temperatures, densities and filling factors

The determination of physical conditions in PN such as temperature, density, ionization degree and abundance of the elements, is based on the observed line intensities and requires a large quantity of accurate atomic data. This need has created a crucial interplay between astronomical observations and atomic physics.

The observed spectra have to be corrected for interstellar reddening caused by dust grains. This is usually carried out by adopting the normal reddening law (e.g. Whitford 1958, Seaton 1979) and by comparing expected intensity ratios with observed ones, either from Balmer line ratios as computed by Brocklehurst (1971) and Hummer and Storey (1987), or from lines that originate in the same upper level and whose ratios are given by the ratios of the Einstein A values, or from radio continuum to Hβ ratios. The intrinsic line intensities, $I(\lambda)$, are related to the observed line intensities, $F(\lambda)$ by

$$\log \frac{I(\lambda)}{I(H\beta)} = \log \frac{F(\lambda)}{F(H\beta)} + f(\lambda)C(H\beta) \tag{3.1}$$

where $f(\lambda)$ is the reddening function, which is practically the same for all galactic PN in the visual region, and $C(H\beta)$ is the logarithmic reddening correction at Hβ, which varies from object to object. Table 2 shows the average reddening law assembled by Seaton (1979).

Most of the observed emission lines are produced by recombination or by electron impact excitation. The parameters that govern their intensities are: (a) the recombination coefficients, (b) the transition probabilities, (c) the collisional excitation cross sections and (d) the ionization cross sections. Sets of H^0 and He^+ recombination coefficients for different densities and temperatures have been computed by Brocklehurst (1971) and Hummer and Storey (1987), similarly a set of recombination coefficients for He^0 has been computed by Brocklehurst (1972) for the conditions

Table 2. Mean interstellar extinction curve from Seaton (1979).

λ (Å)	$1/\lambda(\mu^{-1})$	$f(\lambda)$	λ (Å)	$1/\lambda(\mu^{-1})$	$f(\lambda)$
10 000	1.0	−0.63	2326	4.3	+1.36
8 333	1.2	−0.50	2222	4.5	+1.61
7 143	1.4	−0.39	2174	4.6	+1.71
6 250	1.6	−0.28	2128	4.7	+1.65
5 556	1.8	−0.15	2041	4.9	+1.49
5 000	2.0	−0.03	1923	5.2	+1.25
4 545	2.2	+0.08	1818	5.5	+1.14
4 167	2.4	+0.16	1667	6.0	+1.13
3 846	2.6	+0.23	1538	6.5	+1.19
3 571	2.8	+0.30	1429	7.0	+1.28
3 333	3.0	+0.38	1250	8.0	+1.61
2 857	3.5	+0.61	1111	9.0	+2.12
2 500	4.0	+0.97	1000	10.0	+2.78

present in PN. A compilation of transition probabilities, collisional excitation cross sections and ionization cross sections, together with a review of the different computational approaches to determine these parameters is given by Mendoza (1983). Many of these atomic parameters cannot be determined in terrestrial laboratories due to the very low densities present in PN shells. In fact, PN are excellent low-density laboratories to test theoretical computations of atomic parameters.

3.1. Temperatures and densities derived from forbidden lines

At low densities the relative population of the excited levels of many ions departs from the Boltzmann distribution and is given by the equilibrium between collisional excitation and de-excitation, and spontaneous emission.

The electron de-excitation rate coefficient, q_{ij}, is given by

$$q_{ij}(T_e) = \frac{8.63 \times 10^{-6} \Upsilon_{ij}(T_e)}{\omega_i T_e^{1/2}} \ (\mathrm{cm^3\ sec^{-1}}) \tag{3.2}$$

where ω_i is the statistical weight of the ith level, and $\Upsilon_{ij}(T_e)$ is the effective collision strength, given by

$$\Upsilon_{ij}(T_e) = \int_0^\infty \Omega(i,j) \exp(-\varepsilon_i / kT_e)\, \mathrm{d}(\varepsilon_i / kT_e) \tag{3.3}$$

where $\Omega(i,j)$ is the collision strength and $\varepsilon_i = \frac{1}{2}mv_i^2$ is the initial kinetic energy of the colliding electron. The excitation rate coefficient is given by

$$q_{ji} = (\omega_i / \omega_j) q_{ij} \exp(-\Delta E_{ij} / kT_e) \tag{3.4}$$

where $i > j$.

3.1.1. Forbidden line densities. Ions whose excited levels are close together in energy produce line intensity ratios that are independent of temperature. These line ratios are used to determine the electron density; for example the observed forbidden line ratios

of [O II] (configuration $2p^3$) and those of [S II], [Cl III], [Ar IV] and [K V] (configuration $3p^3$) are given by

$$R(N_e) = I(^4S^0_{3/2} - {}^2D^0_{5/2}) / I(^4S^0_{3/2} - {}^2D^0_{3/2}) \tag{3.5}$$

and are very sensitive to the electron density.

The level populations are determined by electron collisions and spontaneous emission of radiation. At low densities R is equal to the ratio of the collision strengths $\Omega(^4S, {}^2D_{5/2})/\Omega(^4S, {}^2D_{3/2})$ and it is equal to $\frac{3}{2}$, the ratio of the statistical weights in the upper states. For large N_e, R is equal to $\frac{3}{2}$ times the ratio of the transition probabilities, $A(^4S, {}^2D_{5/2})/A(^4S, {}^2D_{3/2})$.

$R(N_e)$ provides a useful comparison between observations and theory of atomic structure; there is excellent agreement for O^+ and S^+ (e.g. Kaler *et al* 1976, Dopita *et al* 1976, Zeippen 1982, Mendoza and Zeippen 1982a, b, Stanghellini and Kaler 1989). From this comparison it was found that higher-order relativistic corrections to the magnetic dipole operator, which are usually negligible, had to be taken into account (the experimental techniques for measuring lifetimes of allowed transitions are in general not suited for forbidden transitions and consequently there have been few experimental results).

3.1.2. Forbidden line temperatures. Electron temperatures are derived from the ratio of two emission lines from the same ion whose excited levels are of very different energies. The classical ratio to derive the electron temperature in PN is given by the [O III] lines $\lambda 5007$ $^3P_2$-$^1D_2$, $\lambda 4959$ $^3P_1$-$^1D_2$ and $\lambda 4363$ $^1D_2$-$^1S_0$ (Menzel *et al* 1941, Seaton 1954). These lines are collisionally excited from the ^3P level and are easily observed in most PN. The excitation energies are $[E(^1D) - E(^3P)] = 2.49$ eV and $[E(^1S) - E(^3P)] = 5.33$ eV. Since typical electron temperatures in PN have associated energies ~ 1 eV, the line ratio is very sensitive to the electron temperature. A good approximation to the ratio is given by

$$\frac{I(4959) + I(5007)}{I(4363} = \frac{7.73 \exp[(3.29 \times 10^4)/T_e]}{1 + 4.5 \times 10^{-4}(N_e/T_e^{1/2})}. \tag{3.6}$$

The accuracy of the atomic parameters used is within 10%, and the accuracy of the best observed line intensity ratios for the brightest PN is also within 10%. Therefore for these objects typical uncertainties of several hundred degrees in the derived electron temperatures are found.

A similar line ratio used to determine electron temperatures is given by the [N II] lines $\lambda 6583$ $^3P_2$-$^1D_2$, $\lambda 6548$ $^3P_1$-$^1D_2$, and $\lambda 5755$ $^1D_2$-$^1S_0$. This ratio is important for PN with regions of a low degree of ionization.

3.2. Density inhomogeneities

Almost all PN show structure on two-dimensional images. In addition to clumpiness, which gives them an inhomogeneous appearance, they show large-scale density gradients, filaments, shells, bipolar geometry, *etc* (e.g. Balick 1987, Balick *et al* 1987). The role that these spatial density variations play in the determination of basic parameters, like the envelope mass and the ionization structure, is paramount to the study and formation of PN.

A global density, $N_e(\text{RMS})$, can be obtained from the PN hydrogen line fluxes. The observed flux in H(β) from a homogeneous sphere after correction for absorption is given by

$$I(\text{H}\beta) = \tfrac{1}{3}(R^3/d^2) N_e(\text{RMS}) N_p(\text{RMS}) \alpha(\text{H}\beta) h\nu(\text{H}\beta) \tag{3.7}$$

where R is the radius of the object, d is the distance to the observer, $\alpha(\text{H}\beta)$ is the Hβ effective recombination coefficient and N_p, the proton density. To a very good approximation, the proton density is given by

$$N_p(\text{RMS}) = N_e(\text{RMS}) \left(1 + \frac{N(\text{He}^+)}{N(\text{H}^+)} + 2\frac{N(\text{He}^{+2})}{N(\text{H}^+)} \right)^{-1}. \tag{3.8}$$

Similar equations can be written for other Balmer lines or for the free-free radio continuum. To solve this equation it is necessary to determine the He^+/H^+ and the $\text{He}^{+2}/\text{H}^+$ abundance ratios (see subsection 4.1). For density homogeneous PN the $N_e(\text{RMS})$ density corresponds to the real electron density.

The densities derived from forbidden line ratios and from global emissions are not identical. In general $N_e(\text{FL})$ is larger than $N_e(\text{RMS})$, indicating the presence of density inhomogeneities. A first approximation to the study of this problem is to assume that a given PN of total volume V_T has two types of regions: high-density ones, which occupy a fraction $\varepsilon = V/V_T$ of the total volume, with an average density given by $N_e(\text{FL})$, and low-density regions with negligible densities.

The filling factor, ε, is given by

$$\varepsilon = N_e^2(\text{RMS})/N_e^2(\text{FL}). \tag{3.9}$$

The concept of filling factor was introduced by Strömgren (1948) (see also Seaton and Osterbrock 1957, Osterbrock and Flather 1959, Mallik and Peimbert 1988 and references therein).

Since for a given nebula the $N_e(\text{FL})$ value is independent of distance while the $N_e(\text{RMS})$ is not, a good distance estimate is needed to derive ε (see (3.7) and (3.9)).

A useful observational quantity is the emission measure (EM) defined as

$$\text{EM} = \int N_e(\text{RMS}) N_i(\text{RMS})\, \text{d}l \tag{3.10}$$

where N_i is the number of ions cm^{-3} and l is given in pc; the EM is proportional to the surface brightness of an object. The brightest PN have EM $\sim 10^7$ cm^{-6} pc and the faintest PN that can be detected in the red Palomar Survey Plates have EM in the range 20-50 (Peimbert *et al* 1975).

3.3. Temperature inhomogeneities

The variations in density, degree of ionization, and chemical composition in PN are likely to produce spatial temperature variations. In addition to these variations, PN are losing mass at supersonic velocities, producing shock waves within the envelopes; these shock waves also produce spatial temperature variations.

There are at least four different methods for deriving temperatures of PN: (a) intensity ratios of auroral to nebular forbidden lines, (b) intensity ratios of a recombination line i times ionized to a collisionally excited line of the same element $i+1$ times ionized like λ4267 of C II to λ1909 of C III, (c) intensity ratios of bound-free continuum to recombination lines of hydrogen, and (d) intensity ratios of free-free continuum to

recombination lines of hydrogen. The first three are used in the UV and optical region of the spectrum, and the fourth one in the radio region.

It can be shown that in the presence of spatial temperature variations over the observed volume, the methods based on collisionally excited lines yield higher temperatures than those based on recombination lines, free-bound or free-free continua. The average temperature weighted by the square of the density over the volume considered is given by

$$T_0(N_i, N_e) = \frac{\int T(\boldsymbol{r}) N_i(\boldsymbol{r}) N_e(\boldsymbol{r}) \, d\Omega \, dl}{\int N_i(\boldsymbol{r}) N_e(\boldsymbol{r}) \, d\Omega \, dl} \tag{3.11}$$

where Ω is the observed solid angle, l is the distance along the line of sight and $\boldsymbol{r}$ is the position vector; for the case of forbidden lines N_i is replaced by $N(X^{+p})$. When the temperature is derived from a parameter that depends on the αth power of the local temperature we have

$$\langle T^\alpha \rangle = \frac{\int T^\alpha(\boldsymbol{r}) N_e(\boldsymbol{r}) N_i \, d\Omega \, dl}{\int N_e(\boldsymbol{r}) N_i(\boldsymbol{r}) \, d\Omega \, dl}. \tag{3.12}$$

For the case of small fluctuations $\langle T^\alpha \rangle$ can be expanded in a Taylor series about the mean temperature, yielding a temperature

$$T_\alpha = \langle T^\alpha \rangle^{1/\alpha} \approx T_0 \left(1 + \frac{\alpha - 1}{2} t^2 \right) \qquad \alpha \neq 0, \text{ for } t^2 \ll 1. \tag{3.13}$$

In this relation terms of order higher than 2 have been neglected. Here t is the root mean square temperature fluctuation and is given by

$$t^2 = \frac{\int T^2 N_e N_i \, d\Omega \, dl - T_0^2 \int N_e N_i \, d\Omega \, dl}{T_0^2 \int N_e N_i \, d\Omega \, dl}. \tag{3.14}$$

For a value of the temperature derived from two processes that depend on different powers of the temperature, it can be shown that

$$T_{\alpha,\beta} = \left(\frac{\langle T^\alpha \rangle}{\langle T^\beta \rangle} \right)^{1/(\alpha-\beta)} \approx T_0 \left(1 + \frac{\alpha - \beta - 1}{2} t^2 \right) \qquad \alpha \neq \beta, \text{ for } t^2 \ll 1. \tag{3.15}$$

Similarly for the case of a temperature derived from the ratio of two forbidden lines, it can be shown that

$$T_{\lambda_1/\lambda_2} \approx T_0 \left[1 + \left(\frac{\Delta E - \Delta E^*}{kT_0} - 3 \right) \frac{t^2}{2} \right] \qquad \Delta E \neq \Delta E^*, \text{ for } t^2 \ll 1 \tag{3.16}$$

where ΔE and ΔE^* represent the differences in energy between the upper levels of each of the transitions and the ground level.

For $t^2 \ll 1$ and the temperature derived from the Balmer continuum and Hβ, it is found that

$$T_{\text{Bac H}\beta} = T_0(1 - 1.70t^2) \tag{3.17}$$

and for the temperature derived from radio lines and continuum:

$$T_{\lambda_1/\lambda_2} = T_0(1 - 1.42t^2) \tag{3.18}$$

while for $\lambda 4363$ and $\lambda 5007$ of O^{++} from equation (3.16) we obtain

$$T_{(4363/5007)} = T_0\left[1+\tfrac{1}{2}\left(\frac{90800}{T_0}-3\right)t^2\right]. \tag{3.19}$$

Consequently for the temperatures calculated from optical lines of PN, the forbidden-line method emphasizes high-temperature regions while the other two methods favour the low-temperature regions.

From recent theoretical models of constant density, homogeneous chemical composition and photon ionization it is found that for PN $0.005 \leq t^2 \leq 0.03$. Obviously each nebula has a different value of t^2.

The derivation of the correct electron temperature is very important for the determination of the chemical abundances. If constant temperature is assumed, $t^2 = 0.00$, instead of $t^2 \simeq 0.02$, an underestimate of 0.3 to 0.2 dex is obtained for the relative abundances based on forbidden-to-permitted line ratios ($10^a = a$ dex). The errors in dismissing spatial temperature fluctuations are negligible when both lines are formed by recombination.

In type-I PN (see subsection 5.1) it is likely that the relative importance of shock waves is higher than in the other objects, and consequently that the electron temperature derived from the 4363/5007 ratio could be considerably higher than the average temperature.

In the presence of chemical inhomogeneities the temperature differences can be very large, a factor of two or more, and sophisticated models of ionization structure are necessary to properly determine the temperature distribution (Torres-Peimbert *et al* 1990).

4. Chemical compositions

One of the most important aspects of the study of PN is the determination of their chemical abundances. The chemical composition of a PN is the result of the galactic chemical evolution prior to the formation of the progenitor star and of the modification of the initial abundances by nuclear reactions in its interior. Therefore the study of the chemical composition of PN can be used as a test of models of stellar evolution and of models of galactic chemical evolution. In this article the term chemical composition is used to describe the relative abundances of all the elements, and not the relative abundances of the molecules.

4.1. Ionic abundances

Hydrogen constitutes ~90%, helium ~10% and all the other elements together ~0.1% of the atoms in the Universe.

The ionic abundances of a PN are always given relative to H^+ not only because H is the most abundant element but because H^+ essentially defines the ionized region. The H^+ abundances are directly derived from the Balmer line intensities that are very bright and easy to observe. The effective recombination coefficients for the Balmer line intensities have been computed by Brocklehurst (1971) and Hummer and Storey (1987) for a wide range of N_e and T_e values; these coefficients are almost independent of N_e and are roughly proportional to T_e^{-1}, therefore precise values of the electron temperature are not needed to obtain accurate H emissivities.

4.1.1. Helium. It is possible to derive the $N(He^{+2})/N(H^{+})$ ratios from equations of the type

$$\frac{N(He^{+2})}{N(H^{+})} = \frac{\alpha_{4,2}(H^{0})}{\alpha_{4,3}(He^{+})} \frac{4686}{4861} \frac{I(4686)}{I(H\beta)} \tag{4.1}$$

where the $4 \rightarrow 3$ transition corresponds to the strongest He II line in the optical region at $\lambda 4686$ Å. Equation (4.1) can be written as

$$\frac{N(He^{+2})}{N(H^{+})} = 2.28 \times 10^{-2} T_e^{0.14} \frac{I(4686)}{I(H\beta)} \tag{4.2}$$

where the effective recombination coefficients have been derived from the computations by Hummer and Storey (1987) interpolated in the 10 000–20 000 K electron temperature range for $N_e = 10\,000\ cm^{-3}$. Since both H and He recombination lines are roughly proportional to T_e^{-1}, accurate $N(He^{+2})/N(H^{+})$ ratios can be derived even if the electron temperature is not well known.

The $N(He^{+})/N(H^{+})$ ratios can be derived from equations of the type

$$\frac{N(He^{+})}{N(H^{+})} = \frac{\alpha_{4,2}(H^{0})}{\alpha_{nm}(He^{0})} \frac{\lambda_{nm}}{4861} \frac{I(\lambda_{nm})_{rec}}{I(H\beta)} \tag{4.3}$$

where the effective recombination coefficients for helium, $\alpha_{nm}(He^{0})$, have been computed by Brocklehurst (1972). The He I line intensities are affected by radiative transfer effects and collisions from the 2^3S metastable level and the observed line intensities are related to the radiative recombination line intensities by

$$I(\lambda) = I(\lambda)_{rec}[1 + \gamma_{ce}(\lambda) + \gamma_{rt}(\lambda)] \tag{4.4}$$

where γ_{ce} is the collisional excitation parameter and γ_{rt} is the radiative transfer parameter. Fortunately each He I line is affected differently by the effects of radiative transfer and collisional excitation, therefore by measuring accurately different He I lines in the same nebula it is possible to evaluate each effect and to derive accurate $N(He^{+})/N(H^{+})$ ratios.

The collisional excitation parameters depend strongly on the T_e and N_e values and are given by

$$\gamma_{ce}(\lambda_{nm}, T_e, N_e) = \gamma_{ce}(\lambda_{nm}, T_e, \infty)/[1 + N_c/N_e(T_e)] \tag{4.5}$$

where N_c is the critical density for radiative depopulation of the 2^3S He^{0} level and corresponds to 3230 cm^{-3} for $10\,000 \leq T_e \leq 20\,000$. The latest estimates of the $\gamma_{ce}(\lambda_{nm})$ values for the different helium lines are those by Clegg (1987) and Peimbert and Torres-Peimbert (1987a, b) based on the 19-state *ab initio* computation for collisions to He^{0} states with $n \leq 4$ by Berrington and Kingston (1987). The possibility of depopulation of the 2^3S He^{0} level by photoionization and by other processes, that could reduce the γ_{ce} values, has been studied by Peimbert and Torres-Peimbert (1987b) and by Clegg and Harrington (1989). The collisional excitation effects typically reduce the $N(He^{+})/N(H^{+})$ ratios by factors ranging from 1.02 to 1.20; the most affected ratios are those of PN with high N_e and T_e values.

The 2^3S-n^3P series with $n > 2$ is weakened by self-absorption and $\lambda\lambda$ 7065 2^3P-3^3S, 5876 2^3P-3^3D and 4472 2^3P-4^3D are strengthened by resonance fluorescence. The self-absorption effect for λ 7065 is considerable while for $\lambda\lambda$ 5876 and 4472 it is substantially smaller. From observations of the $I(7065)/I(4472)$ intensity ratios and the computations by Robbins (1968) and Cox and Daltabuit (1971) it is possible to

estimate the optical thickness in the various triplet lines. For typical PN the self-absorption effect increases the intensity of λ7065 by factors in the 1.1–3 range while the increase on $\lambda\lambda$5876 and 4472 is smaller than a factor of 1.02. A partial energy level diagram showing the He I triplet system is presented in figure 4.

Similarly, self-absorption from the 1^1S ground state has a considerable effect on the emergent line intensities; for example λ5016 2^1P-3^1P is strengthened by a large factor. From observations of the $I(5016)/I(4472)$ intensity ratios (e.g. Aller and Walker 1970) and the computations by Robbins and Bernat (1973) it is possible to estimate the optical thickness in the various singlet lines, from this estimate it follows that the effect on $\lambda\lambda$6678 2^1P-3^1D and 4922 2^1P-4^1D is smaller than a factor of 1.01 and can be neglected.

4.1.2. Ionic abundances from other recombination lines. Faint emission lines of C, N, O and other elements have been detected in bright PN. Some are excited by resonance fluorescence, while others seem to be due to pure recombination processes.

Lines produced by fluorescence cannot be used to determine accurate abundances because radiative transfer effects dominate their intensities. A classic example is provided by the O III lines in the 2800–3800 Å range, the strongest lines being $3p^3S_1$–$3d^3P^0_2$ λ3133 and $3p^3P_2$–$3d^3P^0_2$ λ3444; these lines are produced by a coincidence between the He II Lyα and the [O III] $2p^2\ ^3P_2$–$3d^3P^0_2$ λ303.80 transitions. This coincidence converts He II Lyα into O III Bowen resonance-fluorescence photons (Bowen 1928, Saraph and Seaton 1980, Osterbrock 1989).

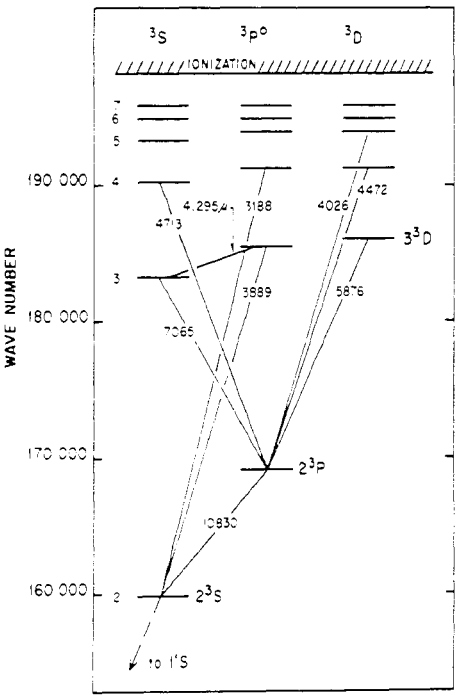

Figure 4. Partial Grotrian diagram of He I, showing the strongest optical lines of the triplet system. The line intensities of the triplet system are affected by collisional excitation and self-absorption from the metastable 2^3S level.

A typical line produced by recombination is $3d^2D\text{-}4f^2F^0\ \lambda 4267$ of C^+, the C^{+2} abundance derived from this line is given by

$$\frac{N(C^{+2})}{N(H^+)} = \frac{\alpha_{4267}(H^0)}{\alpha_{4267}(C^+)} \frac{4267}{4861} \frac{I(4267)}{I(H\beta)}$$

$$= 1.67 \times 10^{-2} T_e^{0.20} \frac{I(4267)}{I(H\beta)} \tag{4.6}$$

where $\alpha_{4267}(C^+)$ was obtained from Seaton (1978) and was interpolated for $10\,000 \leqslant T_e \leqslant 20\,000$ K.

The C^{+2} abundance derived from $\lambda 4267$ is in general higher than that derived from the [C III] $3s^2\ ^1S_0\text{-}3s\ 3p^3\ P_2\ \lambda 1907 + $[C III] $3s^2\ ^1S_0\text{-}3s\ 3p^3\ P_1\ \lambda 1909$ collisionally excited lines; this difference is of an order of magnitude in extreme cases. General discussions of this problem have been given in the literature (e.g. Torres-Peimbert *et al* 1980, Barker 1982, French 1983, Kaler 1986, Clegg 1989, Peimbert 1989). The discrepancy could be due to spatial variations in the electron temperature produced by inhomogeneities in the C/H abundance ratio (Peimbert 1983); the regions with higher C/H abundance ratios would be at lower temperatures and would contribute preferentially to $\lambda 4267$, while the regions with lower C/H abundance ratios would be at higher temperatures and would contribute preferentially to $\lambda\lambda 1907 + 1909$. Torres-Peimbert *et al* (1990) have computed ionization structure models for NGC 4361 that are consistent with this suggestion.

The abundances of C^{+3} and C^{+4} can also be determined from recombination lines present in the visual region of the spectrum (e.g. French 1983); the effective recombination coefficients have been presented by Seaton (1978). For the line C III $4f^3F\text{-}5g^3G$, $\lambda 4070$ the contribution due to dielectronic recombination (Nussbaumer and Storey 1984) has to be taken into account.

Recombination lines of N^+ have also been used to determine N^{+2}/H^+ ratios (Wilkes *et al* 1981, Escalante 1988). Some of the N^+ lines might be affected by fluorescence effects. Escalante (1988) has found that for a group of PN the N^+ lines that originate from F levels are due only to recombination, while those that originate from P levels are affected by fluorescence in some objects. The accuracy of the N^{+2}/H^+ abundance ratios is about a factor of two due to the faintness of the N^+ lines. Non-hydrogenic effective recombination coefficients for the N^+ lines have been computed by Escalante and Victor (1990).

4.1.3. Ionic abundances from collisionally excited lines. The collisionally excited line flux $I(X^{+p}, \lambda_{nm})$ received from a nebula in ergs cm^{-2} s^{-1} is given by

$$I(X^{+p}, \lambda_{nm}) = \int N_n(X^{+p}) A_{nm} h\nu(\lambda_{nm})\, d\Omega\, dl \tag{4.7}$$

where λ_{nm} is the wavelength associated with the emission, $N_n(X^{+p})$ is the number of atoms in the excited level n of the state of ionization p in cm^{-3}, A_{nm} is the Einstein transition probability coefficient in s^{-1}, Ω is the observed solid angle and l is the depth of the nebula along the line of sight in cm. If collisional de-excitations are negligible, equation (4.7) can be written as

$$I(X^{+p}, \lambda_{nm}) = C(\lambda_{nm}) \int N(X^{+p}, \boldsymbol{r}), N_e(\boldsymbol{r}) T_e(\boldsymbol{r})^{-1/2} \exp[-\Delta E/kT_e(\boldsymbol{r})]\, d\Omega\, dl \tag{4.8}$$

where $N(X^{+p})$ is the total number of atoms in the pth state of ionization, $\boldsymbol{r}$ is the position in the nebula, ΔE is the energy difference between the ground and excited levels and C is a constant that can be determined from the atomic parameters.

Analogously, the Hβ flux of a nebula can be expressed as

$$I(\mathrm{H}\beta) = \int N_e(\boldsymbol{r}) N(\mathrm{H}^+, \boldsymbol{r}) \alpha_{4,2}(\mathrm{H}^0) h\nu(\mathrm{H}\beta)\, \mathrm{d}\Omega\, \mathrm{d}l \tag{4.9}$$

where $\alpha_{4,2}(\mathrm{H}^0) = 1.32 \times 10^{-10} T_e^{-0.91}$ for $10\,000 \leq T_e \leq 20\,000$ K (Hummer and Storey 1987). Consequently equation (4.9) can be written as

$$I(\mathrm{H}\beta) = D \int N_e(\boldsymbol{r}) N(\mathrm{H}^+, \boldsymbol{r}) T_e(\boldsymbol{r})^{-0.91}\, \mathrm{d}\Omega\, \mathrm{d}l \tag{4.10}$$

where D is a constant.

For homogeneous nebulae with uniform temperature the relative abundances can be obtained from equations (4.8) and (4.10), and are given by

$$\frac{N(X^{+p})}{N(H^+)} = \frac{D}{C(\lambda_{nm})} \frac{\exp(\Delta E/kT_e)}{T_e^{0.41}} \frac{I(X^{+p}, \lambda_{nm})}{I(\mathrm{H}\beta)}. \tag{4.11}$$

Accurate values of the electron temperature are needed to obtain accurate abundances from collisionally excited lines in the ultraviolet and visual regions of the spectrum because for them $\Delta E \geq 2$ eV and typical temperatures in PN correspond to $kT_e \sim 1$ eV. Alternatively, abundances derived from infrared lines are almost temperature independent since $\Delta E < 1$ eV.

In Tables 3, 4 and 5, we list some of the most important collisionally excited lines used to determined chemical abundances; notice that all the visual and infrared lines are forbidden while in the ultraviolet there are forbidden, semi-forbidden and permitted lines. A review of the relevance of infrared forbidden fine-structure emission lines for the study of PN has been given by Dinerstein (1983). Typical spectra of PN in the UV, optical and infrared regions are shown in figures 5 to 8. Feibelman *et al* (1988) have produced a very useful spectral atlas of PN based on the archives of the International Ultraviolet Explorer satellite.

Table 3. Ultraviolet collisionally excited lines used to determine chemical abundances.

λ (Å)	Ion	Transition
1239	N V	$^2S_{1/2}$–$^2P_{3/2}$
1243	N V	$^2S_{1/2}$–$^2P_{3/2}$
1483	[N IV]	$^1S_0$–$^3P_2$
1486	N IV]	$^1S_0$–$^3P_1$
1548	C IV	$^2S_{1/2}$–$^2P_{3/2}$
1550	C IV	$^2S_{1/2}$–$^2P_{1/2}$
1661	O III]	$^3P_1$–$^5S_2$
1666	O III]	$^3P_2$–$^5S_2$
1907	[C III]	$^1S_0$–$^3P_2$
1909	C III]	$^1S_0$–$^3P_1$
2422	[Ne IV]	$^4S_{3/2}$–$^2D_{5/2}$
2426	[Ne IV]	$^4S_{3/2}$–$^2D_{3/2}$
2854	[Ar IV]	$^4S_{3/2}$–$^2P_{3/2}$
2868	[Ar IV]	$^4S_{3/2}$–$^2P_{1/2}$

Table 4. Optical collisionally excited lines used to determine chemical abundances.

λ (Å)	Ion	Transition
3426	[Ne V]	$^3P_2$-$^1D_2$
3726	[O II]	$^4S_{3/2}$-$^2D_{5/2}$
3729	[O II]	$^4S_{3/2}$-$^2D_{5/2}$
3869	[Ne III]	$^3P_2$-$^1D_2$
4711	[Ar IV]	$^4S_{3/2}$-$^2D_{5/2}$
4724	[Ne IV]	$^2D_{3/2}$-$^2P_{3/2}$
4726	[Ne IV]	$^2D_{3/2}$-$^2P_{1/2}$
4740	[Ar IV]	$^4S_{3/2}$-$^2D_{3/2}$
5007	[O III]	$^3P_2$-$^1D_2$
6583	[N II]	$^3P_2$-$^1D_2$
6716	[S II]	$^4S_{3/2}$-$^2D_{5/2}$
6731	[S II]	$^4S_{3/2}$-$^2D_{3/2}$
7006	[Ar V]	$^3P_2$-$^1D_2$
7136	[Ar III]	$^3P_2$-$^1D_2$
9531	[S III]	$^3P_2$-$^1D_2$

Table 5. Infrared collisionally excited lines used to determine chemical abundances.

λ (μm)	Ion	Transition
6.98	[Ar II]	$^2P_{3/2}$-$^2P_{1/2}$
8.99	[Ar III]	$^3P_2$-$^3P_1$
10.52	[S IV]	$^2P_{1/2}$-$^2P_{3/2}$
12.81	[Ne II]	$^2P_{3/2}$-$^2P_{1/2}$
18.71	[S III]	$^3P_1$-$^3P_2$
24.28	[Ne V]	$^3P_0$-$^3P_1$
25.87	[O IV]	$^2P_{1/2}$-$^2P_{3/2}$
51.81	[O III]	$^3P_1$-$^3P_2$
57.34	[N III]	$^2P_{1/2}$-$^2P_{3/2}$
88.36	[O III]	$^3P_0$-$^3P_1$

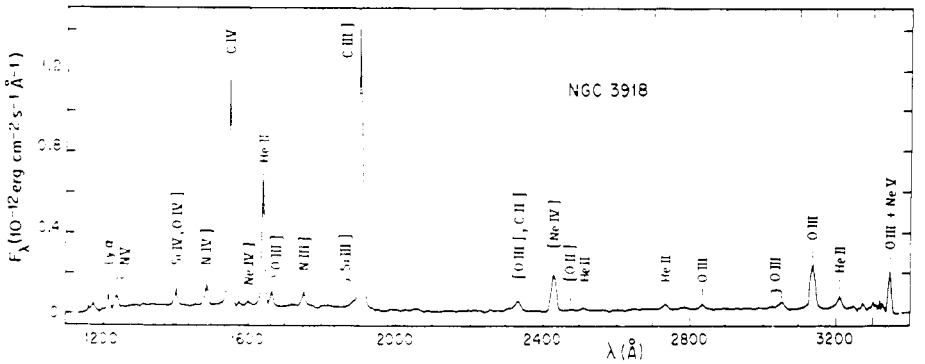

Figure 5. Ultraviolet spectrum of NGC 3918 obtained with the International Ultraviolet Explorer satellite.

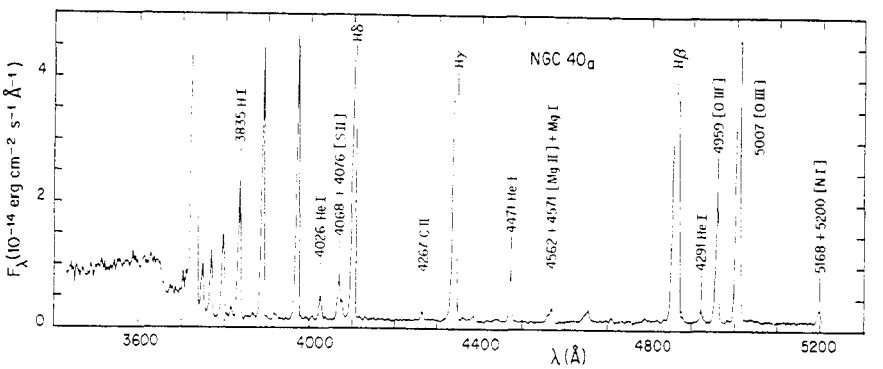

Figure 6. Blue spectrum of NGC 40 taken with the IIDS at Kitt Peak National Observatory (Clegg *et al* 1983).

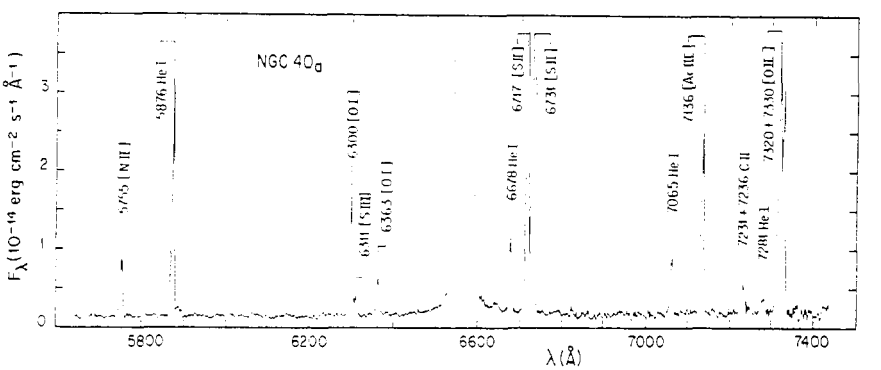

Figure 7. Red spectrum of NGC 40 taken with the same equipment as figure 6 (Clegg *et al* 1983).

4.2. Total abundances

The total abundance of a given object relative to H is given by

$$\frac{N(X)}{N(H)} = \frac{N(X^0) + N(X^+) + N(X^{+2}) + \ldots}{N(H^+)}. \tag{4.12}$$

Ideally all the ions present should be observable. Unfortunately very often not all ions have observable transitions and corrections for the unobservable stages of ionization have to be applied.

4.2.1. Ionization correction factors. To estimate the abundance of unobserved ions it is possible to rely on the abundances of observed ions with similar ionization potentials.

PN can be divided into (a) those with a low degree of ionization, i.e. those without a He^{+2} region and (b) those with a high degree of ionization, i.e. those with a He^{+2} region. In what follows we will mention the most used ionization correction factors for PN with high and low degrees of ionization.

For PN with a low degree of ionization the oxygen abundance is given by

$$\frac{N(O)}{N(H)} = \frac{N(O^+ + O^{+2})}{N(H^+)} \tag{4.13}$$

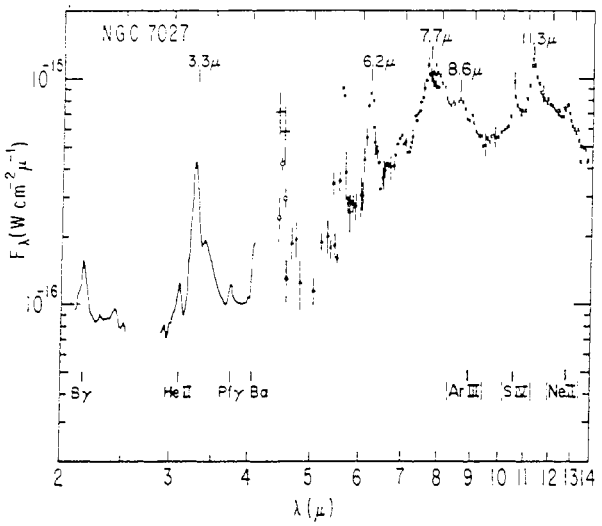

Figure 8. Infrared spectrum of NGC 7027; the data in the 4–8μ region were taken with the UCSD spectrograph on the Kuiper Airborne Observatory and the other data from ground based observatories (Rusell *et al* 1977).

the ionic O^+ and O^{+2} abundances are directly determined from strong lines. The oxygen ratios are used to determine the total abundances of N and Ne when only N^+ and Ne^{+2} abundances are available as follows:

$$\frac{N(N)}{N(H)} = \frac{N(O^+ + O^{+2})}{N(O^+)} \frac{N(N^+)}{N(H^+)} = i_{cf}(N) \frac{N(N^+)}{N(H^+)} \tag{4.14}$$

$$\frac{N(Ne)}{N(H)} = \frac{N(O^+ + O^{+2})}{N(O^{+2})} \frac{N(Ne^{+2})}{N(H^+)} = i_{cf}(Ne) \frac{N(Ne^{+2})}{N(H^+)}. \tag{4.15}$$

Equation (4.15) breaks down for the external regions and at the edges of low-density PN like NGC 7293 and NGC 6720, where there are appreciable quantities of H^0 inside the H^+ zone and the following charge transfer reactions occur

$$O^{+2} + H^0 \rightleftarrows O^+ + H^+ \tag{4.16}$$

$$Ne^{+2} + H^0 \rightleftarrows Ne^+ + H^+. \tag{4.17}$$

The large value of the rate coefficient $\beta(O^{+2})$ relative to $\beta(Ne^{+2})$ produces an increase of $N(Ne^{+2})/N(O^{+2})$ toward the edge of low-density PN (Péquignot *et al* 1978, Hawley and Miller 1978a, Butler *et al* 1979, Péquignot 1980). Equation (4.15) also breaks down for objects with a very low degree of ionization, those with a He^0 zone inside the H^+ region (e.g. Flower 1969, Torres-Peimbert and Peimbert 1977).

For PN with a high degree of ionization the helium abundance is given by

$$\frac{N(He)}{N(H)} = \frac{N(He^+ + He^{+2})}{N(H^+)}. \tag{4.18}$$

From these values it is possible to correct for the higher ionization stages of oxygen,

which are not usually available, as follows:

$$\frac{N(\mathrm{O})}{N(\mathrm{H})} = \frac{N(\mathrm{He}^{+}+\mathrm{He}^{+2})}{N(\mathrm{He}^{+})}\,\frac{N(\mathrm{O}^{+}+\mathrm{O}^{+2})}{N(\mathrm{H}^{+})}$$

$$= i_{\mathrm{cf}}(\mathrm{O})\,\frac{N(\mathrm{O}^{+}+\mathrm{O}^{+2})}{N(\mathrm{H}^{+})}. \tag{4.19}$$

Equation (4.18) breaks down for objects with a very low degree of ionization which have a considerable fraction of He^0 inside the H^+ region. To estimate the He^0 amount in a given PN we need observations along different lines of sight, or a sophisticated ionization structure model.

Ionization correction factors have been proposed for other elements, nevertheless many of them are density dependent and have been of limited use.

4.2.2. Ionization structure models. Photoionization models have been used to estimate the ionization correction factors for unobserved ions. To construct a model we require: (a) atomic data to determine the ionization equilibrium at each point, (b) the integrated electron temperature, (c) line emissivities, (d) the gaseous density distribution, (e) the stellar ionizing flux distribution and (f) the dust distribution and its absorbing properties. The data for ionization cross sections and recombination probabilities can be obtained from Chapman and Henry (1971, 1972), Reilman and Manson (1979), Gould (1978) and the compilation by Osterbrock (1989). The data for charge transfer reactions and dielectronic recombinations can be obtained from Butler and Dalgarno (1980), Butler *et al* (1980) and Nussbaumer and Storey (1983, 1984). The data for transition probabilities and collision strengths have been summarized by Mendoza (1983).

There are several sets of stellar atmosphere fluxes available: the LTE models by Hummer and Mihalas (1970) and the NLTE models by Husfeld *et al* (1984) and by Clegg and Middlemass (1987). Unfortunately the observed properties of the central stars and the degree of ionization of the nebulae predicted by these models often do not match the observations. For example the stellar temperatures and gravities derived by Méndez *et al* (1981, 1988) for NGC 1535 and NGC 4361 were used together with ionization structure models by Adam and Koppen (1985) and Torres-Peimbert *et al* (1990) to try to fit the observed line intensities. These authors were not able to fit the observed nebular ionization structures, to obtain agreement they found that the stellar flux beyond 54.4 eV had to be significantly higher than those of the model atmosphere fluxes available.

On the other hand the model atmosphere fluxes by Clegg and Middlemass (1987) for stars with very different gravities and effective temperatures, but similar ratios of H^0 to He^+ ionizing photons, produce very similar ionization structures and consequently similar i_{cf} values, which implies that if the strong lines of H^0, He^0, He^+, O^+ and O^{+2} are fitted by the photoionization models the i_{cf} for the other elements are almost independent of the stellar atmosphere adopted (e.g. Torres-Peimbert *et al* 1990).

4.2.3. Accuracy of the abundance determinations. The accuracy of the ionic abundances is determined by the accuracy of the line intensities and of the atomic parameters, the relevant line intensities and atomic parameters are not only those that correspond to the ion in question but also those that are needed to determine the distributions of the electron temperature and of the electron density. The errors vary from ion to ion and from object to object. For the best observed PN the accuracy of the ionic concentrations relative to H^+ is better than 0.04 dex for He^+ and He^{+2}, 0.1 dex for N^+, O^+, O^{+2},

Ne^{+2}, S^{+} and Ar^{+2} and 0.2 dex for C^{+}, C^{+2}, Ne^{+3}, Ne^{+4}, S^{+2}, Ar^{+3} and Ar^{+4}; similarly the accuracy of the total abundances relative to H is better than 0.04 dex for He, 0.1 dex for O, 0.15 dex for N and Ne and 0.2 dex for C, Ar and S.

5. Classification of planetary nebulae

5.1. Types of PN

From the range in kinematical properties, galactic distribution, chemical composition and mass of the shell it follows that the progenitors of PN range from population I to extreme population II objects. That is, the masses of the progenitor stars range from a few solar masses to less than one solar mass. In this review we will follow Peimbert's (1978) classification, which divides PN into four types: type I He-N rich; type II (disk or intermediate population); type III (high velocity) and type IV (halo population). From a variety of arguments related to stellar dynamics and stellar evolution it seems that this scheme is not only a chemical composition classification but that it corresponds to progenitor stars of different initial or main sequence masses M_i, with the following approximate values: type I $(2.4\text{-}8)M_\odot$, type II $(1.2\text{-}2.4)M_\odot$, type III $(1\text{-}1.2)M_\odot$ and type IV $(0.8\text{-}1.0)M_\odot$. Faúndez-Abans and Maciel (1987a) have divided type II PN into types IIa and IIb and Maciel (1989) has suggested that PN in the bulge of the Galaxy be called type V. Other classifications have been proposed by Greig (1971, 1972), Kaler (1983b), Heap and Augensen (1987), Balick (1987) and Amnuel *et al* (1989).

As mentioned before, the M_i values are in the 0.8–8 $M_\odot$ range; alternatively, after the envelope ejection most PN central stars have M_c values in the 0.54–0.8 $M_\odot$ range. The difference between M_i and M_c for each object varies from about 0.3 to a few solar masses, part of the difference is due to mass loss during the red giant stage and the rest is due to the mass of the PN shell. The shell masses range from $\sim 0.02\ M_\odot$ for extreme type IV PN to $\sim 1\ M_\odot$ for the most extreme type I PN. In optically thin PN all the shell mass is ionized while in optically thick PN a considerable fraction of the shell mass is in the form of H^0, He^0 and H_2.

Classifications based on chemical abundances depend on the quality of the abundance determinations, particularly for borderline objects between types I and II and between types IIa and IIb.

5.1.1. Type I PN. PN of type I have been defined as those objects with $N(He)/N(H) \geq 0.125$ or $\log N(N)/N(O) \geq -0.3$ (Peimbert 1978, Peimbert and Torres-Peimbert 1983), average abundances have been presented in table 6. Most He-N rich PN are very filamentary and show a bipolar structure (Greig 1971, 1972, Peimbert and Torres-Peimbert 1983, Kaler 1983b); this shape has been given several names: B, bipolar, binebulous, or hourglass. Moreover, in general their spectra present very strong forbidden lines ranging from [O I], [N I], and [S II] up to [Ne V].

Based on morphological arguments, Greig (1971, 1972) divided PN into four main classes: A (annular), B (binebulous), C (centric, surface brightness increases toward the centre) and E (egg shaped). There is a strong overlap between type I PN and class B PN. Different kinematical and galactic distribution studies have shown that class B (Greig 1972, Cudworth 1974) and type I objects (Acker 1980, 1983, Dutra and Maciel 1990) as a group correspond to more massive stellar progenitors than the other types of PN.

Table 6. Chemical abundances of galactic PN, the Sun and the Orion nebula, given in $12+\log N(X)/N(H)$.

Object	He	C	N	O	Ne	Ar	Reference
Type I PN	11.13	8.4-9.1	8.55	8.65	8.00	—	1
Type II PN	11.04	8.3-9.1	8.15	8.70	8.10	6.60	2, 3
Type III PN	11.04	—	8.00	8.40	7.80	—	4, 5
Sun	—	8.67	7.99	8.92	8.03	6.69	6, 7, 8
Orion nebula	11.01	8.57	7.68	8.65	7.80	6.65	9, 10, 11
Population I	11.01	8.62	7.84	8.75	7.98	6.65	12

1. Peimbert and Torres-Peimbert (1987a)
2. Torres-Peimbert and Peimbert (1977)
3. Aller and Czyzak (1983)
4. Barker (1978)
5. Maciel (1990)
6. Lambert (1978)
7. Lambert and Luck (1978)
8. Meyer (1985)
9. Peimbert and Torres-Peimbert (1977)
10. Torres-Peimbert *et al* (1980)
11. Peimbert (1982)
12. The present paper

There are a few type I PN for which estimates of the mass of the progenitor in the main sequence, M_i, are reported in the literature. From the assumption that NGC 2818 belongs to the galactic cluster of the same name, Peimbert and Serrano (1980) and Dufour (1984a) estimate M_i to be $2.2\pm0.3\ M_\odot$. NGC 2346 has a binary nucleus with a current orbital separation of $38\ R_\odot$; from the assumption that a common envelope event has been responsible for NGC 2346, Iben and Tutukov (1989) estimate that M_i was between 2 and $3\ M_\odot$ (see also Calvet and Peimbert 1983). Based on the increase in brightness (0.06 mag year^{-1}), the mass in the molecular shell ($\geq 2\ M_\odot$), and the mass of the central star ($M_c \sim 0.8\ M_\odot$), Kwok and Bignell (1984) estimate that $M_i \geq 3\ M_\odot$ for GL 618.

Several authors have found that, in general, central stars of type I PN lie on higher-mass tracks in the HR diagram than the central stars of other PN (Kaler 1983a, Pottasch 1983, 1989, Gathier and Pottasch 1985, Kaler and Jacoby 1989, 1990, Kaler *et al* 1990, Stasinska and Tylenda 1990); this result implies higher M_i values for type I PN than for other objects (see figure 9).

Sabbadin (1986a) finds that B nebulae spend most of their life as optically thick, whereas C nebulae spend most of their life as optically thin; this result supports the idea that B nebulae have higher-mass progenitors than C nebulae. Amnuel *et al* (1989) based on morphological, kinematic and other characteristics have classified PN in three groups: (a) massive, (b) intermediate mass and (c) low mass. There is a very strong overlap between type I PN and those classified as massive PN by Amnuel *et al*.

5.1.2. Type II PN. PN of type II are defined by the following properties: $N(He)/N(H) < 0.125$, $\log N(N)/N(O) < -0.3$, $\log N(O)/N(H) > -3.9$, $|\Delta v_{pr}| < 60\ km\ s^{-1}$, and $|z| < 0.8$ kpc, where $|v_{pr}|$ is the peculiar radial velocity relative to the galactic rotation curve and z is the distance away from the galactic plane. About 80% of the well studied PN of the solar vicinity belong to this group. Chemical abundances for large groups of

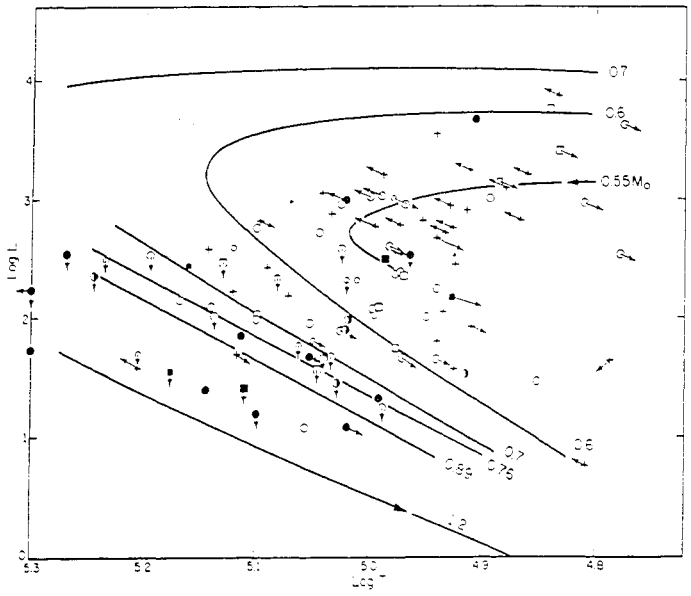

Figure 9. PN central stars on the log L–log T plane from Kaler *et al* (1990). *Filled symbols*: N/O ≥ 0.8, or He/H > 0.15; *half filled*: 0.8 > N/O ≥ 0.5; *open*: N/O < 0.5; *crosses*: no abundance data. *Solid curves*: evolutionary tracks from Wood and Faulkner (1986) for $\phi = 0.5$, mass loss core A, except for $M_c = 1.2\ M_\odot$, which is from Paczynski (1971).

type II PN are present in the literature (e.g. Torres-Peimbert and Peimbert 1977, Kaler 1979, Aller and Czyzak 1983, Aller and Keyes 1987), average abundances are presented in table 6. PN of the solar neighbourhood have an average height above the galactic plane of 150 pc, which corresponds to progenitors of $M_i = 1.5\ M_\odot$ (Osterbrock 1973); these values are typical of intermediate population I stars.

Faúndez-Abans and Maciel (1987a) have divided type II PN in two subtypes: type IIa are those with log $N(\mathrm{N})/N(\mathrm{H}) \geq -4.0$ and type IIb are those with log $N(\mathrm{N})/N(\mathrm{H}) < -4.0$. Dutra and Maciel (1990) find that the kinematic behaviour and the average z value of type IIa PN are intermediate between those of type I and type IIb PN.

5.1.3. Type III PN. Type III PN are defined by the following properties: $\Delta v_{pr} > 60\ \mathrm{km\ s^{-1}}$ and log $N(\mathrm{O})/N(\mathrm{H}) > -3.9$. Kaler (1970) has defined as Population II PN those objects with $\Delta v_{pr} > 60\ \mathrm{km\ s^{-1}}$ or $z > 0.8$ kpc. Barker (1978) studied 22 PN that fit Kaler's definition for population II, most of them are type III PN and their average abundances are presented in table 6.

5.1.4. Type IV PN. Type IV PN or halo PN are defined by having log $N(\mathrm{O})/N(\mathrm{H}) \leq -3.9$, very often they show $\Delta v_{pr} > 60\ \mathrm{km\ s^{-1}}$ and $z > 0.8$ kpc. There are eight known objects including a borderline case. Their abundances are presented in table 7; typical errors are 0.03 dex for He, 0.1 dex for O and less than 0.2 dex for the other elements. The prototype is K648, a PN in the globular cluster M15, with $M_i \sim 0.8\ M_\odot$ and $M_{shell} \sim 0.02\ M_\odot$ (O'Dell *et al* 1964, Peimbert 1973). For NGC 4361: $M_c \sim 0.55\ M_\odot$ and $M_{shell(FL)} \sim 0.07\ M_\odot$ (Méndez *et al* 1988, Torres-Peimbert *et al* 1990).

Table 7. Chemical abundances of type IV PN, given in $[X/H] = \log(X/H) - \log(X/H)_{pop I}$.

Object	He	C	N	O	Ne	Ar	Reference
K648	−0.01	+0.08 (rec)	−1.34	−1.05	−1.28	−2.35	1, 2, 3
BB-1	−0.03	+0.47 (rec)	+0.50	−0.85	+0.02	−2.05	1, 4
H4-1	−0.02	+0.69 (rec)	−0.09	−0.35	−1.28	−1.95	1, 2
NGC 4361	+0.01	+0.66 (rec)	−0.48	−0.92	−0.41	−0.74	5
NGC 2242	−0.01	−0.23 (coll)	−0.12	−0.72	−0.20	−0.76	5
DDDM-1	−0.01	<−1.52 (coll)	−0.44	−0.65	−0.68	−0.85	6, 7
PRMG-1	−0.05	—	—	−0.65	−0.68	−0.85	8
PRTM-1	+0.03	<−1.02 (coll)	<+0.16	−0.35	−0.08	−0.45	9

1. Barker (1980)
2. Torres-Peimbert and Peimbert (1979)
3. Adams *et al* (1984)
4. Torres-Peimbert *et al* (1981)
5. Torres-Peimbert *et al* (1990)
6. Clegg *et al* (1987)
7. Barker and Cudworth (1984)
8. Peña *et al* (1989)
9. Peña *et al* (1990)

5.1.5. Extremely inhomogeneous PN. A30 and A78 show inner regions that are extremely H underabundant, while the outer regions are normal (Jacoby 1979, Hazard *et al* 1980, Jacoby and Ford 1983, Manchado *et al* 1988). The abundances of the most contaminated inner regions of A30 and A78 are presented in table 8. The standard deviations for the abundances of A30 amount to ~0.14 dex; the C abundances were derived from the C^{+} λ4267 line.

5.1.6. Galactic bulge PN. Galactic bulge PN are important for the study of general properties of the bulge: dynamics, star formation history and chemical evolution. Moreover, they are also important for comparing the luminosity of their central stars with stellar evolution predictions since the distance to the bulge is well known. Dust obscuration makes the study of bulge PN in the visual region very difficult. Several recent studies have been made to detect new PN in the galactic bulge (e.g. Kinman *et al* 1988, Pottasch *et al* 1988, Ratag *et al* 1990).

Webster (1988) has studied 65 PN toward, and probably in, the galactic bulge. She obtained He/H, O/H and N/O abundance ratios for 49 of them. Between 10 and 20 per cent of the sample are type I PN, providing evidence for a young component of

Table 8. Chemical abundances of A30 and A78, given in $12 + \log N(X)/N(H)$.

Object	He	C	N	O	Ne	Reference
Abell 30, 3	12.99	11.89	9.14	9.32	8.83	1
Abell 30	12.95	11.96	9.93	9.63	—	2
Abell 78	12.78	<11.73	9.19	9.89	9.52	1
Abell 78, 4	12.43	—	11.09	11.09	10.41	3

1. Jacoby and Ford (1983)
2. Peimbert (1983)
3. Manchado *et al* (1988)

the population of the galactic bulge. Most PN in the sample have O/H ratios similar to those of PN in the solar neighbourhood. Based on these observations Webster proposes that the star formation rate was high early in the history of the bulge and that afterwards it has become considerably smaller.

Webster (1988) also finds that M2-29 might be a type IV PN since its $N(O)/N(H)$ ratio is 2.8×10^{-5}. She also identifies in her sample a few super-oxygen-rich candidates that deserve further study.

5.2. Comparison of the observed abundances with those predicted by stellar evolution models

The evolution of the surface abundances of He, C, N and O for intermediate-mass stars during their asymptotic giant branch phase has been predicted by stellar evolution models (e.g. Iben 1975, Iben and Truran 1978, Becker and Iben 1979, 1980, Renzini and Voli 1981, Iben and Renzini 1983, Renzini 1984, Wood and Faulkner 1986). The abundances predicted by the models have been compared with observations by many authors (e.g. Kaler *et al* 1978, Peimbert 1981, 1984, 1985, Aller 1983, Kaler 1983b, Peimbert and Torres-Peimbert 1983, Torres-Peimbert 1984, Clegg 1985, Kaler and Jacoby 1989, 1990, Henry 1989, Kaler *et al* 1990).

In what follows we will briefly describe the evolutionary models by Renzini and Voli (1981) and the information derived from observational comparisons. The models consider two processes: (a) convective dredge ups, when the envelope convection extends inward mixing to the surface nuclearly processed material and (b) nuclear burning at the base of the convective envelope. Three dredge-up phases prior to the PN ejection have been considered. The first dredge-up corresponds to the inward penetration of the convective envelope when stars reach the red giant branch for the first time, during the H-burning shell phase, enhancing N at the expense of C. The second dredge-up occurs in stars with $M_i \geq 3\ M_\odot$, when following the ignition of the He-burning shell the convective envelope penetrates into the helium core, enhancing the N and He and reducing the O and C surface abundances. The third dredge-up occurs during the asymptotic giant branch (AGB) evolution and consists of one or several individual mixing episodes following each He-shell flash enhancing the He and C surface abundances. The evolution is greatly affected by two mass loss processes: the stellar wind during the AGB and the PN ejection.

The stellar structure computations by Renzini and Voli (1981) have been made considering two parameters: $\alpha = l/H$, the ratio of the mixing length to the pressure scale height, and η which multiplied by the Reimers' rate (1975) gives the mass loss rate during the AGB phase; the computations were made for $\eta = \frac{1}{3}$ and $\frac{3}{3}$ and $\alpha = 0$, 1, 1.5 and 2, with most of them for $\eta = \frac{1}{3}$ and $\alpha = 0$ and 1.5. It has been estimated semi-empirically that η is in the $\frac{1}{3}$–3 range and that for stars with $M_i < 2\ M_\odot$ it is in the $\frac{1}{3}$–$\frac{1}{2}$ range (e.g. Renzini 1984, Iben 1984, and references therein). The values of α and η are not well known and they may vary with stellar evolution stage, initial stellar mass and chemical composition.

5.2.1. Type I PN. The observed range of He/H values in type I PN is well accounted for by the theory and implies that these objects have progenitors with $M_i \geq 3\ M_\odot$. This result is in agreement with the other criteria that indicate that type I PN have the most massive progenitors. For PN with good abundance determinations the He/H and C/O observed values are in fair agreement with predictions for models with M_i in the 3–5 $M_\odot$ range with $0 < \alpha < 2$ and $\eta = \frac{1}{3}$; the exceptions are NGC 6302 (Aller *et al* 1981)

and N97 (Barlow *et al* 1983), which can be matched with models for $M_i \sim 8\ M_\odot$ with $\alpha \sim 2$, and $\eta = \frac{1}{3}$, which makes them the two well observed PN with the highest M_i values known. Gómez *et al* (1989) estimate an envelope mass of 0.75 $M_\odot$ for NGC 6302, again supporting the idea of a massive progenitor. In figure 10 a radio map of NGC 6302 is presented.

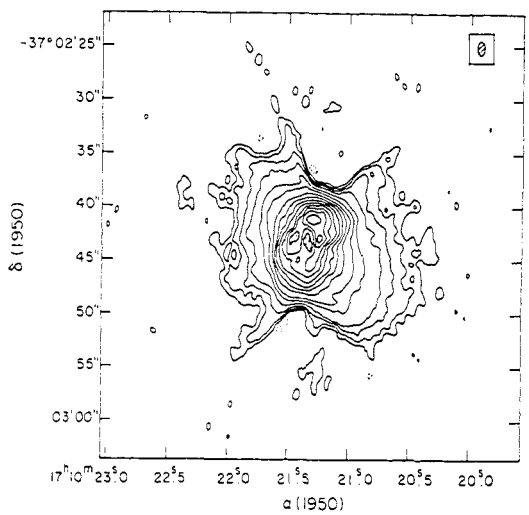

Figure 10. Continuum map at 6 cm of NGC 6302. The synthesized beam was 0.8×1.3 (arc sec) FWHM. The contour levels are: −0.003, 0.003, 0.005, 0.01, 0.02, 0.05, 0.1, 0.2, 0.3, 0.4, 0.5, 0.6, 0.7, 0.8 and 0.9 of the peak flux of 60 mJy per beam (Gómez *et al* 1989).

There is a well established positive correlation between the He/H and N/O ratios. This correlation implies that: (a) if $\eta = \frac{1}{3}$, α diminishes from 2 to 1 as M_i increases from ~3 to ~6 $M_\odot$ or (b) if $\alpha \sim 2$, η increases with M_i. From galactic chemical evolution considerations (Peimbert 1985) the second possibility is more likely.

There is an O/H versus N/O anticorrelation that seems to be real (Peimbert and Torres-Peimbert 1983, 1987a, Henry 1989, 1990, Kaler *et al* 1990) and which cannot be explained by the available models. The O depletion reaches factors of 2-3, while the most favourable theoretical models produce depletions of a factor of 1.4 (Renzini and Voli 1981, Renzini 1984). The O depletion increases with α and the highest depletion is obtained for the model with $\alpha = 2$, $\eta = \frac{1}{3}$ and $Z = 0.02$. It is possible to explain the O depletion with a larger value of α. It is also possible that part of the correlation could be due to an underestimate of the O/H abundance caused by shock wave enhancements of $\lambda 4363$ of [O III] but no models have been made to check this suggestion.

Models predict many more bright AGB stars ($M_{bol} \leq -6.0$) than observed in the Magellanic Clouds (e.g. Iben and Truran 1978, Renzini and Voli 1981, Iben and Renzini 1983, Renzini 1989, and references therein). It has been suggested that this discrepancy might be solved by a radiation pressure mechanism responsible for a rapid hydrodynamical ejection of the stellar envelope (Wood and Faulkner 1986, Renzini 1989). Renzini argues that this mechanism would limit the PN enrichment due to the third dredge-up phase, apparently in contradiction with the C/O > 1 values present in most PN of type I (Peimbert and Torres-Peimbert 1983, 1987a).

5.2.2. Type II and type III PN. The observed range of He/H values in type II PN is well accounted for by theory and implies that those objects have progenitors with $M_i < 3\ M_\odot$.

From the average C/H values it is possible to predict the average M_i value, which turns out to be somewhat higher than the average value derived from their galactic distribution. This result indicates that the third dredge-up phase is more efficient for low-mass stars than predicted by Renzini and Voli (1981); further theoretical developments indicate that this is the case (e.g. Iben and Renzini 1983), therefore the C/H and He/H predictions by Renzini and Voli (1981) for objects with $M_i < 3\ M_\odot$ should be used with caution (Renzini 1983).

There are well established positive correlations between the He/H and N/O ratios and the O/H and N/O ratios. These correlations are in agreement with a secondary production of N and with different initial He, C and N abundances produced by galactic chemical evolution and galactic abundance gradients.

5.2.3. Type IV PN. Of the seven halo PN with C/O abundance determinations, five of them show C/O > 1 (see table 7). These values are difficult to explain because AGB carbon stars are not found in globular clusters, nor are they predicted by current AGB models with $M_c \leq 0.6\ M_\odot$ (e.g. Renzini and Voli 1981, Iben and Renzini 1984). To explain C/O > 1 values, Renzini (1989) has proposed that these objects eject their envelope during one thermal pulse. Thermal pulses, also known as helium shell flashes, have often been regarded as possible triggers for the envelope ejection. The mass that could be ejected during one pulse peak for an object with $M_c = 0.54\ M_\odot$ is about $0.1\ M_\odot$, a value considerably larger than the envelope mass of K648 or NGC 4361. This implies that in type IV PN the envelope ejection may be possible during just a single thermal pulse. Moreover, the inhomogeneous model for NGC 4361 with C/O higher in the inner region (Torres-Peimbert *et al* 1990) and the strong C IV emission lines shown by the central star of NGC 4361 (Méndez 1989) agree with this suggestion.

5.2.4. Extremely inhomogeneous PN. A fraction of post AGB stars is expected to experience a final thermal pulse while descending along the white dwarf cooling track (Schönberner 1979, Iben and Renzini 1983, Iben *et al* 1983). It is thought that A30 and A78 might belong to this group.

6. Distances, masses and birth rates

Two of the main parameters searched for in the study of astronomical objects are their distances and their masses. The distances of PN are needed in order to: (a) compare the central stars of PN with theoretical evolutionary tracks in the HR diagram, (b) calculate the mass of the ionized shell, (c) estimate the number of PN in the galaxy and (d) determine the distances to other galaxies. Similarly the masses of PN are needed to: (a) constrain the mass loss models of asymptotic giant branch evolution, (b) study the chemical enrichment of the interstellar medium, (c) study the shell evolution, and (d) determine the scale for statistical distances.

6.1. Distances derived from individual properties

In the seventies only a handful of PN in the solar vicinity had direct distance determinations; at present the number has grown to about 50. For most objects in the solar

vicinity we only have distances based on statistical properties. A review of recent distance determinations has been given by Lutz (1989). In what follows we will mention the most important methods, not based on statistical arguments, that have been used to determine distances.

6.1.1. Binary stars and clusters. There are four binary PN nuclei with distance determinations based on the spectral type of the secondary star: NGC 246, NGC 1514, NGC 2346 and NGC 3132 (e.g. Minkowski 1965, Kohoutek 1967, Méndez 1975, Maciel and Pottasch 1980, Mallik and Peimbert 1988, and references therein). The distance to K648 has been determined under the assumption that it belongs to the globular cluster M15 (Peimbert 1973). The distance to NGC 2818 has been determined under the assumption that it belongs to the open cluster of the same name (Dufour 1984a, Pedreros 1989).

6.1.2. 21 cm absorption and emission. Gathier *et al* (1986a) have derived distances for 12 PN based on 21 cm observations: (a) in absorption in the direction of the PN, (b) in absorption of background sources within 1 degree of the PN and (c) in emission in directions close to the PN. They combined these observations with information on the galactic rotation curve and on nearby H II regions to determine the distances, the estimated accuracies are in the 0.12–0.25 dex range.

6.1.3. Visual extinction. It is possible to construct extinction versus distance diagrams by measuring the visual extinction of many stars with known distance in directions near a given PN. From a well behaved relation between extinction and distance it is possible to estimate the distance to the PN by measuring its extinction. The method was pioneered by Lutz (1973), and has been used by several authors (Kaler and Lutz 1985, Maciel 1985, Maciel *et al* 1986). Probably the most precise set of determinations based on this method was made by Gathier *et al* (1986b), who determined distances to 12 PN with estimated accuracies in the 0.04–0.18 dex range.

6.1.4. Expansion and radial velocity. By comparing radial velocities of expansion, determined spectroscopically, with measured angular expansions it is possible to estimate distances. The angular expansion is determined by comparing the position of knots, filaments, edges, and other features on two different epochs (e.g. Liller *et al* 1966, Masson 1986). This method is expected to provide reliable results for optically thin objects. For optically thick objects it provides only a lower limit to the distance because the size of the ionized region increases not only due to gas expansion but also due to the advance of the ionization front into the external neutral shell and the inner neutral pockets. The distances determined by this method are usually smaller than those determined by other methods (e.g. Maciel and Pottasch 1980, Méndez *et al* 1988), probably indicating that most of the objects to which this method has been applied are optically thick.

6.1.5. Central stars. It is possible to derive the distance to a PN from the intrinsic luminosity of the central star, since it depends on the surface gravity, g, and the effective temperature, $T_{\rm eff}$. The distance to the central star in pc is given by (Méndez *et al* 1988)

$$d^2 = 3.82 \times 10^{-11} \frac{M_* F_\infty}{g} 10^{(0.4 m_{\rm bol})} \qquad (6.1)$$

where $M_\odot$ is the mass of the star in solar units, F_* is the monochromatic model atmosphere flux at $\lambda 5480$ Å, in erg cm^{-2} s^{-1} cm^{-1}, g is the surface gravity in cm s^{-2} and $m_0(V)$ is the apparent visual magnitude corrected for reddening. F_* depends strongly on $T_{\rm eff}$. From high-dispersion spectra of the central stars and model atmospheres it is possible to derive g and $T_{\rm eff}$. Combined errors of 0.04 dex in $T_{\rm eff}$ and 0.2 dex in g produce an error of 0.08 dex in the distance. Based on this method, Méndez *et al* (1988) have derived distances for 22 PN.

6.2. Masses

The ionized mass of a homogeneous density nebula made of H and He is given by

$$M(\mathrm{RMS}) = (1+4y)m_{\rm H}\int \frac{N_{\rm e}(\mathrm{RMS})}{(1+x)}\,\mathrm{d}V \tag{6.2}$$

where $y = N(\mathrm{He})/N(\mathrm{H})$, $x = N(\mathrm{He}^+)/N(\mathrm{H}^+) + 2N(\mathrm{He}^{+2})/N(\mathrm{H}^+)$. The factor $1/(1+x)$ denotes the contribution of helium to the electron density per hydrogen atom (see equation (3.8)), and $m_{\rm H}$ is the mass of the H atom. For a spherical PN of radius R, equation (6.2) can be written as

$$M(\mathrm{RMS}) = \frac{(1+4y)}{(1+\bar{x})}\, m_{\rm H}\tfrac{4}{3}\pi R^3 N_{\rm e}(\mathrm{RMS}) \tag{6.3}$$

where $\bar{x}$ is the average value within the ionized volume. The linear size is related to the observed angular size in arc sec, ϕ, by

$$R(\mathrm{pc}) = \frac{\phi(\mathrm{arc\ sec})d(\mathrm{pc})}{206265}. \tag{6.4}$$

Compilations of angular sizes can be found in the catalogue by Perek and Kohoutek (1967) or in the list by Cahn and Kaler (1971).

It is well known that PN are not homogeneous in density; in general they present complex density structures with cavities, shells, knots, filaments, etc. For non-homogeneous nebulae, $M(\mathrm{RMS})$ corresponds to an upper limit to the real mass. To derive a more realistic mass it can be assumed that a fraction ε of the volume is filled with dense material and that the remainder of the volume is empty. The density of the dense material is expected to be the one derived from the forbidden line ratios, $N_{\rm e}(\mathrm{FL})$. Therefore the total mass in the nebula is given by

$$M(\mathrm{FL}) = \frac{(1+4y)}{(1+\bar{x})}\, m_{\rm H} V_{\rm T}\varepsilon N_{\rm e}(\mathrm{FL}) \propto V N_{\rm e}(\mathrm{FL}). \tag{6.5}$$

Similarly, from equations (3.7)–(3.9) we have

$$I(\mathrm{H}\beta) \propto V_{\rm T}\varepsilon N_{\rm e}^2(\mathrm{FL})/d^2 \propto V N_{\rm e}^2(\mathrm{FL})/d^2. \tag{6.6}$$

From equations (6.5) and (6.6) it follows that

$$M(\mathrm{FL}) \propto I(\mathrm{H}\beta)d^2/N_{\rm e}(\mathrm{FL}) \tag{6.7}$$

therefore, $M(\mathrm{FL})$ can be derived independently of the filling factor and the assumed geometry (Barlow 1987). Alternatively $M(\mathrm{RMS})$ depends on the geometry and the filling factor, from equations (6.3), (6.5) and (3.9) it follows that

$$M(\mathrm{FL}) = \varepsilon^{1/2} M(\mathrm{RMS}). \tag{6.8}$$

Only a small fraction of the PN have reliable N_e(FL) and N_e(RMS) determinations; consequently, ε values have been derived for only a few PN and most authors have *adopted an average* ε value, usually in the 0.6–0.8 range, for large samples of PN (e.g. O'Dell 1962, Cahn and Kaler 1971, Maciel and Pottasch 1980, Daub 1982, Gathier *et al* 1986a, b, Méndez *et al* 1988). In all the cases where M(FL) values are given, it is possible to derive the corresponding M(RMS) values by means of equation (6.8).

A list of 35 PN with distances derived by direct methods and with individual ε and M(FL) determinations has been presented by Mallik and Peimbert (1988); the M(FL) values vary from $\sim 0.005\ M_\odot$ to $0.3\ M_\odot$ and the ε values vary from 0.01 to 1, with almost half of the sample having ε values smaller than 0.16. These ε values are considerably smaller than the average value adopted in most papers.

For optically thick PN the M(RMS) and M(FL) values are lower limits to the total PN mass because the neutral and molecular components have not been considered. The presence of a neutral and a molecular component can be established by studying: (a) the variation of the degree of ionization with r, (b) the presence of the 21 cm hyperfine transition of H I in absorption and (c) the presence of molecules (e.g. Rodríguez 1989 and references therein).

The envelope masses derived for type IV PN are smaller than those derived for other types of PN, in agreement with the idea that the progenitors of type IV PN had lower masses in the main sequence (e.g. Peimbert 1973, Adams *et al* 1984, Mallik and Peimbert 1988, Torres-Peimbert *et al* 1990).

6.3. Relation between mass and radius

From observations of large samples of PN, several authors have obtained relations between masses and radii of the type

$$M(\mathrm{RMS}) \propto R^{\gamma} \tag{6.9}$$

(see table 9). Moreover, Kwok (1985), using a method based on evolution models of central stars of PN by Schönberner (1983), has obtained that $M(\mathrm{RMS}) \propto R^{5/2}$. Mallik and Peimbert (1988), based on observations of 35 PN, have obtained that

$$M(\mathrm{FL}) \propto R^{1.02 \pm 0.15} \tag{6.10}$$

$$\varepsilon \propto R^{-0.91 \pm 0.18} \tag{6.11}$$

(see figure 11). Other authors, basing their estimates on large samples of PN, have also obtained ε values which decrease with increasing R (Torres-Peimbert and Peimbert

Table 9. Exponent γ for the mass-radius relation given by $M \propto R^{\gamma}$.

R range (pc)	ε range	γ (FL)	γ (RMS)	Reference
0.01–0.33	1.0	—	1.43 ± 0.09	Pottasch (1980)
0.007–0.066	1.0	—	1.47 ± 0.12	Gathier *et al* (1983)
0.004–0.96	1.0	—	2.46	Phillips and Pottasch (1984)
0.032–0.27	1.0	—	1.88	Phillips and Pottasch (1984)
0.004–0.12	0.01–1.0	1.21 ± 0.10	—	Daub (1982)
0.01–0.56	0.01–1.0	1.02 ± 0.15	—	Mallik and Peimbert (1988)

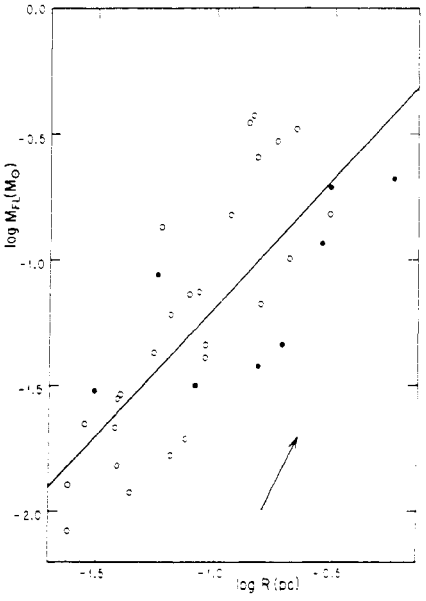

Figure 11. Plot of mass as a function of radius for PN with scale-independent distances (Mallik and Peimbert 1988). *Filled circles*: type I PN; *open circles*: the rest. The arrow indicates the change in mass if an object is 1.4 times farther away than assumed.

1977), Daub 1982, Amnuel *et al* 1984).

From equation (6.9) and the following relations:

$$M(\mathrm{RMS}) \propto N(\mathrm{RMS}) R^3 \tag{6.12}$$

$$E(\mathrm{H}\beta) \propto N^2(\mathrm{RMS}) R^3 \propto Q(\mathrm{H}^0) \tag{6.13}$$

where $E(\mathrm{H}\beta)$ is the total emitted flux in $\mathrm{H}\beta$ and $Q(\mathrm{H}^0)$ is the number of hydrogen ionizing photons per unit time (see equation (2.9)), it follows that

$$Q(\mathrm{H}^0) \propto \frac{M^2(\mathrm{RMS})}{R^3} \propto R^{2\gamma-3} \tag{6.14}$$

which implies that $Q(\mathrm{H}^0)$ is independent of R for $\gamma = 1.5$.

Notice that the derived value of $Q(\mathrm{H}^0)$ is also independent of R if $\rho^{-1/2} M(\mathrm{FL}) \propto R^{3/2}$ (equations (6.8), (6.9), (6.12) and (6.13)).

6.4. Distances derived from statistical properties

Since only a small fraction of PN in the solar vicinity have distance determinations based on individual characteristics, the so-called direct distance determinations, it has been the aim of many investigators to find a good distance scale that can be applied to all PN. This distance scale is based on the assumption that a general property has the same value for a set of PN or that a general relationship holds for a set of PN.

6.4.1. Assumption of constant mass. The Shklovsky (1956) method (see also Minkowski and Aller 1954) applies to optically thin PN, those that are completely ionized, and is

based on the assumption that the ejected mass is the same for all objects. This method has been used extensively to determine distances to PN (e.g. O'Dell 1962, 1963, 1968, Seaton 1966, 1968, Webster 1969, Cahn and Kaler 1971, Osterbrock 1973, Cudworth 1974, Milne and Aller 1975, Acker 1978, Khromov 1979, Schneider and Terzian 1983).

From equations (3.7), (6.4) and (6.5) it follows that the distance is given by

$$d = \left[\frac{3}{16\pi^2}\frac{\alpha(\mathrm{H}\beta)h\nu(\mathrm{H}\beta)}{m_{\mathrm{H}}^2}\frac{(1+\bar{x})}{(1+4y)^2}\right]^{1/5} M(\mathrm{FL})^{2/5}\varepsilon^{-1/5}\phi^{-3/5}I(\mathrm{H}\beta)^{-1/5}$$
$$= KM(\mathrm{FL})^{2/5}\varepsilon^{-1/5}\phi^{-3/5}I(\mathrm{H}\beta)^{-1/5} \qquad (6.15)$$

where K depends weakly on T_e and the He/H abundance ratio. Equation (6.15) can also be written as

$$d = KM(\mathrm{RMS})^{2/5}\phi^{-3/5}I(\mathrm{H}\beta)^{-1/5}. \qquad (6.16)$$

Two calibrations of equation (6.15) have been widely used: Seaton's (1968) based on Webster's (1969) observations of PN in the Magellanic Clouds and employed in the extensive study by Cahn and Kaler (1971) (hereafter to be referred to as the S distance scale) and Cudworth's (1974) based on statistical parallaxes (hereafter to be referred to as the C distance scale). The S distance scale is a factor of 1.47 smaller than the C distance scale. In many applications of this method it has been assumed that objects with $R \geq 0.08$ pc are optically thin and those with $R \leq 0.08$ pc are optically thick.

From the C distance scale it follows that

$$d(\mathrm{pc}) = 108\,\phi^{-3/5}I(\mathrm{H}\beta)^{-1/5}. \qquad (6.17)$$

Under the assumptions that $\langle T_e\rangle = 10\,000$ K, $\langle y\rangle = 0.11$ and $\langle\bar{x}\rangle = 0.13$, equation (6.16) implies that $\langle M(\mathrm{RMS})\rangle = 0.42\,M_\odot$. Similarly, from the S distance scale it follows that $\langle M(\mathrm{RMS})\rangle = 0.16\,M_\odot$.

There are two problems with the Shklovsky method that render the distances derived from equation (6.16) very uncertain: (a) the assumption that the ejected mass is the same for all objects is not valid since values of $M(\mathrm{RMS})$ for individual shells of PN vary from a few hundredths of a solar mass for type IV PN to almost one solar mass for the most massive PN, (b) the method applies to optically thin PN while recent results have shown that most PN in the solar vicinity are optically thick with R values as high as 0.6 pc (Pottasch 1980, Phillips and Pottasch 1984, Gathier 1987, Mallik and Peimbert 1988, Pottasch 1989, Amnuel *et al* 1989). For a given PN, equation (6.16) could yield errors in the distance determination as high as a factor of 4.

Molecules have been detected in many PN that were classified as optically thin based on their large R values; the presence of molecules indicates that these PN are optically thick in at least some directions. For example, Zuckerman and Gatley (1988) have detected H_2 molecules in NGC 6720 and NGC 6853 (see figures 1 and 2), these PN have R values of 0.23 and 0.21 pc, respectively and had been classified as optically thin (e.g. Cudworth 1974).

6.4.2. Assumption of a constant ionizing flux. For optically thick objects it can be assumed that the number of H ionizing photons per unit time, $Q(\mathrm{H}^0)$, is the same for all objects (Zanstra 1931, Vorontsov-Velyaminov 1934, Minkowski 1965). Therefore from equations (2.9) and (3.7) it follows that

$$d = \left[\frac{Q(\mathrm{H}^0)}{4\pi I(\mathrm{H}\beta)}\frac{\alpha(\mathrm{H}\beta)}{\alpha_{\mathrm{B}}}h\nu(\mathrm{H}\beta)\right]^{1/2}. \qquad (6.18)$$

Cudworth (1974) calibrated equation (6.18) based on statistical parallaxes and for objects with $R \leq 0.07$ pc found that

$$d(\mathrm{pc}) = 0.0178\, I(\mathrm{H}\beta)^{-1/2}. \tag{6.19}$$

This calibration is in very good agreement with the earlier calibration by Minkowski (1965). Acker (1978) has also used this method extensively.

Milne (1982) used this method for a sample of PN observed in radio continuum, the observed flux is due to free-free emission which is proportional to the hydrogen recombination flux; he calibrated the radio continuum analogue of equation (6.18) with the distances by Cudworth (1974) and Acker (1978). The distances found by Acker are closer to the S distance scale than to the C distance scale.

Based on a sample of PN with individual distance determinations, Mallik and Peimbert (1988) obtained, for objects in the $0.02 \leq R \leq 0.3$ pc range, the following equation:

$$d(\mathrm{pc}) = 0.0171\, I(\mathrm{H}\beta)^{-1/2} \tag{6.20}$$

in very good agreement with the determination by Cudworth (1974).

Figure 12 presents a plot of $E(\mathrm{H}\beta)$ as a function of R for the distance-independent sample of Mallik and Peimbert (1988); filled circles denote type I PN, open circles the rest. Also this figure presents: (a) the distance scale proposed by Mallik and Peimbert for objects in the $0.02 \leq R(\mathrm{pc}) \leq 0.3$ range, (b) the optically thick distance scale by Cudworth (1974) for $R \leq 0.07$ pc and (c) the optically thin distance scale by Cudworth (1974) for $R > 0.07$ pc. The two largest objects in figures 11 and 12 are NGC 2818 and NGC 7293; the presence of molecules in these PN (Storey 1984) indicates that they are not optically thin in all directions and have not been so in the past. The optically thin distance scale by Cudworth (1974) might yield the proper distance for some large nebulae, not because they are optically thin but because their central star is fading, as it is in the case of NGC 7293 (Méndez *et al* 1988). For any given object the error produced by applying equation (6.20) could be as large as a factor of three, but in

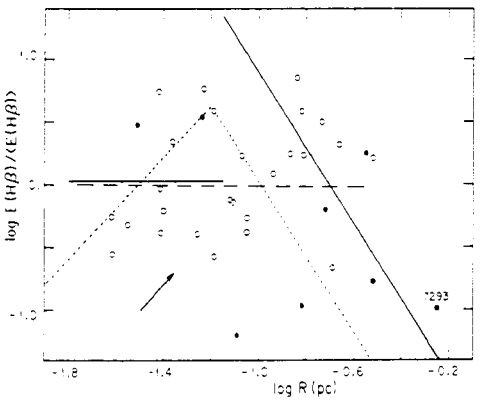

Figure 12. Plot of log $E(\mathrm{H}\beta)$ against log R for the scale-independent sample (Mallik and Peimbert 1988). *Solid horizontal line* and *solid diagonal line*: optically thick and optically thin distance scales, respectively, by Cudworth (1974); *broken horizontal line*: distance scale by Mallik and Peimbert (1988); *dotted diagonal lines*: predicted behaviour by Kwok (1985, 1987). The arrow indicates the displacement of any given point if its distance is increased by a factor of 1.4.

general it will be smaller than a factor of two, which amounts to a difference of 0.6 in the log $E(H\beta)$ value of figure 12.

The spread in masses and $E(H\beta)$ values for a given R in figures 11 and 12 is probably real and could be due to an additional parameter, such as the mass of the central star (Mallik and Peimbert 1988, Maciel 1989, Pottasch 1989).

6.4.3. Assumption of a relationship between mass and radius. Maciel and Pottasch (1980) and Pottasch (1980) developed a method for determining distances to optically thick PN based on an empirical ionized mass to nebular radius relation. Maciel (1981a, b, 1984), Daub (1982), Phillips and Pottasch (1984) and Amnuel *et al* (1984) have also used this method to derive distances to a large number of PN. Each group obtains different distance scales due to differences in their assumptions; the most important differences are: (a) the proportionality constant in equation (6.9), (b) the value of the exponent γ in equation (6.9) and (c) the range of R values for which the method has been used.

The relations between mass and radius found by Pottasch (1980), Gathier *et al* (1983), and Mallik and Peimbert (1988) indicate that $Q(H^0)$ does not vary systematically with R, but variations of an order of magnitude in $Q(H^0)$ for a given R value are present, see figure 12, where $E(H\beta)$ is proportional to $Q(H^0)$. The relation $M(\text{RMS}) \propto R^{5/2}$ derived by Kwok (1985, 1987) should be analysed further.

From equations (6.13) and (6.14) it is seen that if $\gamma = 2.5$ then $E(H\beta) \propto R^2$; i.e. the EM is constant for all objects (equation (3.10)). This implies that the surface brightness is independent of R, and consequently that it is not possible to derive distances based only on the surface brightness or the total observed flux.

In figure 12 we show the behaviour predicted by Kwok (1985, 1987) for $\gamma = 2.5$, which corresponds to $EM = 7.4 \times 10^6$ cm^{-6} pc for $R \leq 0.065$ pc. For $R > 0.065$ pc Kwok assumes that the PN are optically thin, with $M(\text{RMS}) = 0.16\, M_\odot$, which corresponds to $\gamma = 0.0$. From this figure it is clear that γ could be equal to 2.5 for $R \leq 0.065$ pc. Alternatively, for optically thick objects with $R > 0.065$ the $\gamma = 2.5$ solution provides a very poor fit to the observations.

Distance scales based on relations for surface brightness, $N_e(\text{FL})$ and $N_e(\text{RMS})$ as functions of R have been proposed in the literature (Amnuel *et al* 1984, 1989, Sabbadin *et al* 1984b, Phillips and Pottasch 1984, Mallik and Peimbert 1988). Since surface brightness, $N_e(\text{FL})$ and $N_e(\text{RMS})$ are related to the mass, these scales are equivalent to those derived from mass radius relations.

6.4.4. Scale factor. To compare different distance scales it is possible to introduce a relative scale factor, k, with the normalization $k = 1$ for Seaton's distance scale. In Table 10 we present the relative sizes for some of the most frequently used distance scales. For optically thin distance scales $k \propto M(\text{RMS})^{2.5}$. For optically thick distance scales k increases with R and an average value for $0.1 \leq R(\text{pc}) \leq 0.3$ is presented. If objects smaller than 0.1 pc are considered, the spread in k values is even larger (see Gathier 1987). In this comparison the $M(\text{RMS})$ values have been computed under the assumptions that $y = 0.11$, $\bar{x} = 0.13$ and $T_e = 10\,000$ K.

Weidemann (1977) proposed a scale factor of 1.3 (see table 10) to superimpose the observed nuclei of PN over the 0.6 $M_\odot$ track on the HR diagram and to lower the PN birth rate to a value compatible with the white dwarf birth rate. To reach agreement

Table 10. Comparison of distance scales for PN with $0.10 \leq R(\mathrm{pc}) \leq 0.30$.

$k = d/d_{\mathrm{Seaton}}$	$M(\mathrm{RMS})(M_\odot)$	Scale
1.55	—	Mallik and Peimbert (1988)
1.47	0.42	Cudworth (1974)
1.40	0.37	Schneider and Terzian (1983)
1.30	0.31	Weidemann (1977)
1.16	—	Maciel and Pottasch (1980)
1.00	0.16	Seaton (1968)
1.00	0.16	Cahn and Kaler (1971)
1.00	0.16	Milne and Aller (1975)
1.00	0.16	Acker (1978)
1.00	—	Gathier (1987)
0.95	0.14	Daub (1982)

with the lower white dwarf birth rates derived recently (see subsection 6.5) a similar argument to that of Weidemann would increase k by an even larger factor.

In spite of the many objects and their corresponding distances in common between the samples by Gathier (1987) and by Mallik and Peimbert (1988) there is a substantial difference between their scale factors (see table 10). The difference is due to two systematic effects: Mallik and Peimbert do not include in their sample the expansion distances determined by Liller *et al* (1966), which are smaller than those derived by other methods (see subsubsection 6.1.4) and include the distances determined by Méndez *et al* (1988), which are generally larger than those derived by other methods.

6.5. Birth rates

The determination of the local and galactic birth rates of PN are important in order to: (a) find out which is the fraction of the stars in the $0.8 \leq M_i(M_\odot) \leq 8$ range that undergo the PN phase (e.g. Tinsley 1978), and (b) to study the chemical enrichment of the interstellar medium.

6.5.1. Local birth rate. The local PN birth rate is given by

$$\dot{\rho} = \rho / \Delta t = \rho \langle v \rangle / (R_f - R_i) \tag{6.21}$$

where ρ is the density, in the solar vicinity, of PN with $R_i < R < R_f$, Δt is the time needed for R to increase from R_i to R_f, and $\langle v \rangle$ is the average velocity of expansion from R_i to R_f. Usually ρ is given in pc^{-3} and Δt in years.

In the optically thick phase $\langle v \rangle$ denotes the average velocity of the ionization front relative to the central star, v_{ion}; while in the optically thin phase $\langle v \rangle$ denotes the average velocity of expansion of matter, v_{exp}, given by the Doppler effect. The determinations of $\dot{\rho}$ have been carried out under the assumption that there is an interval in size $R_f - R_i$ where all PN are optically thin.

There are several sources of error associated with the use of equation (6.21) (see Phillips (1989) for a review). The main uncertainty is due to the adopted distance scale: since $\dot{\rho}$ is proportional to d^{-4} the $\dot{\rho}$ estimates vary, to a first approximation, like k^{-4} (see table 10). If we divide the distance scales into long, medium and short ($k \geq 1.4$, $1.3 \geq k \geq 1$, $k < 1$) the $\dot{\rho}$ values, in units of 10^{-12} $\mathrm{pc}^{-3}\,\mathrm{y}^{-1}$, are in the ranges 0.6-1, 2-3 and 4-6, respectively (Phillips 1989).

There are two factors that increase the birth rate estimates. While most investigators have used $\langle v_{exp} \rangle = 20\ km\ s^{-1}$, a careful study by Phillips (1989), primarily based on observations by Sabbadin *et al* (1983, 1984*a*, 1985, 1986) and Sabbadin (1984a, b, 1986b) yields $\langle v_{exp} \rangle = 26\ km\ s^{-1}$ for objects with $0.1 \leq R(pc) \leq 0.6$ and $25\ km\ s^{-1}$ for objects with $R \leq 0.6$ pc. As mentioned before (see subsubsection 6.4.1), most PN in the solar vicinity are optically thick, therefore in addition to the expansion of the shell, the ionized size increases further by the expansion of the ionized front into the neutral matter, consequently $\langle v_{ion} \rangle$ should be used instead of $\langle v_{exp} \rangle$ in equation (6.19). The measurement of angular expansions of PN with known distances could provide the direct determinations of v_{ion} which are needed to improve the birth rate estimates.

The $\dot{\rho}$(PN) values have often been compared with the white dwarf birth rate $\dot{\rho}$(WD). Recent results by Downes (1986) and Fleming *et al* (1986) yield $\dot{\rho}$(WD), in units of $10^{-12}\ pc^{-3}\ y^{-1}$, equal to 0.72 ± 0.25 and 0.62 ± 0.13, respectively; in very good agreement with the $\dot{\rho}$(PN) values derived from long distance scales (Alloin *et al* 1976, Phillips 1989).

It has been argued that $\dot{\rho}$(WD) should be increased to take into account those WD in binary systems. On the other hand it has been argued that $\dot{\rho}$(PN) does not include low-mass WD progenitors because the ejected nebula dissipates before the central star becomes hot enough to ionize it. The magnitude of these two effects is similar. Considering all the uncertainties involved, it can be concluded that $\dot{\rho}$(PN) and $\dot{\rho}$(WD) agree within a factor of 2 if a long distance scale is adopted.

6.5.2. Galactic birth rate. The galactic PN birth rate, $\dot{N}$, has been estimated by scaling the surface density birth rate of the solar vicinity to the overall galaxy, $\dot{N}$ is proportional to k^{-3}. Values of 0.5–1.5 PN per year have been derived for $\dot{N}$. As expected, the smaller values correspond to the longer k values (e.g. Phillips 1989 and references therein).

6.5.3. Total number of PN. The total number of PN in the Galaxy with $R \leq 0.6$ pc, N_T, has been derived by multiplying the galactic birth rate by the mean lifetime of a PN. N_T is proportional to k^{-2} and the values that have been determined are in the 10 000–30 000 range (Phillips 1989 and references therein).

7. Extragalactic planetary nebulae

Extragalactic PN allow us to study such properties of PN as: (a) the mass range of the progenitor stars based on their location and velocity distribution; (b) [O III] and Hα luminosity functions, and the masses of their envelopes, based on the common distance of the PN sample in a given galaxy; and (c) characteristics of stellar evolution models by comparing the chemical composition of the PN with that of the general interstellar medium. Moreover, extragalactic PN permit us to study properties of the host galaxy such as: (a) stellar death rate, (b) stellar mass return rate to the interstellar medium, (c) galactic chemical evolution, (d) mass distribution of the host galaxy, and (e) distance to the galaxy. Some results relevant to these problems will be discussed below.

Extragalactic PN are extremely faint and abundance determinations have been possible only for PN in Local Group galaxies, while for PN outside the Local Group only absolute fluxes in the [O III] 5007 line have been determined. These observations have been obtained with the largest telescopes and the best detectors available. Extragalactic PN will be prime targets for the new generation of large telescopes now under construction.

7.1. Magellanic Clouds

The Magellanic Cloud extragalactic planetary nebulae have been the most extensively studied PN, due to their proximity. Recent reviews on MC PN are those by Jacoby (1983), Peimbert (1984) and Barlow (1989).

7.1.1. [O III] luminosity function and number of PN. Jacoby (1980) was able to detect PN in the Magellanic Clouds (MC) spanning a range of 250 in their [O III] luminosity; he established an [O III] luminosity function and from it estimated that the total number of PN in the Small Magellanic Cloud (SMC) and in the Large Magellanic Cloud (LMC) with a limiting envelope size of $R \leq 0.64$ pc, are 285 ± 78 and 996 ± 253, respectively. The limiting envelope size comes from an expansion velocity of 25 km s^{-1} and a lifetime of 25 000 years.

Based on the MC PN luminosity function, Jacoby (1980) estimated that, for Local Group galaxies, the visual luminosity specific number is $6.1 \pm 2.2 \times 10^{-7}$ PN/$L_{\odot}$ and the mass specific number is $2.1 \pm 1.5 \times 10^{-7}$ PN/$M_{\odot}$, where the uncertainties are 1σ values derived from the averaging procedure.

7.1.2. Sizes and masses. Speckle interferometry has been used by Barlow *et al* (1986) and Wood *et al* (1986) to determine the diameter of bright compact PN in the MC. Wood *et al* (1987) used a direct imaging technique to determine the angular diameter of fainter and larger PN.

Wood *et al* (1986, 1987) determined M(RMS) values from the measured diameters and the observed $I(\mathrm{H}\beta)$ fluxes of 24 PN in the MC. From a plot of mass against radius they concluded that the PN become optically thin for $R > 0.12$ pc. For those objects with $R > 0.12$ pc they found that $\langle M(\mathrm{RMS})\rangle = 0.32\ M_{\odot}$, and $\langle M(\mathrm{FL})\rangle = 0.27\ M_{\odot}$ where they assumed that $\varepsilon = 0.7$ (see equation (6.8.)).

Barlow (1987) determined M(FL) values for 32 PN in the MC and was the first to show that the M(FL) values derived from $I(\mathrm{H}\beta)$ and N_e(FL) are independent of geometry and filling factor (equation (6.7)). For the 10 most dense objects, assumed to be optically thick, Barlow found that the average distance is $\langle d(\mathrm{pc})\rangle = 0.0332\ I(\mathrm{H}\beta)^{-1/2}$, which is about a factor of 2 larger than those derived from the calibrations by Cudworth (1974) for PN with $R \leq 0.07$ pc and by Mallik and Peimbert (1988) for PN in the $0.02 \leq R(\mathrm{pc}) \leq 0.3$ range (equations (6.19) and (6.20)). Nevertheless, there is a selection effect in favour of PN with large Hβ fluxes in the sample used by Barlow, therefore even if the difference in distance scales is significant it does not imply that the galactic distance scale should be revised.

From a plot of N_e(FL) against M(FL) Barlow (1987, 1989) concluded that the 12 PN with the lowest N_e(FL) values are optically thin and derived for them a mean mass $\langle M(\mathrm{FL})\rangle = 0.27 \pm 0.06\ M_{\odot}$. Moreover, by adopting $\varepsilon = 0.65$, and equation (6.8), Barlow derived, for this sample, $\langle M(\mathrm{RMS})\rangle = 0.33\ M_{\odot}$. This value corresponds to a distance scale factor, k, of 1.34. Nevertheless this k value is uncertain and should not be applied to galactic distances for two reasons: (a) ε might be considerably smaller than 0.65 (Mallik and Peimbert 1988), which would increase k, and (b) there is a selection effect in favour of PN with large Hβ fluxes; correcting for this effect would decrease k.

7.1.3. Chemical composition. There have been many abundance determinations for PN in the MC (e.g. Peimbert 1984 and references therein), some of the more recent ones are those by Aller *et al* (1987), Monk *et al* (1988), Peña and Ruiz (1988) and Henry *et al* (1989).

Table 11 presents the mean abundances of He, N, O and Ne for the PN samples by Monk *et al* (1988) and the mean abundances of C for the PN samples by Aller *et al* (1987), the mean values exclude type I nebulae, which are discussed below, and P25 of the sample by Aller *et al* which is C poor. Also table 11 presents the mean abundances for H II regions derived by Dufour (1984c). The standard deviations of the PN mean abundances are typically of 0.05 dex for He and of 0.2 dex for C, N, O and Ne, while for the H II regions they are about half as large. Presumably the H II region abundances are similar to the initial abundances of most PN progenitors, particularly those formed recently, and by comparing them it should be possible to estimate the enrichment produced by the evolution of the progenitor star.

The main results derived from samples that exclude type I PN are: (a) the He/H ratio is about the same in PN and in H II regions of the same galaxy, which implies that these PN do not contain significant amounts of freshly made helium (Monk *et al* 1988, Henry *et al* 1989); (b) the N/H ratios in the SMC and LMC samples are 0.94 dex and 0.84 dex higher than those of H II regions in the same galaxies, which implies that PN progenitors are producing substantial amounts of N; (c) by comparing the PN N abundances with the H II region C abundances, it follows that in PN most of the initial C has been converted into N, alternatively the N/H excess in PN of type II in the solar vicinity (see table 6) amounts to only about one third of the C abundance of population I objects, these results are in agreement with the computations by Renzini and Voli (1981), where it is expected that the smaller the initial metallicity, the higher the fraction of original C that is transformed into N (Monk *et al* 1988); (d) the C/H ratios in the SMC and LMC samples are 1.49 dex and 0.66 dex higher than those of H II regions in the same galaxies, which implies that C produced by the triple α reaction has been brought up to the surface by the third dredge-up phase (Renzini and Voli 1981, Aller and Czyzak 1983); (e) the O/H, Ne/H and Ar/H ratios in PN are similar to those of H II regions, indicating that IMS are not important sources of O, Ne and Ar.

Table 12 lists abundances for a group of type I PN. The C abundances were derived from UV collisionally excited lines. The He/H abundance ratio of N67 has not been corrected for the effect of collisional excitation from the 2^3S He^{0} state, the correction would reduce the ratio by about 0.1 dex.

Monk *et al* (1988) have classified MC PN as type I using only the criterion that $N/O \geq -0.3$ dex. They did not use the He/H abundance criterion because the initial He/H ratios are much lower than those found in the Galaxy, so a significantly larger He enhancement would have been necessary before a MC PN could satisfy the He/H

Table 11. Mean abundances for PN and H II regions in the Magellanic Clouds, given in $12+\log N(X)/N(H)$. The mean values for the PN samples exclude type I nebulae.

Sample	He	C	N	O	Ne	Reference
SMC PN	10.92	8.65	7.44	8.26	7.36	1, 2
SMC H II	10.90	7.16	6.46	8.02	7.22	3
LMC PN	10.94	8.56	7.81	8.49	7.64	1, 2
LMC H II	10.93	7.90	6.97	8.43	7.64	3

1. Monk *et al* (1988)
2. Aller *et al* (1987)
3. Dufour (1984c)

Table 12. Abundances for type I PN in the Magellanic Clouds given in $12+\log N(X)/N(H)$.

Object	He	C	N	O	Ne	Reference
N67 (SMC)	11.17:	6.27	7.47:	7.15	6.54	1
N66 (LMC)	11.07	7.45	8.17	8.26	7.60	2
N97 (LMC)	11.09	7.47	8.44	8.09	7.48	1, 2, 3, 4
N102 (LMC)	11.13	7.49	8.39	8.12	7.39	1, 2, 4

1. Aller *et al* (1987)
2. Peña and Ruiz (1988)
3. Barlow *et al* (1983)
4. Monk *et al* (1988)

abundance criterion for galactic PN. Nevertheless the LMC type I PN are extremely He-N rich since they show an average He/H enrichment of 0.17 dex and an average N/H enrichment of 1.36 dex, relative to the values found in H II regions of the LMC. Their very high He/H and N/H ratios combined with their very low C/O ratios are in agreement with models by Renzini and Voli (1981) for $\alpha \sim 2$ and $M_i \sim 8\ M_\odot$, where α is the ratio of the convective mixing length to the pressure scale height. The PN in table 12 have similar C/O and N/O ratios to those of NGC 6302 (Aller *et al* 1981, Barral *et al* 1982), which is probably the most extreme type I PN known in the Galaxy.

The O/H mean value of the LMC type I PN is smaller than that of the LMC H II regions. Furthermore, the (N+O)/H mean value of the LMC type I PN is similar to that of the LMC H II regions, probably indicating that the ON cycle has contributed to the N enrichment (Aller *et al* 1987, Monk *et al* 1988, Peña and Ruiz 1988, Henry *et al* 1989).

Monk *et al* (1988) find that 14% of the PN in the SMC and 20% in the LMC are of type I; these values are similar to those found in the solar neighbourhood. Maran *et al* (1982), on the evidence of the large C abundances of PN compared to those of H II regions (table 11), concluded that most of the C enrichment in the MC is due to PN.

Henry *et al* (1989) determined the average net yield of N due to PN for the LMC and the SMC and compared it with the yield needed to explain the current interstellar (H II region) level of N, assuming a simple, closed system model for chemical evolution of galaxies. They conclude that while PN have contributed significantly to the N enrichment in the LMC, they have made only a small contribution to it in the SMC.

7.2. Chemical abundances in other Local Group galaxies

The chemical composition of PN in galaxies of the Local Group, excluding the Magellanic Clouds and the Galaxy, has been reviewed by Ford (1983).

Table 13 presents abundances for PN of the Local Group of galaxies. The He/H abundance ratios have not been corrected for the effect of collisional excitation from the 2^3S He^0 state, this correction is in general smaller than 0.04 dex, but for the NGC 185 and NGC 6822 PN it can be as high as 0.10 dex.

The O/H ratio in the Fornax PN is relatively high, considering that the galaxy is metal poor, it probably implies that there are two stellar populations: an old metal-poor population characterized by Fornax's four globular clusters that predominates, and an intermediate-age population characterized by the PN listed in table 13 and the carbon stars present (Frogel *et al* 1982, Ford 1983).

Table 13. Chemical abundances of extragalactic PN and H II regions, given in 12+ log $N(X)/N(H)$.

Object	He	N	O	Ne	Reference
PN (Fornax)	11.08	7.41	8.51	—	1
PN (NGC 185)	11.32:	>8.14	7.88	6.81:	2, 3
PN (NGC 6822)	11.27:	8.79	8.12	6.91	4
H II (NGC 6822)	10.92	6.52	8.24	7.58	5
PN (M31-290)	11.20:	7.81	8.55	7.79	6
PN (M31-363)	11.21:	7.88	8.67	8.11	6
H II (M31-BA 685)	10.93	7.39	8.51	7.66	6
PN (M31-372)	—	<7.71	8.06	7.49	6

1. Danziger *et al* (1978)
2. Jenner and Ford (1978)
3. Ford (1983)
4. Dufour and Talent (1980)
5. Lequeux *et al* (1979)
6. Jacoby and Ford (1986)

The NGC 185 PN in table 13 is of type I, probably with an initial stellar mass $M_i \geq 3\ M_\odot$. This indicates that its progenitor is relatively young and that it might be associated with the OB stars present in this galaxy.

The NGC 6822 PN in table 13 is also of type I. Its N/H enrichment relative to the NGC 6822 H II regions is very high, of 2.27 dex which probably constitutes a record. Its O/H ratio is slightly smaller than those of the NGC 6822 H II regions, in agreement with other type I PN in other galaxies. Its Ne/O ratio is smaller than that of the NGC 6822 H II regions and of the other type I PN known. This latter result is difficult to explain and could be due to errors in the abundance determinations; if real it would imply that the Ne/O ratio is not homogeneous in the ISM or that its progenitor star produced O. Both possibilities are unlikely and the object should be reobserved.

In the spiral galaxy M31, Jacoby and Ford (1986) have determined the chemical composition of three PN: M31-290, M31-363 and M31-372. These objects are at projected distances from the nucleus of 3.5, 18 and 33 kpc. From their radial velocities it is found that only the second one might belong to the disk while the other two belong to the halo. The O/H ratios of the PN M31-363 and of the H II region BA 685 are similar, which implies that disk PN are good tracers of the ISM O/H ratios. The O/H values of the two halo PN, M31-290 and M31-372, are considerably higher than the O/H ratios derived for galactic halo PN and imply that the chemical evolution of M31 was different from that of the Galaxy. M31-290 seems to correspond to a metal-rich halo population and M31-372 to a relatively metal-poor one; this division has also been found from the study of globular clusters in M31. Highly accurate observations of PN in M31 are needed to study further its chemical evolution: more data on disk PN would permit us to evaluate abundance gradients, and more data on halo PN would permit us to study its early chemical evolution.

7.3. Extragalactic distance scale

Jacoby and collaborators (Jacoby 1989, Jacoby *et al* 1989, 1990, Ciardullo 1989a, b, Ford *et al* 1989) have presented the physical rationale for using the planetary nebula [O III] luminosity function (PNLF) to derive highly accurate extragalactic distances.

The PNLF was established by observing galaxies with two filters: an [O III] filter corrected for the peculiar velocity of the galaxy and an off-band [O III] filter. Both images were blinked to detect stellar objects emitting in the [O III] 5007 Å line. Objects that were extended or that appeared in the off-band image were rejected as PN candidates.

Distances to the galaxies were obtained by adjusting the shape of a given PNLF to that of M31. The M31 PNLF has a sharp cutoff in the bright end of the observed luminosity function and a plateau about one magnitude below the sharp cutoff (the PNLF of other galaxies show a very similar behaviour). They assumed that the size of the galaxy affects only the number of PN, but not the shape of the PNLF.

Jacoby (1989) simulated [O III] luminosity functions for Gaussian M_c distributions with different central values, $\langle M_c \rangle$, and widths, b. He obtained an excellent match to the observations of the M31 PNLF for a model based on helium-burning central stars with $\langle M_c \rangle = 0.61\ M_\odot$ and $b = 0.02\ M_\odot$.

For the Sb spiral galaxy M81 Jacoby *et al* (1989) derived a PNLF distance of 3.50 ± 0.40 Mpc, which is in excellent agreement with the distance derived from I-band observations of Cepheids, indicating that the accuracy of the PNLF method is as good as the Cepheids' one. Ciardullo *et al* (1989a) have applied the PNLF method to three galaxies of the Leo I Group with different Hubble types: NGC 3379 an E0 elliptical, NGC 3377 and E6 elliptical, and NGC 3384 S0 spiral; the derived distances are 9.8, 10.3 and 10.1 Mpc with a formal 1σ error of about 10%

Jacoby *et al* (1990) applied the PNLF method to six galaxies of the Virgo Cluster, with elliptical or S0 Hubble types (M49, M60, M84, M85, M86, M87), to derive their distances. They found a very small dispersion in the distances and an average distance of 14.7 ± 1.0 Mpc. By merging the six PNLF into a single one, a distance of 14.9 ± 0.3 Mpc is derived, the 1σ uncertainty is less than 2%. This result illustrates the power of the method when large samples of bright PN are available.

Table 14 lists the distances to the Virgo Cluster of galaxies derived by different methods and different observers.

Table 14. Distances to the Virgo cluster of galaxies.

Method	Distance (Mpc)	Reference
Mean of six methods	11.9 ± 0.6	de Vaucouleurs (1985)
Luminosity fluctuations	13.9 ± 1.2	Tonry *et al* (1989)
$L-\sigma-\Sigma$ relation	14.4 ± 1.6	Pierce (1989)
IR Tully–Fisher relation	14.6 ± 0.8	Aaronson *et al* (1986)
PN luminosity function	14.7 ± 1.0	Jacoby *et al* (1990)
H II region luminosities	15.1 ± 1.0	Melnick *et al* (1988)
Novae	18.2 ± 3.0	Capaccioli *et al* (1990)
Globular cluster luminosity function	21.9 ± 2.2	Harris (1988)
Mean of six methods	21.9 ± 0.9	Sandage and Tammann (1990)

To determine the Hubble constant, H_0, from the distance to the Virgo cluster it is necessary to determine the infall velocity of the Local Group of galaxies toward Virgo. A recent determination of this velocity by Sandage and Tammann (1990) of 168 ± 50 km s^{-1}, combined with the observed redshift of Virgo of 976 ± 45 km s^{-1} yields $H_0 = 52 \pm 2$ km s^{-1} Mpc^{-1}.

On the other extreme, from the infall velocity of the Local Group toward Virgo by Sandage and Tamman (1990) and the distance by de Vaucouleurs (1985), a value of $H_0 = 96 \pm 5$ km s^{-1} Mpc^{-1} is derived. The distance to Virgo derived by Jacoby *et al* (1990) and the infall velocity by Sandage and Tammann implies that $H_0 = 77 \pm 6$ km s^{-1} Mpc^{-1}, safely in the middle between de Vaucouleurs' and Sandage and Tammann's determinations. Notice that there are other estimates in the literature of the infall velocity of the Local Group toward Virgo; adopting that of Kraan-Korteweg (1985), the distance to Virgo given by Jacoby *et al* would imply that $H_0 = 81 \pm 6$ km s^{-1} Mpc^{-1}, while adopting that of Aaronson *et al* (1986), the distance given by Jacoby *et al* would imply that $H_0 = 94 \pm 6$ km s^{-1} Mpc^{-1}. It is beyond the scope of this review to discuss the error estimates of the different Hubble constant determinations.

7.4. Birth rate and total number of PN

Table 15 presents the PN birth rate per solar luminosity, $\dot{\xi}$, and the total number of PN, N_T, for 16 galaxies.

For M31 the $\dot{\xi}$ and N_T values were obtained from: a solar bolometric absolute magnitude, $M(\odot)_{bol} = +4.75$ (Allen 1973), a visual absolute magnitude for the galaxy,

Table 15. PN birth rates per unit luminosity, $\dot{\xi}$, and total numbers of PN, N_T, for the Galaxy and other galaxies. $(B\text{-}V)_0$ is the intrinsic colour index and M_{bol} is the absolute bolometric magnitude.

Object	$(B\text{-}V)_0$	M_{bol}	$\dot{\xi}$ (10^{-12} yr^{-1} $L_\odot^{-1}$)	N_T (10^3)	References
M49	0.98	−23.29	2.7 ± 0.6	11.1 ± 2.5	1
M87	0.97	−23.08	3.4 ± 0.6	11.5 ± 2.0	1
M60	1.00	−22.85	2.6 ± 0.8	7.1 ± 2.2	1
M86	0.96	−22.78	5.4 ± 0.8	13.9 ± 2.1	1
M84	0.95	−22.60	6.8 ± 1.3	14.8 ± 2.8	1
M85	0.88	−22.31	8.0 ± 1.2	13.3 ± 2.0	1
M31	0.80	−21.96	6.6 ± 1.2	8.0 ± 1.5	2, 3, 4
M81	0.84	−21.88	8.4 ± 1.8	9.4 ± 2.0	5, 6
NGC 3379	0.89	−21.57	8.5 ± 1.7	7.2 ± 1.4	7
NGC 3384	0.84	−21.25	15.0 ± 3.0	9.4 ± 1.9	7
The Galaxy	0.53:	−21.2:	12.0 ± 3.0	7.2 ± 1.8	4, 8
The Galaxy	—	—	—	9.1 ± 3.3	9
NGC 3377	0.79	−20.69	15.0 ± 3.8	5.6 ± 1.4	7
LMC	0.43	−19.0:	12.6 ± 2.7	1.0 ± 0.25	4, 9, 10
SMC	0.44	−17.2:	19.2 ± 5.3	0.29 ± 0.08	4, 9, 10
M32	0.85	−17.14	10.1 ± 2.5	0.14 ± 0.04	3, 4
NGC 205	0.75	−16.99	14.5 ± 4.2	0.18 ± 0.05	3, 4

1. Jacoby *et al* (1990)
2. Freeman (1970)
3. Ciardullo *et al* (1989b)
4. Peimbert (1990)
5. Brandt *et al* (1972)
6. Jacoby *et al* (1989)
7. Ciardullo *et al* (1989a)
8. de Vaucouleurs and Pence (1978)
9. Jacoby (1980)
10. Hindman (1967)

$M_V = -21.2$ (Freeman 1970), a bolometric correction, BC $= -0.8$ mag and an estimated number of 970 PN for a region of M31 with $M_{bol} = -19.68$ (Ciardullo *et al* 1989b).

In figures 13 and 14 we plot $\dot{\xi}$ against M_{bol} and $\dot{\xi}$ against B-V using values for the sample in table 15, excluding the Galaxy (Peimbert 1990). It is found that there is a strong correlation between M_{bol} and $\dot{\xi}$, in the sense that the brighter the galaxy, the smaller the $\dot{\xi}$ value. From the same sample it is also found that there is a strong correlation between B-V and $\dot{\xi}$ in the sense that the redder the galaxy, the smaller the $\dot{\xi}$ value.

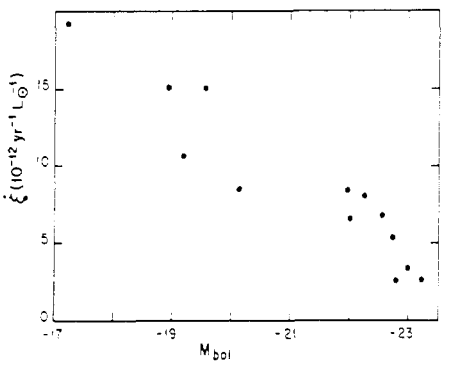

Figure 13. Plot of PN birth rate per solar luminosity, $\dot{\xi}$, against bolometric magnitudes, M_{bol}, for a group of fifteen galaxies.

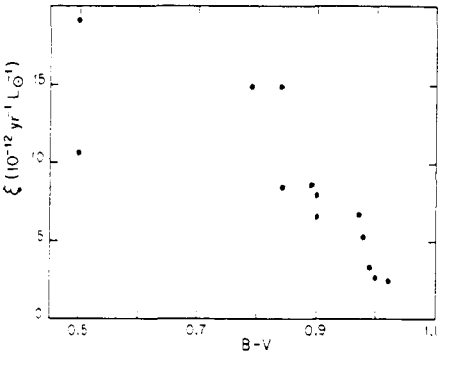

Figure 14. Plot of $\dot{\xi}$ against the colour index, B-V, for the sample of objects in figure 13.

The $\dot{\xi}$ value for the Galaxy in table 15 was estimated from the ($\dot{\xi}$, M_{bol}) relation presented in figure 13 (a higher and less precise $\dot{\xi}$ value would have been obtained from the relationship between B-V and $\dot{\xi}$, see figure 14). The N_T value was obtained from the M_V value by de Vaucouleurs and Pence (1978) and the $\dot{\xi}$ value in table 15.

It is possible to compare $\dot{\xi}$ with the stellar death rate per solar bolometric luminosity, $\dot{s}$. Renzini and Buzzoni (1986) computed $\dot{s}$ values as a function of time from models with a single burst of star formation and three widely different initial mass functions. They found that the $\dot{s}$ values are extremely insensitive to the population age or to the initial mass function. For a stellar population with an age of 1×10^{10} years the $\dot{s}$ values derived by Renzini and Buzzoni are $\sim 20 \times 10^{-12}$ yr L^{-1}. These values apply to elliptical galaxies dominated by a very old stellar population.

For spiral and irregular galaxies, models with continuous star formation have to be considered to determine the $\dot{s}$ values. To compare spiral and irregular galaxies with the models by Renzini and Buzzoni (1986), an average age for the stellar content has to be estimated. In these galaxies the stellar death rate and the total luminosity are dominated by the younger generations of stars, and an average age, weighted by the higher luminosity of the younger generations, of about 10^9 years should be used. Moreover, $1\text{-}2 \times 10^9$ years is the time that a star with $M_i \sim 1.5\ M_\odot$ spends in the main sequence and corresponds to the (M_i) derived from the height of PN above the galactic plane. An age of $\sim 10^9$ years would reduce $\dot{s}$ to $\sim 15 \times 10^{-12}$ yr^{-1} L^{-1} (Renzini and Buzzoni 1986).

For the LMC, the SMC, M81, M31 and the Galaxy the $\dot{\xi}$ values are very similar to the $\dot{s}$ values derived from the models by Renzini and Buzzoni (1986), considering all the uncertainties that enter into both types of determinations. In particular, for the Galaxy $\dot{\xi} \sim (\frac{2}{3})\dot{s}$; this result implies that the majority of the intermediate-mass stars undergo the PN phase.

Moreover, for the Galaxy the N_T value derived from the $\dot{\xi}$ value is concordant with the N_T values derived from the PN surface density of the solar neighbourhood and long distance scales like those of Cudworth (1974) and Mallik and Peimbert (1988) (see section 6).

For all the galaxies in table 15 a value of $15 \leq \dot{s}\,(10^{-12}\,\mathrm{yr}^{-1}\,L_\odot^{-1}) \leq 20$ can be expected and, if anything, slightly higher $\dot{s}$ values for the more luminous galaxies. Therefore the decrease of $\dot{\xi}$ with B-V and with bolometric luminosity is not due to a decrease in $\dot{s}$ and should be explored further.

Most of the PN luminosity functions used for the determinations of $\dot{\xi}$ in table 15 are complete only at the high-luminosity end; the completeness limit of the observations extends only ~2.5, 1.5, 1.1 and 0.8 mag below the bright-end cutoff for M31, M81, the Leo I Group, and the Virgo Cluster, respectively. The shape of the entire PNLF is obtained by scaling the observed upper end with the PNLF for the Magellanic Clouds derived by Jacoby (1980). Since the PNLF spans about eight magnitudes (Ciardullo *et al* 1989b), the $\dot{\xi}$ values represent the upper end of the PNLF. Therefore, strictly speaking, it can only be said that the number of bright PN decreases with increasing luminosity of the galaxy.

There are at least three possible causes for the decrease in the number of bright PN with the increase of B-V and luminosity: (a) an increase of the heavy-element abundances, (b) a decrease of $\langle M_c \rangle$ due to an age effect, and (c) a decrease of the fraction of intermediate-mass stars that produce luminous PN. In what follows we will analyse these possibilities.

There is a well known positive correlation between the total mass of the galaxy and the heavy-element abundances that includes irregular, spiral and elliptical galaxies (e.g. Lequeux *et al* 1979, Mould 1984, Garnett and Shields 1987). From the relatively close relationship between mass and luminosity, a positive correlation between luminosity and heavy-element abundances is also expected. Even if a higher heavy-element abundance produces a decrease of the [O III] luminosity, the expected effect is very small (Jacoby 1989) and cannot explain the correlation present in figures 13 and 14.

It is also possible that the $\langle M_c \rangle$ decreases with the luminosity of the galaxy and consequently the luminosities of all PN. This possibility seems unlikely because the three galaxies of the Leo I Group, at practically the same distance, have different $\dot{\xi}$ values and the six galaxies of the Virgo Cluster, also at practically the same distance, also have different $\dot{\xi}$ values.

The third possibility is that there are two stellar populations in each galaxy: a relatively young one, with an average age of $\sim 1\text{-}2 \times 10^9$ years, and an old one, with an average age of $\sim 10^{10}$ years. The observed bright end of the PNLF would be due to the younger population with $\langle M_c \rangle \sim 0.61\,M_\odot$, while the older population would seldom produce PN or would produce PN with $\langle M_c \rangle \leq 0.57\,M_\odot$, which are considerably fainter (e.g. Jacoby 1989). The brighter the galaxy, the more important the old population relative to the young population. The older population is expected to produce fainter and fewer PN per star due to the following reasons: (a) lower luminosity of the central star, (b) smaller mass of the shell and (c) longer stellar evolutionary times that might prevent the star from becoming hot enough to ionize the nebula before it has dissipated.

8. Chemical evolution of galaxies

To fit the observed abundances in the interstellar medium (ISM) of the Galaxy and of other galaxies into a consistent picture it is necessary to construct models of galactic chemical evolution. Such models predict the time variation of the chemical composition of the ISM depending on assumptions for: (a) the mass distribution of the recently formed stars, the so-called initial mass function, (b) the time dependence of the stellar birth rate, (c) the chemical composition of the material ejected by the stars during their evolution, and (d) the large-scale mass flows, like infall from the halo, outflow to the intergalactic medium or radial flows within the galaxy. The observed abundances are used as tests for the input assumptions, since these physical parameters are not generally known.

Massive stars, those with $M_i \geq 8\ M_\odot$, produce supernovae of types Ib and II, while some binary stars with $M_i \leq 8\ M_\odot$ produce SN of type Ia. The ISM enrichment of elements heavier than N, like O, Ne, S, Ar and Fe is mainly due to SN. Intermediate-mass stars, those with masses in the $0.8 \leq M_i/M_\odot \leq 8$ range, undergo the PN phase and enrich the ISM with He, N and C (e.g. Kaler 1979, Peimbert and Serrano 1980, Torres-Peimbert *et al* 1980, Aller and Czyzak 1983, Clegg 1989, Barlow 1989, and references therein). Stars with $M_i \leq 0.8\ M_\odot$ do not enrich the ISM with heavy elements because they are still transforming H into He in their nuclei without producing any ejecta. It is important to know which is the relative contribution of PN and SN to the enrichment of any given element.

PN can be used to study the chemical composition of the ISM at the time they were formed, particularly the abundances of elements heavier than Ne, like S and Ar that are not affected by the evolution of the PN progenitors. PN can also be used to determine the pregalactic He abundance and their He, C and N contribution to the enrichment of the ISM.

8.1. Evolution of the halo of the Galaxy

Type IV PN are located in the halo and probably were born in it; from the study of those elements not affected by stellar evolution it is possible to estimate the chemical composition of the halo at the time the progenitor stars were formed.

From studies of K648, H4-1 and BB-1, it has been found that Ar, Fe and S are underabundant by about two orders of magnitude, while O and Ne are underabundant by about one order of magnitude relative to the solar vicinity (see table 7). Two possibilities have been discussed in the literature to explain the different underabundances: (a) that the enrichment of O and Ne in the ISM has proceeded faster than that of Ar, Fe and S; and (b) that the O and Ne excesses relative to Ar, Fe and S were produced by the progenitors of the PN themselves (Peimbert 1973, 1981, Hawley and Miller 1978b, Torres-Peimbert and Peimbert 1979, Barker 1980, 1983, Clegg *et al* 1987, Clegg 1989, Torres-Peimbert *et al* 1990).

Clegg (1989) suggested that possibly most of the Fe, Ar and S atoms are made by supernovae of type Ia while most of the O atoms are made by supernovae of types Ib and II; the delay in the Fe, Ar and S enrichment of the ISM relative to that of O is due to the smaller mass of the progenitors of SN of type Ia relative to those of types Ib and II. Similarly, Torres-Peimbert *et al* (1990) have suggested that most of the Ne enrichment of the ISM is due to SN of types Ib and II.

Figure 15 presents a plot of the [O/Ar] against [Ar/H] abundance ratios for the type IV PN (see table 7) as well as those for the Orion nebula, the Sun, and type II PN (see table 6). From this figure it follows that the eight halo PN show significant deficiencies relative to Orion, the Sun, and type II PN. Moreover, based on their chemical composition, the eight PN can be divided into two groups: one composed by K648, BB-1 and H4-1 and the other one composed by the other five.

Based on their distances to the plane of the galaxy, z, and on their velocities relative to the local standard of rest, v_{lsr} (see table 16), it seems that DDDM-1 and PRMG-1

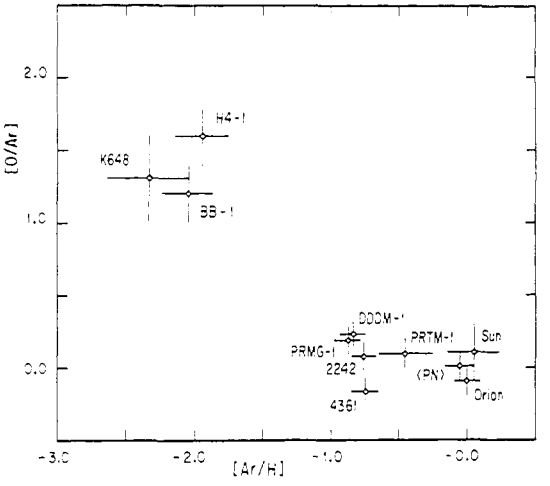

Figure 15. Plot of [O/Ar] against [Ar/H] abundances for Halo PN, where $[A/B] = \log(A/B) - \log(A/B)_{popI}$. We have also plotted the abundances for the Sun, the Orion nebula and an average for type II PN.

Table 16. Velocities relative to the local standard of rest and distances from the plane of the Galaxy for type IV PN.

Object	v_{lsr} (km s^{-1})	z (kpc)	Reference
K648	-128 ± 17	11.8	1, 2
BB-1	-192 ± 10	10.5	1, 3
H4-1	-133 ± 12	6.0	1, 3
NGC 4361	$+8 \pm 2$	0.83	1, 3
NGC 2242	$+15 \pm 21$	1.09	3, 4, 5
DDDM-1	-285 ± 20	14.9	6, 7
PRMG-1	—	5.1	8
PRTM-1	—	3.0	9

1. Schneider *et al* (1983)
2. O'Dell *et al* (1964)
3. Torres-Peimbert *et al* (1990)
4. Maehara *et al* (1986)
5. Huchra (1984)
6. Barker and Cudworth (1984)
7. Clegg *et al* (1987)
8. Peña *et al* (1989)
9. Peña *et al* (1990)

belong to the halo and NGC 2242 and NGC 4361 to the thick disk (see the discussion by Freeman (1987) on the different components of the galaxy). If DDDM-1 and PRMG-1 were formed in the halo it follows that the chemical enrichment of the ISM was not significant between the formation of the metal-rich halo stars and the formation of the metal-poor stars that now belong to the thick disk.

8.2. Abundance gradients across the disk of the Galaxy

The presence of O/H abundance gradients across the disks of spiral galaxies based on the study of H II regions is now well established (e.g. Pagel and Edmunds 1981, Shields 1990 and references therein). Studies of galactic H II regions show a similar O/H gradient to those of other spiral galaxies (Peimbert *et al* 1978, Hawley 1978, Shaver *et al* 1983). Gradients in He/H, N/O and S/O in the Galaxy and other spiral galaxies have been reported by some authors but not by others.

PN present several advantages over H II regions for the study of chemical abundance gradients across the disk of the Galaxy because: (a) a considerably larger sample of objects is available; (b) PN show a larger scatter in the direction perpendicular to the plane, it is therefore possible to observe them in the optical domain over a larger range of galactocentric distances; (c) in general small PN have higher surface brightness than galactic H II regions observable in the optical domain. On the other hand they also present several disadvantages: (a) the initial He, C, N and O could have been modified by the evolution of their parent stars, (b) their orbits may be non-circular, (c) the stellar progenitors have a large age spread.

Abundance gradients derived from PN have been reported in the literature by many authors (D'Odorico *et al* 1976, Aller 1976, Torres-Peimbert and Peimbert 1977, Barker 1978, Peimbert and Serrano 1980, Faúndez-Abans and Maciel 1986, 1987a, b). In table 17 we present abundance gradients derived by Faúndez-Abans and Maciel (1986) for PN of type II, see also figure 16. The PN results are similar to those derived for H II

Table 17. Solar neighbourhood abundance gradients given in $\Delta \log(X/H)/\Delta R$, with R in kiloparsecs, (from Peimbert *et al* 1978, Shaver *et al* 1983, Faúndez-Abans and Maciel 1986).

Ratio	H II regions (kpc^{-1})	Planetary nebulae (kpc^{-1})
He/H	-0.02 ± 0.01	-0.019 ± 0.003
O/H	-0.07 ± 0.015	-0.072 ± 0.012

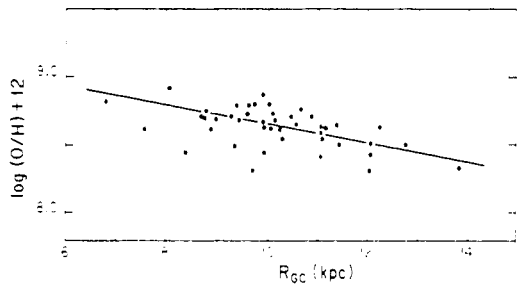

Figure 16. Log (O/H) + 12 plotted against galactocentric distance, R_{GC}, for type II PN (Faúndez-Abans and Maciel 1986).

regions and imply that most of the PN in these samples show orbits of relatively low eccentricity and that their ages are small compared with the age of the disk of the Galaxy.

Maciel and Faúndez-Abans (1985) have derived a well defined electron temperature gradient from type II galactic PN given by $\sim 600 \pm 120$ K kpc^{-1}; this value is about 1.5 times larger than that derived from galactic H II regions (Lichten *et al* 1979, Garay and Rodríguez 1983, Shaver *et al* 1983). The difference could be real since there are many different factors affecting each gradient. The main factor producing the T_e gradient in the galactic disk is the radial decrease of the abundance of the heavy elements that are responsible for the cooling of the PN shells.

There are two effects that could affect the derived values of the PN abundance and electron temperature gradients: (a) for a larger PN distance scale the derived gradients are smaller because they are proportional to k^{-1}, (b) the presence of objects in the sample with elliptical orbits tends to smooth out the gradients.

Several models of galactic chemical evolution have been proposed to explain the abundance gradients present in the ISM (e.g. Pagel 1989, Matteucci and Francois 1989, Matteucci *et al* 1989). These models explore several hypotheses: (a) variations in the initial mass function, (b) variations in the gas fraction, (c) variations in the ratio of star formation rate to inflow rate and (d) gas flows across the disk of the Galaxy. There are several possible combinations of hypotheses that can explain the gradients and other observational constraints are needed to produce a unique model.

8.3. The pregalactic helium abundance and the $\Delta Y/\Delta Z$ ratio

The fractional abundances of hydrogen, helium and all the other elements, normalized to unit mass, are denoted by X, Y and Z, respectively. The pregalactic, or primordial helium abundance, Y_p, is an important parameter for models of galactic chemical evolution and its value has several cosmological implications (e.g. Boesgaard and Steigman 1985, Pagel and Simonson 1989). To determine Y_p from the observed Y value of a given PN it is necessary to estimate two effects: the helium enrichment of matter previous to the formation of the progenitor star due to galactic evolution, ΔY_{GE}, and the helium enrichment due to the stellar evolution of its progenitor, ΔY_{SE}, i.e.

$$Y = Y_p + \Delta Y_{GE} + \Delta Y_{SE} = Y_i + \Delta Y_{SE} \tag{8.1}$$

where Y_i is the initial helium abundance of the star, and ΔY_{SE} is given by

$$\Delta Y_{SE} = \Delta Y^1 + \Delta Y^2 + \Delta Y^3 \tag{8.2}$$

where the terms on the right-hand side are due to the three dredge-up episodes (see subsection 5.2).

Type I PN are not good candidates to determine Y_p for the following reasons: (a) their ΔY_{SE} values are higher than those of other PN, probably due to their higher M_i values and the effects of the second dredge-up, (b) they are expected to have higher ΔY_{GE} values than those of other PN due to their younger ages.

In what follows we will discuss the Y_p and $\Delta Y_{GE}/\Delta Z_{GE}$ determinations presented in table 18. The first determinations of Y_p and $\Delta Y_{GE}/\Delta Z_{GE}$ based on PN were made by D'Odorico *et al* (1976) under the following considerations: (a) they obtained the ΔY^1 values from Torres-Peimbert and Peimbert (1971), (b) they assumed that oxygen constitutes 45% by mass of the heavy elements, Z, at the time the PN were formed and that the O/H ratio is not affected by the evolution of the PN progenitor, (c) they adopted a value of 0.055 for the mean square temperature fluctuation, t^2, to determine

Table 18. Pregalactic helium abundance by mass, Y_p, and the relative helium to heavy elements enrichment ratio produced by galactic evolution, $\Delta Y_{GE}/\Delta Z_{GE}$.

Sample	Y_p	$\Delta Y_{GE}/\Delta Z_{GE}$	ΔY^1	ΔY^3	Reference
7 type II	0.227	2.95	0.006	0	D'Odorico *et al* (1976)
6 type II	0.227 ± 0.012	3.0	0.016	0.013	Peimbert (1983)
16 type II + III	0.220 ± 0.010	3.6 ± 0.8	0.016	0.013	Peimbert (1983)
3 type IV	0.218 ± 0.03	—	0.02	0.037	Peimbert (1983)
4 type IV	0.23 ± 0.003	—	0.015	0.026	Clegg (1989)
H II + type IIb	0.227 ± 0.003	6.1 ± 0.6	0	0	Maciel and Leite (1990)
H II + type IIb	0.230 ± 0.003	5.2 ± 0.5	0.010	0	Maciel and Leite (1990)
H II	0.232 ± 0.004	4.0 ± 1	—	—	Pagel (1987a)
H II	0.229 ± 0.004	7.0 ± 2	—	—	Pagel and Simonson (1989)
H II	0.230 ± 0.006	3.8 ± 0.7	—	—	Torres-Peimbert *et al* (1989)

the chemical abundances. At present values of $t^2 \leq 0.03$ are favoured for PN (Torres-Peimbert *et al* 1980, Harrington *et al* 1982).

Peimbert (1983) determined Y_p from a sample of six type II PN of intermediate and high degree of ionization (i.e. without neutral helium in the H$^+$ zone). The procedure followed was: (a) ΔY^1 and ΔY^3 were taken from stellar evolution models by Renzini and Voli (1981), the ΔY^1 value for $M_i = 1.45\ M_\odot$ was adopted and ΔY^3 was computed from the difference between the observed C/O ratio and the interstellar C/O ratio, (b) it was assumed that O constitutes 45% by mass of Z_i, and that the O/H ratio is not affected by the evolution of the PN progenitor, (c) that $\Delta Y_{GE} = 3\Delta Z_{GE} = 3\Delta Z_i$ and (d) a value of $t^2 = 0.00$ was adopted.

Peimbert (1983) derived the Y_p and $\Delta Y_{GE}/\Delta Z_{GE}$ values in table 18 from the sample of 16 PN of types II and III of Peimbert and Serrano (1980) based on the stellar evolution models by Renzini and Voli (1981), the ΔY^1 value for $M_i = 1.45\ M_\odot$, the average ΔY^3 determined from the six best observed type II PN and $t^2 = 0.00$. For $t^2 = 0.02$ the ratio derived is $\Delta Y_{GE}/\Delta Z_{GE} = 3.0 \pm 0.7$ and the primordial helium is $Y_p = 0.223$, while for $t^2 = 0.035$ the derived quantities are $\Delta Y_{GE}/\Delta Z_{GE} = 2.2 \pm 0.5$ and $Y_p = 0.225$.

For type IV PN, ΔY_{GE} can be neglected and therefore $Y_p = Y_i$ (see equation (8.1)). Peimbert (1983) and Clegg (1989) determined Y_p from three and four type IV PN, respectively. The ΔY^1 and ΔY^3 values were also obtained from the computations by Renzini and Voli (1981) and from the observed C abundances. The main source of error is the large correction due to ΔY^3, moreover the computations by Renzini and Voli were made for stars with higher heavy-element abundances, consequently a new set of stellar evolution models is needed to improve the accuracy of these determinations.

Maciel (1988) and Maciel and Leite (1990) combined the abundances for type IIb PN with those for galactic H II regions by Shaver *et al* (1983) and for extragalactic H II regions by Pagel (1987a) to derive Y_p. For their sample of type II PN they found that $Z = 3.88\ Z(16)$, where $Z(16)$ is the O abundance by mass, while from H II regions it is found that $Z = 2.22\ Z(16)$, the difference is mainly due to freshly made C by the PN progenitor. To compare the $\Delta Y_{GE}/\Delta Z_{GE}$ ratio derived from PN with that derived from H II regions it is necessary to compare with $Z(16)$ which is not expected to be affected by the evolution of the PN progenitor. Therefore we have defined $\Delta Z_{GE} = 2.22\ Z(16) = Z_i$, in agreement with the other entries for ΔZ_{GE} in table 18. Consequently

the $\Delta Y_{GE}/\Delta Z_{GE}$ ratio is different from that defined by Maciel (1988) and Maciel and Leite (1990), but it can be derived from their data since they also present a relation for Y against Z(16). The Y_p values by Maciel and Maciel and Leite depend mainly on the O-poor H II regions, while the $\Delta Y_{GE}/\Delta Z_{GE}$ values depend mainly on the PN. By increasing the $\Delta Y^1 + \Delta Y^3$ value adopted by Maciel and Leite to ~0.03, a value of $\Delta Y_{GE}/\Delta Z_{GE} \sim 3.4$ is obtained, in excellent agreement with the H II region value (e.g. Peimbert 1986, Torres-Peimbert *et al* 1989), and with the value derived by Peimbert (1983) from PN.

To compare the PN results with those for H II regions, we present in table 18 three recent Y_p and $\Delta Y_{GE}/\Delta Z_{GE}$ determinations. Pagel and Simonson (1989) argue that their $\Delta Y_{GE}/\Delta Z_{GE}$ value is probably too large, being biased by a few nitrogen-rich objects. It is no surprise that the Y_p values by Maciel and Leite (1990) are very similar to that derived by Pagel (1987a) since, as mentioned before, the Y_p values by Maciel and Leite depend mainly on the data by Pagel for O-poor H II regions. The Y_p values by Peimbert (1983) and by Clegg (1989), derived exclusively from PN, are not as accurate as those derived from H II regions, but are in agreement with them.

The $Y_p = 0.23 \pm 0.01$ value is in agreement with standard big-bang nucleosynthesis with three families of light neutrinos ($m_\nu < 1$ MeV) and implies that the ratio of the nucleon density to the critical density required to close the universe, $\Omega_N = \rho_N/\rho_C$, is given by $0.007 \leq \Omega_N h(50) \leq 0.05$, where $h(50)$ is the present value of the Hubble parameter in units of 50 km s^{-1} Mpc^{-1} (e.g. Boesgaard and Steigman 1985, Pagel and Simonson 1989, Denegri *et al* 1990, Steigman 1990, Olive *et al* 1990). Therefore if most of the matter in the universe is baryonic, then the standard big-bang model coupled with the Y_p value implies an open universe.

8.4. Interstellar medium enrichment

8.4.1. The $\Delta Y_{GE}/\Delta Z_{GE}$ enrichment ratio. From models of galactic chemical evolution, Serrano and Peimbert (1981), Chiosi and Matteucci (1982), Schild and Maeder (1985) and Mallik and Mallik (1985) have obtained for $\Delta Y_{GE}/\Delta Z_{GE}$ values of 3.1, 2, 1 and 0.6, respectively. The differences are due to the adopted initial mass functions and stellar evolution models.

Schild and Maeder (1985) and Mallik and Mallik (1985) have considered the possibility that stars with initial masses above a critical mass, M(BH), produce black holes without enriching the ISM with heavy elements. Schild and Maeder have suggested that $M(\text{BH}) \sim 50\ M_\odot$, for which $\Delta Y_{GE}/\Delta Z_{GE} \sim 1.4$. To be able to explain the observed $\Delta Y_{GE}/\Delta Z_{GE}$ values, Mallik and Mallik conclude that stellar evolution models still required considerable improvements or that M(BH) is very small, of the order of $20\ M_\odot$; for the latter M(BH) value they obtain $\Delta Y_{GE}/\Delta Z_{GE} \sim 2.1$.

An important contribution to the enrichment of the ISM by He-rich objects, like type I PN and supernovae of the Crab nebula type (e.g. Péquignot and Dennefeld 1983, Davidson and Fesen 1985, Henry 1986, MacAlpine *et al* 1989) would help to explain the high $\Delta Y_{GE}/\Delta Z_{GE}$ values presented in table 18.

8.4.2. Nitrogen and helium. PN of type I show very high He/H and N/H overabundances relative to those of the ISM, probably due to the three dredge-up phases (see subsection 5.2); while PN of type II show moderate N/H overabundances, of about a factor of three to four, and very small He/H overabundances, probably due to the first and third dredge-up phases.

Peimbert (1987) has estimated that the He enrichment of the ISM due to PN of type I is five to six times larger than that produced by PN of types II and III. This result is based on the following assumptions: (a) an ISM helium abundance by mass of 0.28, (b) a production rate of type I PN of 20% relative to the total PN production rate, and (c) an average envelope mass for type I PN three times higher than that for PN of types II and III. Similarly, Peimbert has estimated that the N enrichment produced by PN of type I is about three times larger than that produced by PN of types II and III.

The N enrichment of the ISM is due to intermediate-mass stars and massive stars. Moreover, it could have had a primary or a secondary origin, where primary elements are those that are directly synthesized in the star from H and He, and secondary elements are those synthesized from heavy elements that were already present in the star when it was formed. Different models of galactic chemical evolution have been made to study the N enrichment of the ISM, nevertheless there is still an open discussion on the relative importance of different stellar mass ranges for N production and on the fraction of N that is of secondary origin (e.g. Edmunds and Pagel 1978, Peimbert and Serrano 1980, Serrano and Peimbert 1983, White and Audouze 1983, Matteucci 1986, Diaz and Tosi 1986, Forieri 1986, Pagel 1986, 1987b, Peimbert 1987, Tosi 1988a, b).

8.4.3. Carbon. Tinsley (1978) considered that the observed solar C/O ratio and estimates of nucleosynthesis in massive stars indicate that PN are a major source of C enrichment of the ISM. Further work showed that most of the C in the ISM comes from intermediate mass stars (e.g. Dufour 1984b, 1985, Mallik and Mallik 1985, Sarmiento and Peimbert 1985, Matteucci 1986).

Sarmiento and Peimbert (1985) found that intermediate mass stars produce from 60 to 80% of the C present in the ISM and that massive stars produce the rest. Their result is based on three independent determinations: (a) the variation of C/H in the ISM of galaxies with different O/H ratio; (b) the comparison of the solar C/O ratio with the C/O ratio predicted by Arnett and Thielemann (1984) for a single star with an $8\,M_\odot$ He-core, corresponding to a 20–$25\,M_\odot$ main sequence star; and (c) the comparison of the solar-vicinity ISM C/H ratio with the predicted C/H ratio from the models by Renzini and Voli (1981).

SN of type Ia are not important sources of C production since carbon deflagration models produce very high Fe/C ratios. Even if these objects were responsible for all of the Fe in the solar vicinity their contribution to the C abundances would be negligible (Nomoto 1984, Woosley *et al* 1984, Mallik and Mallik 1985). The contribution of novae to the C abundance of the ISM is also negligible (Sarmiento and Peimbert 1985).

9. Concluding remarks

PN correspond to one of the main stages of stellar evolution. The PN birth rate in the Galaxy and other galaxies indicates that most IMS go through the PN stage. Therefore a complete stellar evolution theory should contemplate the transition from red giants to white dwarfs and the relation between Miras, OH/IR stars, protoplanetary nebulae, PN and white dwarfs.

Stellar evolution computations for a wide variety of masses and chemical composition exploring the parameters α and η, the ratio of the mixing length to the pressure scale height and the mass loss rate during the asymptotic giant branch phase, are needed to produce a better fit with the observations.

From future observations it will be possible to place the central stars of Magellanic Cloud PN in the luminosity-temperature diagram, providing us with a very powerful tool to test stellar evolution predictions.

The ejection mechanism of the shell should be better understood. It is hoped that the study of the shell evolution can lead us to an improved knowledge of the ejection mechanism. Advances on the interaction of the stellar wind with the previous ejected shell are being made, as well as on the study of multiple shells and their relation to stellar evolution. Observations of molecules with higher angular resolution and of atomic hydrogen in the shells will also help us to advance in the study of the shell's evolution.

The relation between binarity, morphology of the nebulae and chemical composition should be studied further.

The determination of the chemical composition of PN with known M_i values and with known kinematical properties will permit us to evaluate the chemical composition at the time PN were formed as well as the chemical enrichment of the Galaxy produced by the PN themselves. This type of study is beginning to be carried out for other galaxies and appears very promising.

Inhomogeneous models with a varying C/H ratio as a function of distance to the central star, coupled with stellar atmospheric abundances will provide strong constraints for stellar evolution models.

PN have been used as test particles to study dynamical aspects of external galaxies and the Galaxy. These studies should be extended further.

The data on extragalactic PN have already yielded important results for the study of the properties of PN and for the general properties of the Universe. It is expected that the study of extragalactic PN will flourish in the next few years.

Acknowledgements

Over the years I have profited enormously by discussions on PN with: L H Aller, G Haro, R Minkowsky, C R O'Dell, D E Osterbrock, M J Seaton and S Torres-Peimbert. I am greatly indebted to J Fierro, J B Kaler, W J Maciel, M Peña, S R Pottasch, A Sarmiento, Y Terzian and S Torres-Peimbert for critical readings of drafts of this article and for constructive suggestions.

References

Aaronson M, Bothun G, Mould J, Huchra J, Schommer R A and Cornell M E 1986 *Astrophys. J.* **302** 536-63
Acker A 1978 *Astron. Astrophys. Suppl. Ser.* **33** 367-81
—— 1980 *Astron. Astrophys.* **89** 33-40
—— 1983 *IAU Symp. 103 Planetary Nebulae* ed D R Flower (Dordrecht: Reidel) p 241
Adam J and Koppen J 1985 *Astron. Astrophys.* **142** 461-75
Adams S, Seaton M J, Howarth I D, Aurriere M and Walsh J R 1984 *Mon. Not. R. Astron. Soc.* **207** 471-89
Allen C W 1973 *Astrophysical Quantities* (London: Athlone)
Aller L H 1976 *Publ. Astron. Soc. Pacific* **88** 574-84
—— 1983 *IAU Symp. 103 Planetary Nebulae* ed D R Flower (Dordrecht: Reidel) pp 1-13
—— 1984 *Physics of Thermal Gaseous Nebulae* (Dordrecht: Reidel)
Aller L H and Czyzak S J 1983 *Astrophys. J. Suppl. Ser.* **51** 211-48
Aller L H and Keyes C D 1987 *Astrophys. J. Suppl. Ser.* **65** 405-28
Aller L H, Keyes C D, Maran S P, Gull T R, Michalitsianos A G and Stecher T P 1987 *Astrophys. J.* **320** 159-77

Aller L H, Ross J E, O'Mara B J and Keyes C D 1981 *Mon. Not. R. Astron. Soc.* **197** 95-106
Aller L H and Walker M F 1970 *Astrophys. J.* **161** 917-45
Alloin D, Cruz-González C and Peimbert M 1976 *Astrophys. J.* **205** 74-81
Amnuel P R, Guseimov O H, Novruzova H I and Rustamov Yu S 1984 *Astrophys. Sp. Sci.* **107** 19-50
Amnuel P R, Guseimov O H and Rustamov Yu S 1989 *Astrophys. Sp. Sci.* **154** 21-88
Arnett W D and Thielemann F K 1984 *Stellar Nucleosynthesis* ed C Chiosi and A Renzini (Dordrecht: Reidel) pp 145-50
Balick B 1987 *Astron. J.* **94** 671-8
Balick B, Reston H L and Icke V 1987 *Astrophys. J.* **94** 1641-52
Barker T 1978 *Astrophys. J.* **220** 193-209
—— 1980 *Astrophys. J.* **237** 482-5
—— 1982 *Astrophys. J.* **253** 167-73
—— 1983 *Astrophys J.* **270** 641-4
Barker T and Cudworth K M 1984 *Astrophys J.* **278** 610-4
Barlow M J 1987 *Mon. Not. R. Astron. Soc.* **227** 161-83
—— 1989 *IAU Symp. 131 Planetary Nebulae* ed S Torres-Peimbert (Dordrecht: Kluwer) pp 319-34
Barlow M J, Adams S, Seaton M J, Willis A J and Walker A R 1983 *IAU Symp. 103 Planetary Nebulae* ed D R Flower (Dordrecht: Reidel) p 538
Barlow M J, Morgan B L, Standley C and Vine H 1986 *Mon. Not. R. Astron. Soc.* **223** 151-72
Barral J F, Cantó J, Meaburn J and Walsh J R 1982 *Mon. Not. R. Astron. Soc.* **199** 817-32
Becker S A and Iben I, Jr 1979 *Astrophys. J.* **232** 831-53
—— 1980 *Astrophys. J.* **237** 111-29
Berrington K and Kingston A E 1987 *J. Phys. B: At. Mol. Phys.* **29** 6631
Boesgaard A M and Steigman G 1985 *Ann. Rev. Astron. Astrophys.* **23** 319-78
Bowen I S 1928 *Astrophys. J.* **67** 1-15
Brandt J C, Kalinowski J K and Roosen R G 1972 *Astrophys. J. Suppl.* **24** 421-48
Brocklehurst M 1971 *Mon. Not. R. Astron. Soc.* **153** 471-90
—— 1972 *Mon. Not. R. Astron. Soc.* **157** 211-27
Butler S E, Bender C F and Dalgarno A 1979 *Astrophys. J.* **230** L59-61
Butler S E and Dalgarno A 1980 *Astrophys. J.* **241** 838-43
Butler S E, Heil T G and Dalgarno A 1980 *Astrophys. J.* **241** 442-7
Calvet N and Peimbert M 1983 *Rev. Mexicana Astron. Astrof.* **5** 319-28
Cahn J H and Kaler J B 1971 *Astrophys. J. Suppl. Ser.* **22** 319-68
Capaccioli M, Cappellaro E, Della Valle M, D'Onofrio M, Rosino L and Turatto M 1990 *Astrophys. J.* **350** 110-18
Chapman R D and Henry R J W 1971 *Astrophys. J.* **168** 169-171
—— 1972 *Astrophys. J.* **173** 243-5
Chiosi C and Matteucci F 1982 *Astron. Astrophys.* **105** 140-8
Chu Y H 1989 *IAU Symp. 131 Planetary Nebulae* ed S Torres-Peimbert (Dordrecht: Kluwer) pp 105-15
Ciardullo R, Jacoby G H and Ford H C 1989a *Astrophys. J.* **344** 715-25
Ciardullo R, Jacoby G H, Ford H C and Neill J D 1989b *Astrophys. J.* **339** 53-69
Clegg R E S 1985 *Production and Distribution of C, N, O Elements* ed I J Danziger, F Matteucci and K Kjar (Garching: European Southern Observatory) pp 261-75
—— 1987 *Mon. Not. R. Astron. Soc.* **229** 31-39
—— 1989 *IAU Symp. 131 Planetary Nebulae* ed S Torres-Peimbert (Dordrecht: Kluwer) pp 139-56
Clegg R E S and Harrington J P 1989 *Mon. Not. R. Astron. Soc.* **239** 869-83
Clegg R E S and Middlemass D 1987 *Mon. Not. R. Astron. Soc.* **228** 759-78
Clegg R E S, Peimbert M and Torres-Peimbert S 1987 *Mon. Not. R. Astron. Soc.* **224** 761-79
Clegg R E S, Seaton M J, Peimbert M and Torres-Peimbert S 1983 *Mon. Not. R. Astr. Soc.* **205** 417-34
Cox D P and Daltabuit E 1971 *Astrophys. J.* **167** 257-9
Cudworth K M 1974 *Astron. J.* **79** 1384-95
Danziger I J, Dopita M A, Hawarden T G and Webster B L 1978 *Astrophys. J.* **220** 458-66
Daub C T 1982 *Astrophys. J.* **260** 612-24
Davidson K and Fesen R A 1985 *Ann. Rev. Astron. Astrophys.* **23** 119-46
Denegri D, Sadoulet B and Spiro M 1990 *Rev. Mod. Phys.* **62** 1-42
de Vaucouleurs G 1985 *ESO Workshop on The Virgo Cluster of Galaxies* ed O-G Richter and B Binggeli (Garching: European Southern Observatory) p 413
de Vaucouleurs G and Pence W D 1978 *Astron. J.* **83** 1163-73
Diaz A I and Tosi M 1986 *Astron. Astrophys.* **158** 60-6
Dinerstein H L 1983 *IAU Symp. 103 Planetary Nebulae* ed D R Flower (Dordrecht: Reidel) pp 79-88

D'Odorico S, Peimbert M and Sabbadin F 1976 *Astron. Astrophys.* **47** 341-4
Dopita M A, Mason D J and Robb W D 1976 *Astrophys. J.* **207** 102-9
Downes R A 1986 *Astrophys. J. Suppl. Ser.* **61** 569-84
Dufour R J 1984a *Astrophys. J.* **287** 341-52
—— 1984b *Bull Astron. Soc. Pacific* **16** 888-9
—— 1984c *IAU Symp. 108 Structure and Evolution of the Magellanic Clouds* ed S van den Bergh and K S de Boer (Reidel: Dordrecht) pp 353-61
—— 1985 *Future of Ultraviolet Astronomy based on Six Years of IUE Research* ed J M Mead, R D Chapman and Y Kondo (NASA CP) pp 107-10
Dufour R J and Talent D L 1980 *Astrophys. J.* **235** 22-9
Dutra C M and Maciel W J 1990 *Rev. Mexicana Astron. Astrof.* **21** 264-7
Edmunds M G and Pagel B E J 1978 *Mon. Not. R. Astron. Soc.* **185** 77p-80p
Escalante V 1988 *Thesis* Harvard University
Escalante V and Victor G A V 1990 *Astrophys. J. Suppl. Ser.* **73** 513-53
Faúndez-Abans M and Maciel W J 1986 *Astron. Astrophys.* **158** 228-32
—— 1987a *Astron. Astrophys.* **183** 324-6
—— 1987b *Astrophys. Space Sci.* **129** 353-60
Feibelman W A, Oliversen N A, Nichols-Bohlin J and Garhart M P 1988 *International Ultraviolet Explorer, Spectral Atlas of Planetary Nebulae, Central Stars, and Related Objects (NASA Reference Publication* **1203**) (Greenbelt, MD: NASA)
Fleming T A, Liebert J, and Green R F 1986 *Astrophys. J.* **308** 176-89
Flower D R 1969 *Mon. Not. R. Astron. Soc.* **146** 243-63
—— 1983 *IAU Symp. 103 Planetary Nebulae* ed D R Flower (Dordrecht: Reidel)
Ford H C 1983 *IAU Symp. 103 Planetary Nebulae* ed D R Flower (Dordrecht: Reidel) pp 443-60
Ford H C, Ciardullo R, Jacoby G H and Hui X 1989 *IAU Symp. 131 Planetary Nebulae* ed S Torres-Peimbert (Dordrecht: Kluwer) pp 335-50
Forieri C 1986 *Spectral Evolution of Galaxies* ed C Chiosi and A Renzini (Dordrecht: Reidel) pp 473-5
Freeman K C 1970 *Astrophys. J.* **160** 811-30
—— 1987 *Ann. Rev. Astron. Astrophys.* **25** 603-32
French H B 1983 *Astrophys. J.* **273** 214-8
Frogel J A, Blanco V M, McCarthy M F and Cohen J G 1982 *Astrophys. J.* **252** 133-46
Garay G and Rodríguez L F 1983 *Astrophys. J.* **266** 263-70
Garnett D R and Shields G A 1987 *Astrophys. J.* **317** 82-101
Gathier R 1987 *Astron. Astrophys. Suppl. Ser.* **71** 245-53
Gathier R and Pottasch S R 1985 *Production and Distribution of C, N, O Elements* ed I J Danziger, F Matteucci and K Kjar (Garching: European Southern Observatory) pp 307-12
Gathier R Pottasch S R and Goss W M 1986a *Astron. Astrophys.* **157** 191-203
Gathier R, Pottasch S R, Goss W M and van Gorkom J H 1983 *Astron. Astrophys.* **128** 325-34
Gathier R, Pottasch S R and Pel J W 1986b *Astron. Astrophys.* **157** 171-90
Gómez Y, Moran J M, Rodríguez L F and Garay G 1989 *Astrophys. J.* **345** 862-70
Gould R J 1978 *Astrophys. J.* **219** 250-61
Greig W E 1971 *Astron. Astrophys.* **10** 161-74
—— 1972 *Astron. Astrophys.* **18** 70-8
Harrington J P, Seaton M J, Adams S and Lutz J H 1982 *Mon. Not. R. Astron. Soc.* **199** 517-64
Harris W E 1988 *A.S.P. Conf. Series no 4, The Extragalactic Distance Scale* ed S van den Bergh and C J Pritchet (Provo: Brigham Young University Press) pp 231-254
Hawley S A 1978 *Astrophys. J.* **224** 417-36
Hawley S A and Miller J S 1978a *Publ. Astron. Soc. Pacific* **90** 39-44
—— 1987b *Astrophys. J.* **220** 609-13
Hazard C, Terlevich R, Morton D C, Sargent W L W and Ferland G 1980 *Nature* **285** 463-4
Heap S R and Augensen H J 1987 *Astrophys. J.* **313** 268-83
Henry R B C 1986 *Publ. Astron. Soc. Pacific* **98** 1044-8
—— 1989 *Mon. Not. R. Astron. Soc.* **241** 453-68
—— 1990 *Astrophys. J.* **356** 229-40
Henry R B C, Liebert J and Boroson T A 1989 *Astrophys. J.* **339** 872-88
Hindman J V 1967 *Australian J. Phys.* **20** 147-71
Huchra J 1984 *Preprint 2067 Center for Astrophysics*
Hummer D G and Mihalas D 1970 *Mon. Not. R. Astron. Soc.* **147** 339-54
Hummer D G and Storey P J 1987 *Mon. Not. R. Astron. Soc.* **224** 801-20
Husfeld D, Kudritzki R P, Simon K P and Clegg R E S 1984 *Astron. Astrophys.* **134** 139-46

Iben I, Jr 1975 *Astrophys. J.* **196** 525–47
—— 1984 *Astrophys. J.* **277** 333–54
Iben I, Jr, Kaler J B, Truran J W and Renzini A 1983 *Astrophys. J.* **264** 605–12
Iben I, Jr and Renzini A 1983 *Ann. Rev. Astron. Astrophys.* **21** 271–342
—— 1984 *Phys. Rep.* **105** 329
Iben I, Jr and Rood R T 1970 *Astrophys. J.* **159** 605–17
Iben I, Jr and Truran J W 1978 *Astrophys. J.* **220** 980–95
Iben I, Jr and Tutukov A V 1989 *IAU Symp. 131* ed S Torres-Peimbert (Dordrecht: Kluwer) pp 505–22
Jacoby G H 1979 *Publ. Astron. Soc. Pacific* **91** 754–60
—— 1980 *Astrophys. J. Suppl.* **42** 1–18
—— 1983 *IAU Symp. 103 Planetary Nebulae* ed D R Flower (Dordrecht: Reidel) pp 427–42
—— 1989 *Astrophys. J.* **339** 39–52
Jacoby G H, Ciardullo R and Ford H 1990 *Astrophys. J.* **356** 332–49
Jacoby G H, Ciardullo R, Ford H C and Booth J 1989 *Astrophys. J.* **344** 704–14
Jacoby G H and Ford H C 1983 *Astrophys. J.* **266** 298–308
—— 1986 *Astrophys. J.* **304** 490–500
Jenner D C and Ford H C 1978 *IAU Symp. 76 Planetary Nebulae* ed Y Terzian (Dordrecht: Reidel) p 246
Kaler J B 1970 *Astrophys. J.* **160** 887–913
—— 1979 *Astrophys. J.* **228** 163–78
—— 1983a *IAU Symp. 103 Planetary Nebulae* ed D R Flower (Dordrecht: Reidel) pp 245–57
—— 1983b *Astrophys. J.* **271** 188–220
—— 1985 *Ann. Rev. Astron. Astrophys.* **23** 89–117
—— 1986 *Astrophys. J.* **308** 337–46
Kaler J B, Aller L H, Czyzak S J and Epps H W 1976 *Astrophys. J. Suppl. Ser.* **31** 163–86
Kaler J B, Iben I, Jr and Becker S A 1978 *Astrophys. J.* **224** L63–6
Kaler J B and Jacoby G H 1989 *Astrophys. J.* **345** 871–80
—— 1990 *Astrophys. J.* **362** 491–502
Kaler J B and Lutz J H 1985 *Publ. Astron. Soc. Pacific* **97** 700–6
Kaler J B, Shaw R A and Kwitter K B 1990 *Astrophys. J.* **359** 392–418
Khromov G 1979 *Astrofisika* **15** 269–84
—— 1989 *Space Sci. Rev.* **51** 339–423
Kinman T D, Feast M W and Lasker B M 1988 *Astron. J.* **95** 804–20
Kohoutek L 1967 *Bull. Astron. Inst. Czech.* **18** 103–13
Kraan-Korteweg R C 1985 *ESO Workshop on The Virgo Cluster of Galaxies* ed O-G Richter and B Binggeli (Garching: European Southern Observatory) p 397
Kwok S 1985 *Astrophys. J.* **290** 568–77
—— 1987 *Phys. Rep.* **156** 111–46
Kwok S and Bignell R C 1984 *Astrophys. J.* **276** 544–50
Lambert D L 1978 *Mon. Not. R. Astron. Soc.* **182** 249–72
Lambert D L and Luck R E 1978 *Mon. Not. R. Astron. Soc.* **183** 79–100
Lequeux J, Peimbert M, Rayo J F, Serrano A and Torres-Peimbert S 1979 *Astron. Astrophys.* **80** 155–66
Lichten S M, Rodríguez L F and Chaisson E J 1979 *Astrophys. J.* **229** 524–32
Liller M H, Welther B L and Liller W 1966 *Astrophys. J.* **144** 280–90
Lutz J H 1973 *Astrophys. J.* **181** 135–45
—— 1989 *IAU Symp. 131 Planetary Nebulae* ed S Torres-Peimbert (Dordrecht: Kluwer) pp 65–72
MacAlpine G M, McGaugh S S, Mazzarella J M and Uomoto A 1989 *Astrophys. J.* **342** 364–73
Maciel W J 1981a *Astron. Astrophys.* **98** 406–7
—— 1981b *Astron. Astrophys. Suppl. Ser.* **44** 123–5
—— 1984 *Astron. Astrophys. Suppl. Ser.* **55** 253–8
—— 1985 *Rev. Mexicana Astron. Astrof.* **10** 199–202
—— 1988 *Astron. Astrophys.* **200** 178–84
—— 1989 *IAU Symp. 131 Planetary Nebulae* ed S Torres-Peimbert (Dordrecht: Kluwer) pp 73–82
Maciel W J 1990 private communication
Maciel W J and Faúndez-Abans M 1985 *Astron. Astrophys.* **149** 365–71
Maciel W J, Faúndez-Abans M and de Oliveira M 1986 *Rev. Mexicana Astron. Astrof.* **12** 233–9
Maciel W J and Leite C C M 1990 *Rev. Mexicana Astron. Astrof.* **21** 197–200
Maciel W J and Pottasch S R 1980 *Astron. Astrophys.* **88** 1–7
Maehara H, Okamura S, Noguchi T, He X-T and Liu J 1986 *Second Japan–China Workshop on Stellar Activities and Observational Techniques* (Kyoto: University of Tokyo) p 71
Mallik D C V and Mallik S V 1985 *J. Astrophys. Astron.* **6** 113–30

Mallik D C V and Peimbert M 1988 *Rev. Mexicana Astron. Astrof.* **16** 111–21
Manchado A, Pottasch S R and Mampaso A 1988 *Astron. Astrophys.* **191** 128–36
Masson C R 1986 *Astrophys. J.* **302** L27–30
Maran S P, Aller L H, Gull T R and Stecher T P 1982 *Astrophys. J.* **253** L43–7
Matteucci F 1986 *Publ. Astron. Soc. Pacific* **98** 973–8
Matteucci F, Franco J, Francois P and Treyer M A 1989 *Rev. Mexicana Astron. Astrof.* **18** 145–52
Matteucci F and Francois P 1989 *Mon. Not. R. Astron. Soc.* **239** 885–904
Melnick J, Terlevich R and Moles M 1988 *Mont. Not. R. Astron. Soc.* **235** 297–313
Méndez R H 1975 *Astrophys. J.* **199** 411–7
—— 1989 private communication
Méndez R H, Kudritzki R P, Gruschinke J and Simon K P 1981 *Astron. Astrophys.* **101** 323–31
Méndez R H, Kudritzki R P, Herrero A, Husfeld D and Groth H G G 1988 *Astron. Astrophys.* **190** 113–36
Mendoza C 1983 *IAU Symp. 103 Planetary Nebulae* ed D R Flower (Dordrecht: Reidel) pp 143–72
Mendoza C and Zeippen C J 1982a *Mon. Not. R. Astron. Soc.* **198** 127–39
—— 1982b *Mon. Not. R. Astron. Soc.* **199** 1025–32
Meyer J-P 1985 *Astrophys. J. Suppl.* **57** 151–71
Menzel D H, Aller L H and Hebb M H 1941 *Astrophys. J.* **93** 230–5
Milne D K 1982 *Mon. Not. R. Astron. Soc.* **200** 51p–54p
Milne D K and Aller L H 1975 *Astron. Astrophys.* **38** 183–96
Minkowski R 1965 *Galactic Structure* ed A Blaauw and M Schmidt (Chicago: University of Chicago Press) pp 321–43
Minkowski R and Aller L H 1954 *Astrophys. J.* **120** 261–4
Monk D J, Barlow M J and Clegg R E S 1988 *Mon. Not. R. Astron. Soc.* **234** 583–624
Mould J R 1984 *Publ. Astron. Soc. Pacific* **96** 773–8
Nomoto K 1984 *Stellar Nucleosynthesis* ed C Chiosi and A Renzini (Dordrecht: Reidel) pp 205–37
Nussbaumer H and Storey P J 1983 *Astron. Astrophys.* **126** 75–9
—— 1984 *Astron. Astrophys. Suppl.* **56** 293–312
O'Dell C R 1962 *Astrophys. J.* **135** 371–84
—— 1963 *Astrophys. J.* **138** 67–78
—— 1968 *IAU Symp. 34 Planetary Nebulae* ed D E Osterbrock and C R O'Dell (Dordrecht: Reidel) pp 361–75
O'Dell C R, Peimbert M and Kinman T D 1964 *Astrophys. J.* **140** 119–29
Olive K A, Schramm D N, Steigman G and Walker T P 1990 *Phys. Lett. B* in press
Osterbrock D E 1973 *Mém. Soc. R. Sci. Liege* Ser 6 **5** 391–402
—— 1989 *Astrophysics of Gaseous Nebulae and Active Galactic Nuclei* (California: University Science Books)
Osterbrock D E and Flather E 1959 *Astrophys. J.* **129** 26–43
Paczynski B 1971 *Acta Astron.* **21** 417–35
Pagel B E J 1986 *Advances in Nuclear Astrophysics* ed E Vangioni-Flan, J Adouze, M Casse, J P Chieze and J Tran Thanh Van (France: Frontieres) p 53
——1987a *A Unified View of the Macro- and the Micro-Cosmos* ed A de Rujula, D V Nanopoulos and P A Shaver (Singapore: World Scientific) pp 399–423
—— 1987b *The Galaxy* ed G Gilmore and B Carswell (Dordrecht: Reidel) p 341
—— 1989 *Rev. Mexicana Astron. Astrof.* **18** 161–72
Pagel B E J and Edmunds M G 1981 *Ann. Rev. Astron. Astrophys.* **19** 77–113
Pagel B E J and Simonson E A 1989 *Rev. Mexicana Astron. Astrof.* **18** 153–9
Pedreros M 1989 *Astron. J.* **98** 2146–55
Peimbert M 1973 *Mem. Soc. R. Sci. Liege* Ser 6 **5** 307–16
—— 1978 *IAU Symp. 76 Planetary Nebulae* ed Y Terzian (Dordrecht: Reidel) pp 215–23
—— 1981 *Physical Processes in Red Giants* ed I Iben, Jr and A Renzini (Dordrecht: Reidel) pp 409–20
—— 1982 *Ann. N.Y. Acad. Sci.* **295** 24–42
—— 1983 *Primordial Helium* ed P A Shaver, D Kunth and K Kjar (Garching: European Southern Observatory) pp 267–79
—— 1984 *IAU Symp. 108 Structure and Evolution of the Magellanic Clouds* ed S van den Bergh and K S de Boer (Dordrecht: Reidel) pp 363–74
—— 1985 *Rev. Mexicana Astron. Astrof.* **10** 125–34
—— 1986 *Publ. Astron. Soc. Pacific* **98** 1057–60
—— 1987 *Planetary Nebulae and Protoplanetary Nebulae: from IRAS to ISO* ed A Preite-Martinez (Dordrecht: Reidel) pp 91–100
—— 1989 *IAU Symp. 131 Planetary Nebulae* ed S Torres-Peimbert (Dordrecht: Kluwer) pp 577–87
—— 1990 *Rev. Mexicana Astron. Astrof.* **237** 454–60
Peimbert M, Rayo J F and Torres-Peimbert S 1975 *Rev. Mexicana Astron. Astrof.* **1** 289–97

Peimbert M and Serrano A 1980 *Rev. Mexicana Astron. Astrof.* **5** 9-18
Peimbert M and Torres-Peimbert S 1977 *Mont. Not. R. Astron. Soc.* **179** 217-34
—— 1983 *IAU Symp. 103 Planetary Nebulae* ed D R Flower (Dordrecht: Reidel) pp 233-42
—— 1987a *Rev. Mexicana Astron. Astrof.* **14** 540-58
—— 1987b *Rev. Mexicana Astron. Astrof.* **15** 117-23
Peimbert M, Torres-Peimbert S and Rayo J F 1978 *Astrophys. J.* **220** 516-24
Peña M and Ruiz M T 1988 *Rev. Mexicana Astron. Astrof.* **16** 55-62
Peña M, Ruiz M T, Maza J and González L E 1989 *Rev. Mexicana Astron. Astrof.* **17** 25-30
Peña M, Ruiz M T, Torres-Peimbert S and Maza J 1990 *Astron. Astrophys.* **257** 654-60
Péquignot D 1980 *Astron. Astrophys.* **81** 356-8
Péquignot D, Aldrovandi S M V and Stasinska G 1978 *Astron. Astrophys.* **63** 313-24
Péquignot D and Dennefeld M 1983 *Astron. Astrophys.* **120** 249-62
Perek L and Kohoutek L 1967 *Catalog of Galactic Planetary Nebulae* (Prague: Czechoslovakian Academy of Science)
Perinotto M 1989 *IAU Symp. 131 Planetary Nebulae* ed S Torres-Peimbert (Dordrecht: Kluwer) pp 293-300
Phillips J P 1989 *IAU Symp. 131 Planetary Nebulae* ed S Torres-Peimbert (Dordrecht: Kluwer) pp 425-34
Phillips J P and Pottasch S R 1984 *Astron. Astrophys.* **130** 91-6
Pierce M J 1989 *Astrophys. J. Lett.* **344** L57-60
Pottasch S R 1980 *Astron. Astrophys.* **89** 336-41
—— 1983 *IAU Symp. 103 Planetary Nebulae* ed D R Flower (Dordrecht: Reidel) pp 391-409
—— 1984 *Planetary Nebulae* (Dordrecht: Reidel)
—— 1989 *IAU Symp. 131 Planetary Nebulae* ed S Torres-Peimbert (Dordrecht: Kluwer) pp 481-92
Pottasch S R, Bignell C, Olling R and Zijlstra A A 1988 *Astron. Astrophys.* **205** 248-56
Preite-Martinez A 1987 *Planetary Nebulae and Protoplanetary Nebulae: from IRAS to ISO* ed A Preite-Martinez (Dordrecht: Reidel)
Ratag M A, Pottasch S R, Zijlstra A A and Menzies J 1990 *Astron. Astrophys.* **28** 525-60
Reilman R F and Manson S T 1979 *Astrophys. J. Suppl. Ser.* **40** 815-80
Reimers D 1975 *Mem. Soc. R. Sci. Liege* ser 6 **8** 369-82
Renzini A 1983 *IAU Symp. 103 Planetary Nebulae* ed D R Flower (Dordrecht: Reidel) pp 267-80
—— 1984 *Stellar Nucleosynthesis* ed C Chiosi and A Renzini (Dordrecht: Reidel) pp 99-114
—— 1989 *IAU Symp. 76 Planetary Nebulae* ed Y Terzian (Dordrecht: Reidel)
Renzini A and Buzzoni A 1986 *Spectral Evolution of Galaxies* ed C Chiosi and A Renzini (Dordrecht: Reidel) pp 195-235
Renzini A and Voli M 1981 *Astron. Astrophys.* **94** 175-93
Robbins R R 1968 *Astrophys. J.* **151** 511-29
Robbins R R and Bernat A P 1973 *Mém. Soc. R. Sci Liege* ser 6 **5** 263-74
Roche P F 1989 *IAU Symp. 131 Planetary Nebulae* ed S Torres-Peimbert (Dordrecht: Kluwer) pp 117-27
Rodríguez L F 1989 *IAU Symp. 131 Planetary Nebulae* ed S Torres-Peimbert (Dordrecht: Kluwer) pp 129-37
Russell R W, Soifer B T and Willner S P 1977 *Astrophys. J.* **217** L149-53
Sabbadin F 1984a *Mon. Not. R. Astron. Soc.* **209** 889-94
—— 1984b *Mon. Not. R. Astron. Soc.* **210** 341-58
—— 1986a *Astron. Astrophys.* **160** 31-8
—— 1986b *Astron. Astrophys. Suppl. Ser.* **64** 579-89
Sabbadin F and Bianchini A 1983 *Astron. Astrophys. Suppl. Ser.* **52** 395-8
Sabbadin F, Bianchini A and Hamzaoglu E 1984a *Astron. Astrophys.* **136** 200-5
Sabbadin F, Gratton R G, Bianchini A and Ortalani S 1984b *Astron. Astrophys.* **136** 181-92
Sabbadin F, Ortolani S and Bianchini A 1985 *Mon. Not. R. Astron. Soc.* **213** 563-73
Sabbadin F, Strafella F and Bianchini A 1986 *Astron. Astrophys. Suppl. Ser.* **65** 259-65
Sandage A and Tammann G A 1990 *Astrophys. J.* in press
Saraph H E and Seaton M J 1980 *Mon. Not. R. Astron. Soc.* **193** 617-29
Sarmiento A and Peimbert M 1985 *Rev. Mexicana Astron. Astrof.* **11** 73-81
Schild H and Maeder A 1985 *Astron. Astrophys.* **143** L7-10
Schneider S E and Terzian Y 1983 *Astrophys. J.* **274** L61-4
Schneider S E, Terzian Y, Purgathofer A and Perinotto M 1983 *Astrophys. J. Suppl.* **52** 399-423
Schönberner D 1979 *Astron. Astrophys.* **79** 108-14
—— 1983 *Astrophys. J.* **272** 708-14
—— 1989 *IAU Symp. 131 Planetary Nebulae* ed S Torres-Peimbert (Dordrecht: Kluwer) pp 463-71
Seaton M J 1954 *Mon. Not. R. Astron. Soc.* **114** 154-71
—— 1960 *Rep. Prog. Phys.* **23** 313-54

—— 1966 *Mon. Not. R. Astron. Soc.* **132** 113-35
—— 1968 *Astrophys. Lett.* **2** 55-8
—— 1978 *IAU Symp. 76 Planetary Nebulae* ed Y Terzian (Dordrecht: Reidel) pp 131-7
—— 1979 *Mon. Not. R. Astron. Soc.* **187** 73p-76p
Seaton M J and Osterbrock D E 1957 *Astrophys. J.* **125** 66-83
Serrano A and Peimbert M 1981 *Rev. Mexicana Astron. Astrof.* **5** 109-24
—— 1983 *Rev. Mexicana Astron. Astrof.* **8** 117-29
Shaver P A, McGee R X, Newton L M, Danks A C and Pottasch S R 1983 *Mont. Not. R. Astron. Soc.* **204** 53-112
Shields G A 1990 *Ann. Rev. Astron. Astrophys.* **28** 525-60
Shklovsky I R 1956 *Soviet Astron.* **33** 222-35
Stanghellini L and Kaler J B 1989 *Astrophys. J.* **343** 811-27
Stasinska G and Tylenda R 1990 *Astron. Astrophys.* in press
Steigman G 1990 *Fundamental Symmetries in Nuclei and Particles* ed P Vogel (Singapore: World Scientific) in press
Storey J W V 1984 *Mon. Not. R. Astron. Soc.* **206** 521-7
Strömgren B 1939 *Astrophys. J.* **89** 526-47
—— 1948 *Astrophys. J.* **188** 242-75
Terzian Y 1978 *IAU Symp. 76 Planetary Nebulae* ed Y Terzian (Dordrecht: Reidel)
Tinsley B M 1978 *IAU Symp. 76 Planetary Nebulae* ed Y Terzian (Dordrecht: Reidel)
Tonry J L, Ajhar E A and Luppino G A 1989 *Astrophys. J. Lett.* **346** L57-60
Torres-Peimbert S 1984 *Stellar Nucleosynthesis* ed C Chiosi and A Renzini (Dordrecht: Reidel) pp 3-14
—— 1989 *IAU Symp. 131 Planetary Nebulae* ed S Torres-Peimbert (Dordrecht: Kluwer)
Torres-Peimbert S and Peimbert M 1971 *Bol. Obs. Tonantzintla y Tacubaya* **6** 101-11
—— 1977 *Rev. Mexicana Astron. Astrof.* **2** 181-207
—— 1979 *Rev. Mexicana Astron. Astrof.* **4** 341-50
Torres-Peimbert S, Peimbert M and Daltabuit E 1980 *Astrophys. J.* **238** 133-9
Torres-Peimbert S, Rayo J F and Peimbert M 1981 *Rev. Mexicana Astron. Astrof.* **6** 315-9
Torres-Peimbert S, Peimbert M and Fierro J 1989 *Astrophys. J.* **345** 186-95
Torres-Peimbert S, Peimbert M and Peña M 1990 *Astron. and Astrophys.* **233** 540-52
Tosi M 1988a *Astron. Astrophys.* **197** 33-46
—— 1988b *Astron. Astrophys.* **197** 47-51
Vorontsov-Velyaminov B A 1934 *Z. Astrophys.* **8** 195-207
Webster B L 1969 *Mon. Not. R. Astron. Soc.* **143** 79-95
—— 1988 *Mon. Not. R. Astron. Soc.* **230** 377-401
Weidemann V 1977 *Astron. Astrophys.* **61** L27-30
White S D M and Audouze J 1983 *Mon. Not. R. Astron. Soc.* **203** 603-18
Whitford A E 1958 *Astron. J.* **63** 201-7
Wilkes B J, Ferland G J, Hanes D and Truran J W 1981 *Mon. Not. R. Astron. Soc.* **197** 1-6
Wood P R, Bessell M S and Dopita M A 1986 *Astrophys. J.* **311** 632-6
Wood P R, Meatheringham S J, Dopita M A and Morgan D H 1987 *Astrophys. J.* **320** 178-81
Wood P R and Faulkner D J 1986 *Astrophys. J.* **307** 659-74
Woosley S E, Axelrod T S and Weaver T A 1984 *Stellar Nucleosynthesis* ed C Chiosi and A Renzini (Dordrecht: Reidel) pp 263-93
Zanstra H 1931 *Zs. f. Astrophys.* **2** 329
Zeippen C J 1982 *Mon. Not. R. Astron. Soc.* **198** 111-25
Zuckerman B and Gatley I 1988 *Astrophys. J.* **324** 501-15